

12-2011

Dynamic Botanical Filtration System for Indoor Air Purification

Zhiqiang Wang
Syracuse University

Follow this and additional works at: http://surface.syr.edu/mae_etd

 Part of the [Mechanical Engineering Commons](#)

Recommended Citation

Wang, Zhiqiang, "Dynamic Botanical Filtration System for Indoor Air Purification" (2011). *Mechanical and Aerospace Engineering - Dissertations*. Paper 63.

This Dissertation is brought to you for free and open access by the College of Engineering and Computer Science at SURFACE. It has been accepted for inclusion in Mechanical and Aerospace Engineering - Dissertations by an authorized administrator of SURFACE. For more information, please contact surface@syr.edu.

Abstract

A dynamic botanical air filtration (DBAF) system was developed, tested and modeled for indoor air purification. The DBAF system consisted of an activated-carbon/hydroculture-based root bed for potted-plant, a fan for driving air through the root bed for purification, and an irrigation system for maintaining proper moisture content in the root bed. Results from test conducted in a full-scale open office space indicated that the filtration system had ability to supply clean air equivalent to 80% of required outdoor air supply for the space. The DBAF was effective for removing both formaldehyde and toluene at 5 to 32% volumetric water content of the root bed. It also performed consistently well over the relatively long testing period of 300 days while running continuously.

In order to improve the understanding of the mechanisms of the DBAF system in removing the volatile organic compounds, a series of further experiments were conducted to determine the important factors affecting the removal performance, and the roles of different transport, storage and removal processes. It was found that passing the air through the root bed with microbes was essential to obtain meaningful removal efficiency. Moisture in the root bed also played an important role, both for maintaining a favorable living condition for microbes and for absorbing water-soluble compounds such as formaldehyde. The role of the plant was to introduce and maintain a favorable microbe community that effectively degraded the VOCs that were adsorbed or absorbed by the root bed. While the moisture in a wet bed had the scrubber effect for water-soluble compounds such as formaldehyde, presence of the

plant increased the removal efficiency by about a factor of two based on the results from the reduced-scale root bed experiments.

A mathematical model was also developed for predicting the short and long term performance of the DBAF with model parameters estimated from the experiments. The simulation results showed that the model could describe the pressure drop and airflow relationship well by using the air permeability as a model parameter. The water source added in the model also led to the similar bed moisture content and outlet air RH as that in real test case. The simulation results also showed that the developed model worked well in analyzing the effect of different parameters. It was also found that the critical bio-degradation rate constant was $1 \times 10^{-5} \text{ s}^{-1}$, below which the DBAF would not be able to sustain the formaldehyde removal performance. The bio-degradation rate constant of the reduced scale DBAF tested was estimated to be in the range of $0.8\text{--}1.5 \times 10^{-4} \text{ s}^{-1}$.

Whole building energy simulation results showed that using the DBAF to substitute 80% of the outdoor air supply without adversely affecting the indoor air quality could result in 30% saving in heating, 3% in cooling and 0.7% in pump energy consumption per year at the climate of Syracuse, NY (Zone 5). A higher percentage of energy savings was found to be achievable for climate zones with a higher annual heating load (e.g., climate zone 6 and 7).

DYNAMIC BOTANICAL FILTRATION SYSTEM FOR INDOOR AIR PURIFICATION

By

Zhiqiang Wang

B.S. Tianjin University, 2003

M.S. Tianjin University, 2007

DISSERTATION

Submitted in partial fulfillment of the requirement for the
Degree of Doctor of Philosophy in Mechanical Engineering
in the Graduate School of Syracuse University

December 2011

Copyright © 2011 Zhiqiang Wang

All right reserved

Table of Contents

LIST OF FIGURES	IX
LIST OF TABLES	XII
NOMENCLATURE.....	XIV
ACRONYM	XVI
ACKNOWLEDGEMENT	XVII
CHAPTER 1. INTRODUCTION	1
1.1 BACKGROUND AND PROBLEM DEFINITION	1
1.2 OBJECTIVES AND SCOPES	8
1.3 DISSERTATION ORGANIZATION	10
CHAPTER 2. LITERATURE REVIEW	11
2.1 INTRODUCTION.....	11
2.2 METHODS OF IMPROVING INDOOR AIR QUALITY	12
2.3 BIOFILTER AND INDOOR AIR QUALITY	16
2.3.1 Biodegradability of VOC.....	19
2.3.2 Influence of Low Concentration on Biomass Productivity and Transfer Rates.....	22
2.3.3 Impact of Design on Purification Efficiency.....	27
2.3.4 Design of Biological Purifiers.....	28
2.3.5 Humidification Effect and Biohazards.....	30
2.3.6 Summary.....	31
2.4 BIOFILTER MODELING	32
2.4.1 Biofilter and Biotrickling Filter Mechanics	32
2.4.2 Air Flow	33
2.4.3 Phase Transfer	34

2.4.4 Diffusion within the Bio-film	36
2.4.5 Adsorption on the Solid Phase	37
2.4.6 Biomass Growth and Biodegradation	39
2.4.7 Summary.....	40
2.5 MAJOR FINDINGS.....	40
CHAPTER 3. PERFORMANCE TESTING, EVALUATION, AND ANALYSIS	42
3.1 INTRODUCTION.....	42
3.2 METHODS.....	43
3.2.1 Experiments in a Full-scale Environmental Chamber.....	44
3.2.2 Experiments as Part of an Office HVAC System	48
3.3 RESULTS AND DISCUSSIONS	52
3.3.1 Full-scale Chamber Experiments.....	52
3.3.2 Experiments as Part of an Office HVAC System	60
3.4. MAJOR FINDINGS.....	70
CHAPTER 4. VOC REMOVAL MECHANISMS AND DETERMINATION OF BIO-DEGRADATION RATE	
CONSTANT	73
4.1 INTRODUCTION.....	73
4.2 METHODS.....	74
4.2.1 Formaldehyde Removal by Potted Plant Without Air Passing the Root Bed.....	76
4.2.2 Formaldehyde Removal by Microbial Community with Air Flow Passing Through.....	79
4.2.3 Formaldehyde and Toluene Removal Rate by the DBAF.....	83
4.3 RESULTS.....	88
4.3.1 Formaldehyde Removal by Potted Plant Without Air Passing the Root Bed.....	88
4.3.2 Formaldehyde Removal by Microbial Community with Air Flow Passing through	93
4.3.3 Formaldehyde Removal by Dynamic Botanical Air Filtration System	100

4.3.4 Toluene Removal by Dynamic Botanical Air Filtration System.....	110
4.4 MAJOR FINDINGS.....	111
CHAPTER 5. MODEL SIMULATION AND VALIDATION.....	113
5.1 INTRODUCTION.....	113
5.2 MODEL DEVELOPMENT.....	114
5.2.1 Model Description and Assumptions.....	114
5.2.2 Governing Equations.....	117
5.2.3 Determination of Model Parameters.....	123
5.3 MODEL IMPLEMENTATION.....	124
5.4 SIMULATION RESULTS.....	124
5.4.1 Model Verification.....	124
5.4.2 Comparison with Experimental Data and Discussion.....	134
5.5 MAJOR FINDINGS.....	135
CHAPTER 6. BUILDING ENERGY EFFICIENCY SIMULATION AND ANALYSIS.....	137
6.1 INTRODUCTION.....	137
6.2 METHODS.....	138
6.3 SIMULATION RESULTS.....	143
6.3.1 Base Case for Syracuse, NY Climate.....	143
6.3.2 Cases for Other U.S. Climate.....	146
6.4 CONCLUSIONS.....	149
CHAPTER 7. SUMMARY AND CONCLUSIONS.....	150
REFERENCES.....	155
APPENDIX A. FULL-SCALE CHAMBER PULL-DOWN TEST PROCEDURE.....	166
A.1 TEST FACILITY AND INSTRUMENT.....	166
A.2 TEST PROCEDURE.....	167

A.3 CALCULATION OF CADR AND REMOVAL EFFICIENCY	169
APPENDIX B. APPLICATION IN REAL-WORLD CONDITIONS AND TEST PROCEDURE	173
B.1 SOURCE INTRODUCTION	173
B.2 VOC IDENTIFICATION.....	173
B.3 FILTER BED SINGLE PASS EFFICIENCY MEASUREMENT.....	175
B.4 EFFECT OF BED WATER CONTENT TO THE SINGLE PASS EFFICIENCY	176
B.5 TEST ROOM CONTAMINANTS CONCENTRATION MONITORING.....	178
APPENDIX C. COE BUILDING HUMIDITY LOAD CALCULATION	180

List of Figures

Figure 1-1 Main mechanisms of the air purification in this combined technique .	6
Figure 1-2 Overview of objectives and scopes	9
Figure 3-1 Schematic of full-sized dynamic botanical air filtration system: (a) side view, (b) top view. Moisture content sensor (M.C. sensor).	44
Figure 3-2 Schematic of the environmental chamber test setup: (a) top-view, (b) side-view. Air handling unit (AHU).	46
Figure 3-3 Integration of botanical filter into an HVAC system and setup for monitoring. Air handling unit (AHU). Proton Transfer Reaction Mass Spectrometer (PTR-MS).	49
Figure 3-4 Normalized formaldehyde concentration at different air flow rate: (a) 250 m ³ /h airflow rate passing the bed, (b) 600 m ³ /h airflow rate, (c) 930 m ³ /h air flow rate. Volumetric water content (VWC) in the filter bed.	53
Figure 3-5 Normalized toluene concentration at different air flow rate: (a) 250 m ³ /h airflow rate passing the bed, (b) 600 m ³ /h airflow rate, (c) 930 m ³ /h air flow rate. Volumetric water content (VWC) in the filter bed.	54
Figure 3-6 Test set-up and test chamber concentration vary with time: (a) test set-up (photo), (b) test results. The red dotted vertical lines represent the 8-hour operation period of the DBAF.	59
Figure 3-7 Effect of DBAF on room air temperature and RH: (a) Temperature, (b) RH.	61
Figure 3-8 Comparison of room pollutants concentration: (a) Formaldehyde, (b) Toluene. Outdoor air (OA). Normalized formaldehyde concentration (NFC). Emission factor (EF). Normalized toluene concentration (NTC).	63
Figure 3-9 Effect of bed water content on removal of pollutants.	66

Figure 3-10 Botanical filter single pass efficiency (SPE) over 300 days.	68
Figure 4-1 Schematic of reduced-sized dynamic botanical air filtration system: (a) side view, (b) top view. Moisture content sensor (M.C. sensor).....	75
Figure 4-2 Schematics of the test set-up for formaldehyde removal by microbial community with air passing by	80
Figure 4-3 Schematic of the mid-scale chamber system for low concentration (ppb) test	84
Figure 4-4 Formaldehyde removed by one 8” potted plant	89
Figure 4-5 Effect of potted plant number on formaldehyde removal	91
Figure 4-6 Effect of light in the chamber on formaldehyde removal	92
Figure 4-7 Test system relative humidity change over time.....	94
Figure 4-8 Formaldehyde removal by microbes with single-injection.....	95
Figure 4-9 Desorption of formaldehyde from sorbent bed with and without microbes	96
Figure 4-10 Formaldehyde removal by microbes in multi-injection test	97
Figure 4-11 Formaldehyde removal isotherm by wet-bed with and without microbes	99
Figure 4-12 Sorbent bed moisture retention curve	99
Figure 4-13 Chamber formaldehyde equilibrium concentrations at different RHs	101
Figure 4-14 Long term formaldehyde removal efficiency by DBAF at 90% RH	102
Figure 4-15 CADR and SPE after one day	104
Figure 4-16 CADR and SPE after one week	104

Figure 4-17 Chamber monitored RH at different RHs	105
Figure 5-1 Schematic of the root bed system and associated transport and storage processes	116
Figure 5-2 Bed average moisture content and outlet air relative humidity.....	126
Figure 5-3 Vertical distribution of bed moisture content over time	126
Figure 5-4 Effect of partition coefficient	128
Figure 5-5 Effect of gas to solid mass transfer coefficient	129
Figure 5-6 Effect of gas to liquid coefficient constant without irrigation	131
Figure 5-7 Effect of gas to liquid coefficient constant with irrigation	131
Figure 5-8 Effect of bio-degradation rate constant	133
Figure 5-9 Simulation results with all the processes involved	134
Figure 6-1 Building image for simulation (generated in DesignBuilder).....	139
Figure 6-2 First and second floor plan of COE building main tower	140
Figure 6-3 Third, fourth, and fifth floor plan of COE building main tower	140
Figure 6-4 U.S. Climate zones (by county) for the 2004 Supplement to the IECC, the 2006 IECC, and ASHRAE 90.1-2004	146
Figure A-1 Test facility and instrument.....	167
Figure A-2 Schematics of the test chamber	169
Figure B-1 Contaminant source introduced into the test room by using particleboards.....	173

List of Tables

Table 2-1 Current and emerging indoor air treatment methods, principle and limitations.....	14
Table 2-2 Biodegradability of typical indoor VOC	20
Table 3-1 CADR and SPE for formaldehyde and toluene removal.....	55
Table 3-2 Average temperature and RH change “Δ” in chamber return air from the initial conditions of 23±0.6 °C and 60±3 % RH.....	57
Table 3-3 CADR and SPE of DBAF for VOC emitted from an office furniture during a 4-day test.....	59
Table 3-4 Average temperature and RH at different periods in a 24-hr-test	61
Table 4-1 Tests conducted to investigate the VOC removal mechanisms of DBAF.....	75
Table 4-2 Tests conducted for formaldehyde removal by potted plant without air passing the root bed at 23±0.6 °C and 50±3 % RH.	77
Table 4-3 Tests conducted for formaldehyde removal by microbial community with air flow passing through at 23±0.6 °C and 90±3 % RH	80
Table 4-4 Tests conducted for formaldehyde removal by DBAF.....	84
Table 4-5 Tests conducted for toluene removal by DBAF.....	85
Table 4-6 Comparison of calculated and measured adsorbed formaldehyde mass	99
Table 4-7 Concentration, SPE and CADR at different RHs.....	102
Table 4-8 Chamber ventilation and DBAF bed moisture content at different RHs	105

Table 4-9 The formaldehyde SPE and CADR of the DBAF at different RHs ..	106
Table 4-10 Comparison of CADR at different series of tests.....	107
Table 4-11 Determination of formaldehyde bio-degradation rate constant.....	109
Table 4-12 The SPE and CADR of the DBAF in removing toluene at different RHs	111
Table 5-1 Model key parameters determination	123
Table 5-2 The fitted bio-degradation rate constant.....	135
Table 6-1 COE building envelope information (from COE building design manual)	141
Table 6-2 COE building internal loads (from COE building design manual) ...	142
Table 6-3 Yearly energy and cost saving related to HVAC system	144
Table 6-4 Selected cities for different U.S. climate zones in the simulation.....	146
Table 6-5 Yearly operation energy and cost saving due to use of DBAF at different U.S. climate zones.....	148
Table B-1 Test room VOC identification (By GC/MS).....	174
Table B-2 Target compounds monitored by PTR-MS (Ion Mass of 21).....	175
Table B-3 The schedule for the two-week test	179
Table B-4 Air change rate for different operation modes.....	179
Table C-1 COE building humidity load calculation	180
Table C-2 Determination of note A, B, and C in Table C-1	181

Nomenclature

A_{tol}	- Surface area of the pellets exposed to the bulk air, m^2 ;
c_g	- Gas phase concentration in the fixed bed, ppm or mg/m^3 (air);
$c_{air}^{m_{VOC}}$	- Gas phase VOC concentration (mass fraction), $kg(VOC)/kg(air)$;
c_p	- Gas phase concentration in the pores of sorbent pellet, ppm or mg/m^3 (air);
c_s	- Sorbed phase concentration, ppm or mg/m^3 (matrix);
d	- Diameter of the spherical sorbent pellet, m;
D_m	- Molecular diffusion coefficient, m^2/s ;
h	- Sorbent bed depth, m;
H	- Henry's law constant, m^3/m^3 ;
$k_{m,g \rightarrow s}$	- The VOC mass transfer coefficient between gas and solid, m/s;
$k_{m,g \rightarrow l}$	- The VOC mass transfer coefficient between gas and liquid, m/s;
K_a	- Air permeability through the media, s^{-1} ;
K_{ma}	- VOC partition coefficient between concentration in sorbent material and in gas (air), corresponding to c_m , kg/m^3 (material)/ (kg/m^3 (gas))
r_p	- Mean pore radius, cm;
r_s	- Radius of the sorbent pellet, m;
T	- Temperature, K;
M	- Molecular weight of target compound, g/mol;
Q	- Air flow rate through the sorbent bed, m^3/s ;
u_s	- Superficial velocity or face velocity (=flow rate/ bed cross section area), m/s;
u	- Interstitial velocity of sorbent bed, $u = u_s \epsilon_b$, m/s;
V_{bed}	- Volume of the sorbent fixed bed, m^3 ;
V_{REV}	- Representative elementary volume, m^3 ;
ϵ_b	- Sorbent bed porosity, m^3 (gas)/ m^3 (REV);

ε_p	- Sorbent pellet porosity, $\text{m}^3(\text{pore})/\text{m}^3(\text{sorbent})$;
σ	- Adsorption flux into sorbent pellet, kg/s ;
$\sigma_{g \rightarrow l}^{m_{\text{VOC},g}}$	- Exchange between gas and liquid, $\text{kg}/(\text{m}^3 \text{s})$;
$\sigma^{m_{\text{VOC},g}}$	- Any source or sink of gas phase VOC components, $\text{kg}/(\text{m}^3 \text{s})$;
$\rho_{\text{REV}}^{\text{VOC}}$	- Total VOC mass density per REV, kg/m^3 (REV);
$\rho_{\text{REV}}^{\text{VOC},g}$	- Gas phase VOC mass density per REV, kg/m^3 (REV);
$\rho_{\text{gas}}^{\text{VOC},g}$	- Intrinsic gas phase VOC mass density in gas, kg/m^3 (gas)
$\rho_{\text{REV}}^{\text{VOC},p}$	- Pore VOC mass density per REV, $\text{kg}/\text{m}^3_{\text{REV}}$;
$\rho_{\text{por}}^{\text{VOC},p}$	- Intrinsic gas phase VOC mass density in the pore, $\text{kg}/\text{m}^3_{\text{pore}}$;
$\rho_{\text{REV}}^{\text{VOC},s}$	- Sorbed phase VOC (in sorbent material) mass density per REV in chemisorption model, $\text{kg}/\text{m}^3_{\text{REV}}$;
$\rho_{\text{mat}}^{\text{VOC},s}$	- Intrinsic sorbed phase VOC mass density in sorbent material in chemisorption model, $\text{kg}/\text{m}^3_{\text{material}}$;
ρ_{air}	- Density of air, kg/m^3 ;
ρ_m	- Density of sorbent material, kg/m^3 ;
ρ_{VOC}	- Density of liquid VOC, kg/m^3 ;
ν	- Kinetic viscosity, m^2/s ;

Acronym

Term	Definition
ACH	- Air change per hour
CADR	- Clean air delivery rate
CFM	- Cubic feet per minute
DBAF	- Dynamic botanical air filtration
EPA	- Environmental protection agency
GC/MS	- Gas chromatography-mass spectrometry
HVAC	- Heating, ventilation, and air conditioning
HPLC	- High-performance liquid chromatography
IAQ	- Indoor air quality
LPM	- Liter per minute
ppb	- Part per billion
ppm	- Part per million
PTR-MS	- Proton transfer reaction - mass spectrometer
RH	- Relative humidity
SPE	- Single pass efficiency
VOC	- Volatile organic compound
VWC	- Volumetric water content

Acknowledgement

This research work was conducted at the Building Energy and Environmental Systems Laboratory (BEESL), Department of Mechanical and Aerospace Engineering at Syracuse University. It took about 4 years (2007~2011) to complete the research works and this dissertation. I would like to thank many people who helped to make it possible.

First of all and foremost, I would like to sincerely thank my supervisor, Dr. Jianshun S. Zhang. With his creative ideas, inspirations and enthusiasm, my PhD experience was productive and exciting. I benefited much from his rigorous scholarship, energetic and aspiring attitude and kind instruction, which impressed me so much. I express my greatest gratitude and respect for him.

Secondly, I would like to sincerely thank Dr. Dacheng Ren and his students, WenHsuan Huang and Geetika. The collaboration with them enriched my knowledge of microbiology. They provided me a lot of suggestions and help.

My further thanks should be given to my doctoral committee members: Dr. Utpal Roy, Dr. Thong Quoc Dang, Dr. Jeongmin Ahn, Dr. Suresh Santanam, and Dr. Dacheng Ren, for their time, helpful comments and insightful questions.

I would like to specially thank my M.S. supervisor, Dr. Junjie Liu from Tianjin University, China. Without his strong encouragement and support, I would not have been in United States for further study.

The members of BEESL group have contributed intensively to both my professional and personal life in Syracuse. I appreciate the help of Mr. Jim Smith. Without his help in building the experimental system, I could not have obtained so many valuable data. I also want to thank Ms. Beverly Guo, who gave me so much guide and assistance in VOC sampling and measurement. I also want to send my thanks to other colleagues and friends, who made my study and life in BEESL fruitful and enjoyable.

The financial supports through sponsored projects from New York State Energy Research and Development Authority (NYSERDA), Syracuse Center of Excellent (CoE), and Phytofilter technologies Inc. are also gratefully acknowledged.

Finally, I would like to thank my family. My wife, Jingjing Pei, who is also a member of BEESL, has helped me so much in the lab. My son, who came between us during the end of my PhD period, brought me so much more energy and enthusiasm for life! I also thank my parents and all other family members for their continuous encouragement and support.

Zhiqiang Wang

Syracuse, August, 2011

Chapter 1. Introduction

1.1 Background and Problem Definition

Indoor air quality (IAQ) is a very important issue today because it can significantly affect people's health, comfort, satisfaction and productivity. U.S. Environmental Protection Agency (EPA) studies of human exposure to air pollutants indicated that indoor air levels of many pollutants may be two to five times – and occasionally, more than 100 times – higher than outdoor level (U.S. EPA, 2000). In recent years, comparative risk studies performed by the EPA and science advisory board (SAB) have consistently ranked indoor air pollution among the top five environmental risks to public health. The importance of indoor air quality is also due to the amount of time that people spend indoors. People nowadays in industrialized countries spend more than 90% of their lifetimes indoors (NRC, 1981). In the United States, for example, every day an average working person spends 22 hours and 15 minutes indoors and one hour in cars or in other modes of transportation – another type of indoor environment (Meyer, 1983).

Three strategies for improving indoor air quality are commonly used: pollution source control, ventilation and air purification. Air purification, as an important part of integrated control strategies to improve IAQ in an energy-efficient and cost-effective manner, has received more and more attentions in recent years. In general, indoor air purification includes removal of particulates, bio-contaminants and gaseous contaminants. Volatile organic compounds (VOC), which belong to the

category of gaseous contaminants, represent a major class of indoor pollutants and can cause offensive odors, skin and membrane irritations and chronic health problems including cancer at elevated exposure level.

Presently, there is no single fully satisfactory method for VOC removal from indoor air due to the difficulties linked to the very low concentration ($\mu\text{g}/\text{m}^3$ range), diversity, and variability at which VOC are typically found in the indoor environment. Technologies used in current products for removing gaseous pollutants include: sorption by activated carbon, ultraviolet photocatalytic oxidization or UV-PCO, plasma ionization, ozone ionization, and bio-trickling filtration. Each of them has its own limitation. Sorption by activated carbon is a highly effective way to remove indoor VOC, but at the same time it has the problem of high pressure drop and does not perform well in removing lighter compound like formaldehyde. Some commercially available ionization and UV-PCO were found to have little effect in removing VOC (Chen et al., 2005). Plasma and ionization products emit ozone as a by-product, which could cause health concerns in rooms with low ventilation rates. In ozone ionization, residential ozone due to incomplete reaction is also of concern not only because O_3 is a harmful compound by itself, but also because of the harmful reaction byproducts it can produce. The bio-trickling filtration is usually applied in removing high concentration pollutants and specified for water soluble compounds, such as acetone and methanol.

Several studies have demonstrated the potential of biological methods to remove indoor VOC (Wolverton et al., 1984; Wolverton et al., 1989; Darlington et al., 2000;

Darlington et al., 2001; Chen et al., 2005; Orwell et al., 2006; Wood et al., 2006).

Nevertheless, there are very limited data available to understand the intrinsic removal mechanisms in these systems and there are apparent mismatches between experimental observations and theoretical results from transfer-based models (S. M. Zarook et al., 1996; Joseph S. Devinnny and J. Ramesh, 2005) on biological air treatment.

Common indoor plants may provide a valuable weapon in the fight against rising level of indoor air pollution. Wolverton et al (1984 and 1993) found that many decorative plants to be surprisingly useful in absorbing potentially harmful gases and cleaning the air inside modern buildings. However, there are very limited data demonstrating the effectiveness of botanical air filtration at realistic and full-scale ventilation conditions and inadequate understanding of the true removal mechanisms in these systems (Guieysse et al., 2008).

How well do house plants perform when they are used as cleaner for improving indoor air quality? In the 1990s, a published research indicated that potted plant can remove 9.2–90% formaldehyde, benzene or xylene in a small-sealed-chamber (Wolverton et al., 1993). The pollutant reduction by plant seems remarkable at first glance. Nevertheless, another study clearly explained that the pollutant reduction from above research was achieved by a high plant loading in chamber (approximately one plant per 0.5 m³), which is far in excess of what would be reasonable for indoor environment (Girman et al., 2009). To achieve the results equivalent to those of chamber studies, 680 plants would be needed for a 340 m³ (1500 ft³) resident house.

Therefore, the authors' conclusion was that indoor plants have little benefit for removing indoor air VOC in residential and commercial buildings.

Still, because all the studies reviewed by Girman were based on a single potted plant and most of these studies focused on the pollutant static removal by plant leaves, it is still too early to make the general statement that indoor plant is not efficient to remove indoor air VOC. One study has shown that three plants in a real office of average area 13 m² (volume 32.5 m³) were more than enough reduce TVOC by up to over 75% (indoor ambient level, without plants, ranging from 80 to 450 ppb), maintaining level at below 100 ppb, with or without air-conditioning (Wood et al., 2006). Studies have shown that VOC could become the potential carbon source for microbial communities in soil from the rhizosphere of plant (Wolverton et al., 1989; Fan et al., 1993; Holden et al., 1997; Owen et al., 2007). Moreover, assimilation and metabolism of formaldehyde by plant leaves appear unlikely to be of value for indoor air purification due to the low uptake rate (Schmitz et al., 2000). Especially, studies had demonstrated that it was the microorganisms of the potting mix that were the primary removal agents, with the plant mainly being responsible for maintaining root-zone microbial community (Orwell et al., 2004 & 2006). Therefore, if the polluted air also can be introduced into plant root system and degraded by the microorganisms there, the removal capacity of the plant would be higher than the potted plant with leaf effect only.

A dynamic botanical air filtration system based on the principle of absorption by wet-scrubbers, physical adsorption by activated carbon, and VOC consumption by

microbes in the plant's root system was developed (Figure 1-1). The system applies a mixture of activated carbon and porous shale pebbles as root bed of some special plants, which will have microbes growing in the root system. The filtration system is operated with periodical irrigation and airflow passing-through, therefore indoor gas pollutant, especially VOC will be adsorbed by the activated carbon sorbent, and the wet root bed will be a scrubber for formaldehyde, which is a water soluble compound. The adsorbed and/or absorbed organic compound can be degraded by the microorganisms, which will regenerate the sorbent based root bed. At the same time, the purified air will be returned to indoor environment to improve indoor air quality.

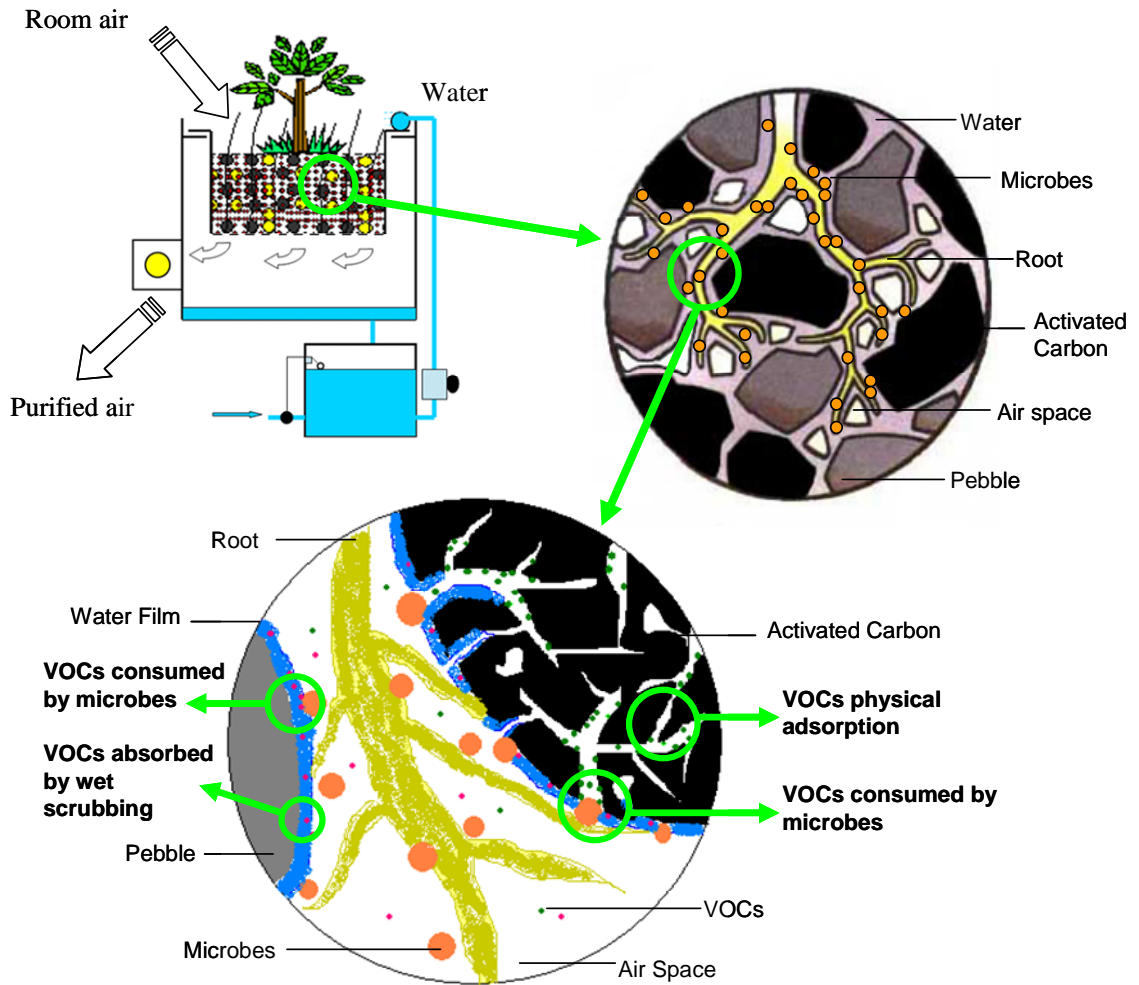


Figure 1-1 Main mechanisms of the air purification in this combined technique

In general, the VOC transport, adsorption/absorption and decomposition mechanism in the whole bio-filtration system may include:

VOC Mass Transfer between Pellets. In fixed-bed adsorption, in addition to convection by mean airflow, diffusion and mixing of adsorbates in fluid occur as a result of the adsorbate concentration gradients and the nonuniformity of fluid flow. This effect gives rise to the dispersion of adsorbates, which takes place along both the direction of main fluid flow (axial dispersion) and the direction transverse to the main

flow direction (radial dispersion).

VOC Interphase Mass Transfer. The transport of adsorbable compounds from the bulk of the gas phase to the external surface of adsorbent pellets (activated carbon) constitutes an important step in the overall uptake process.

VOC Absorption by Wet-scrubbing. In the context of air-pollution control, absorption involves the transfer of a gaseous pollutant from the air into a contacting liquid, such as water. The liquid serves as a solvent for the pollutant. Water film formed on the surface of pebbles or activated carbon pellets act as wet scrubbers, on which water soluble compounds like formaldehyde in the air can be absorbed.

VOC Physical Adsorption by Activated Carbon. Activated carbon is a widely used adsorbent to remove indoor air VOC. When indoor air passes through the sorbent bed, these water insoluble compounds like toluene will be physically adsorbed by activated carbon.

VOC Consumption by Microorganisms. The microbes formed by the root system of plant may consume the absorbed or adsorbed VOC as a food source. In this way, the saturated activated carbon might be reactivated, which means more VOC could be removed and there is no need to replace the activated carbon as long as the microorganisms remain active.

1.2 Objectives and Scopes

The primary goal of the present study was to improve the understanding of VOC removal mechanisms and factors impacting the performance of dynamic botanical air filtration system, and model the processes involved in the filter system, including VOC adsorption, absorption and their biodegradation by microorganisms in the plant root under realistic conditions. This was attempted through the following specific objectives:

1. Characterize the air flow, thermal and moisture conditions in the root bed and their effect on VOC removal efficiency, as well as indoor air temperature and humidity;
2. Study the influence of water content (WC) of sorbent material on the adsorption of water soluble/insoluble VOC, such as formaldehyde/toluene;
3. Conduct experimental investigation of the performance of the full-scale filter in laboratory condition (relatively high concentration level: 1~3 ppm), as well as in real-world condition (relatively low concentration level: 2~17 ppb);
4. Conduct further experimental investigation of VOC removal mechanisms and determination of bio-degradation rate by using a small-scale filter;
5. Develop a numerical model to simulate the processes with a combination of VOC adsorption, absorption and bio-degradation that exist in the filter system, and improve the filter design;

6. Use the model to propose an improved design of a sorbent biofilter system and predict potential energy benefit for commercial building due to the use of dynamic botanical air filtration system.

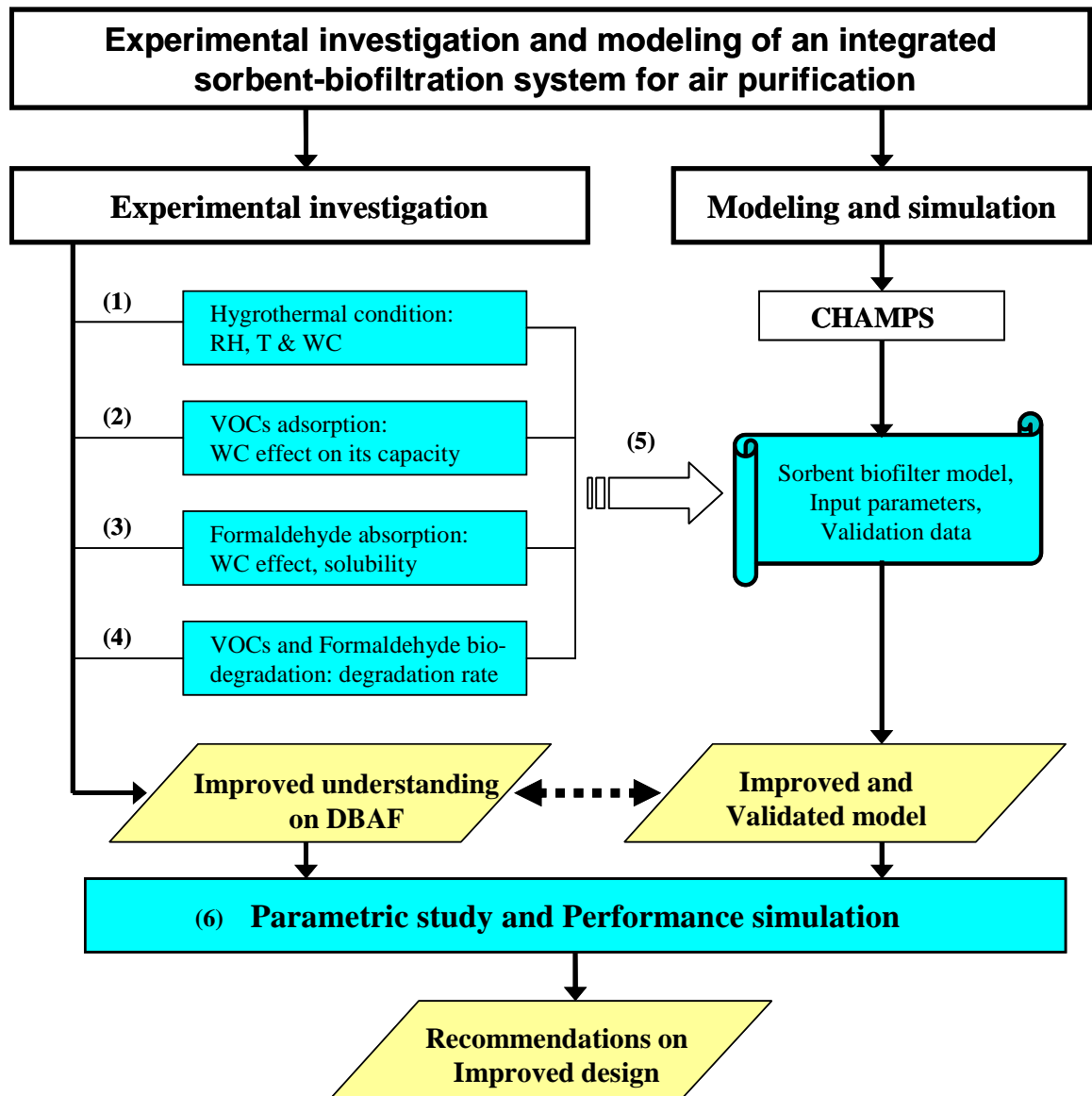


Figure 1-2 Overview of objectives and scopes

1.3 Dissertation Organization

The rest of this dissertation is organized as follows: in Chapter 2 the literature review of currently available methods of improving indoor air quality were first presented, including the principle and limitation. Later, it was focused on literature review of biofilter and indoor air quality and biofilter modeling. Major findings of literature review are summarized and further required research regarding the biofilter is also identified. Chapter 3 presents the performance testing and evaluation of dynamic botanical air filtration system at both laboratory relatively high pollutant concentration level (ppm) and real-world relatively low pollutant concentration level (ppb). In Chapter 4, results from laboratory experiments are discussed to improve the understanding of VOC removal mechanisms and determine the bio-degradation rate. Chapter 5 describes the numerical model development and implementation. Chapter 6 presents results from the energy simulation for a commercial building with the DBAF integrated under different U.S. climate conditions. Finally, Chapter 7 presents conclusions and recommendations for future work.

Dynamic botanical air filtration system research involves several disciplines, including botany, microbiology, chemical engineering as well as mechanical engineering. This study is primarily from a mechanical engineer's point of view. We hope that the techniques, tools, methods and results described here will help identify research opportunities as well as provide a solid foundation for future work in botanical air filter experimental investigation and numerical modeling.

Chapter 2. Literature Review

2.1 Introduction

As indoor air quality plays a more and more important role in people's life, the improvement of indoor air quality becomes one of the critical concerns in buildings. It is necessary to conduct a literature review to list all the current available methods of improving indoor air quality, compare the difference of their principle, and find out the limitation of each method. Moreover, the major objectives of the this study was to improve the understanding of VOC removal mechanisms of dynamic botanical air filtration system and model the processes involved in the filter system. It is necessary to review the research that has been done in terms of biofilter experimental investigation and modeling. It is also necessary to summarize the achievement and limitations of studies that have been done and present the further required researches regarding the botanical air filtration.

The objectives of this chapter were to: 1) review the methods of improving indoor air quality; 2) review the studies related to bio-filter and indoor air quality; 3) review the studies of bio-filter modeling.

2.2 Methods of Improving Indoor Air Quality

Current solutions to poor indoor air quality include removing the pollutant sources, increasing ventilation rates, and cleaning the indoor air (US EPA). Although certain furniture or appliance manufacturers are already phasing out the use of formaldehyde, removing the pollutant sources is only possible when these are known and control is technically or economically feasible, which is actually seldom the case. New substances are constantly detected and classified as hazardous and many sources can release compounds for years. In addition, there is fear that many air pollutants are still to be discovered (Otake et al., 2001; Carlsson et al., 2000; Muir and Howard, 2006) and preventive approaches might therefore be needed to ensure indoor air contaminants are maintained below satisfactory levels at all times. Natural ventilation is the easiest alternative but it is often not possible because of outdoor weather, external pollution conditions (Ekberg, 1994; Daisey et al., 1994), or issues of security, safety in high buildings, climate control and noise, or being not easy for building internal zone to realize. Periodical air refreshing is often not efficient because many indoor air pollutants are constantly released. Hence, forced ventilation is still one of the most common methods used for air treatment (Wargoeki et al., 2002). The improvement of indoor air quality and energy savings are encouraged in the European Union (EU) and by movements such as the “Green Building” (US Green Building Council), which means that forced ventilation should be reduced at the same time as IAQ should be improved. Consequently, there are few alternatives left than purifying

the air inside the building.

Existing methods for air purification include combinations of air filtration, ionization, activated carbon adsorption, ozonation, and photocatalysis (Table 2-1). These processes can be integrated into the central ventilation system (in duct) or used in portable air purifiers (or air cleaner) designed for limited spaces. Efficient strategies for particle removal are now well established and include combinations of filtration and electrostatic precipitation. The situation is still very different for VOC removal. For instance, in a study conducted to compare several commercial air purifiers, Shaugnessy et al. (1994) concluded that, although high efficiency particles air filters (HEPA filters) and electrostatic precipitators were highly efficient for particle removal, none of the techniques tested (HEPA filtration, electrostatic precipitation, ionization, ozonation, activated carbon adsorption) could significantly remove formaldehyde.

A similar study was recently conducted to compare 15 air cleaners with a mixture of 16 representative VOC (Chen et al., 2005). The technologies evaluated included sorption filtration, ultraviolet-photocatalytic oxidation (UVPCO), ozone oxidation, air ionization and a botanical purifier prototype (where contaminated air was blown through the rhizosphere of plants and contaminants were in principle removed by soil microorganisms, the plants or their enzymes through various mechanisms). The authors concluded that only the botanical system significantly removed volatile organic compounds, such as formaldehyde, in contrast to the

Table 2-1 Current and emerging indoor air treatment methods, principle and limitations

Method	Principle	Limitation
Current methods		
Filtration	Air is passed through a fibrous material (often coated with a viscous substance)	<ul style="list-style-type: none"> • Not work for gaseous pollutant • Pressure drop increases as they become saturated. • Microorganisms can also develop in filters • Particles reemission might occur.
Electrostatic precipitator with ionization	An electric field is generated to trap charged particles	<ul style="list-style-type: none"> • Electrostatic precipitators are often combined with ion • can generate hazardous charged particles
Adsorption	Air pollutants are adsorbed onto porous media, such as activated carbon or zeolites	<ul style="list-style-type: none"> • There is a potential risk of pollutant reemission. • High pressure drop
Ozonation	Ozone is generated to oxidize pollutants	<ul style="list-style-type: none"> • Only remove some fumes and certain gaseous pollutants • Might generate unhealthy ozone and degradation products • Ozone-based purifiers are not recommended by the American Lung Association.
Photolysis	High energy ultra violet radiation oxidizes air pollutants and kills pathogens.	<ul style="list-style-type: none"> • can only remove some fumes and some gaseous pollutants • might release toxic photoproducts. • Accidental exposure to UV light is harmful

Photocatalysis	High energy ultra violet radiation is used in combination with a photocatalyst (TiO ₂) to generate highly reactive hydroxyl radicals that can oxidize most pollutants and kill pathogens.	<ul style="list-style-type: none"> • UV irradiation is energy consuming • Suitable for a broad range of organic pollutants.
<hr/>		
Emerging methods		
Membrane separation	Pollutants are passed through a membrane into another fluid by affinity separation	<ul style="list-style-type: none"> • This method is normally recommended for highly loaded streams and has not yet been proven at low VOC levels • If the separated VOC are not reused, membrane filtration must be completed with a destruction step.
Enzymatic oxidation	Air pollutants are transferred into an aqueous phase where they are degraded by suitable enzymes	<ul style="list-style-type: none"> • Little information is however available concerning the efficiency of the commercial system • New enzymes must be supplied periodically.
Botanical purification	Air is passed through a planted soil or directly on the plants. The contaminants are then degraded by microorganisms and/or plants.	<ul style="list-style-type: none"> • The precise mechanisms being unclear • Although the efficiency of botanical purification has not been fully proven, a number of devices have been patented and several commercial products are available.
Biofilters and biotrickling filter	Air is passed through a packed bed of a solid support colonized by attached microorganisms that biodegrade the VOC	<ul style="list-style-type: none"> • In one configuration, air was purified through lava rocks covered with a geotextile cloth supporting mosses (Darlington et al., 2001).

adsorption processes that generally only satisfactorily removed the poorly soluble contaminants.

2.3 Biofilter and Indoor Air Quality

Several studies have demonstrated the potential of biological methods to remove indoor VOC (Wolverton et al., 1984; Wolverton et al., 1989; Darlington et al., 2000; Darlington et al., 2001; Chen et al., 2005; Orwell et al., 2006; Wood et al., 2006). Nevertheless, there is little data available on the biological removal of VOC from indoor air and the removal mechanisms were rarely studied. In a pioneer study supported by the NASA, Wolverton and co-authors demonstrated the potential of plants (and their rhizosphere) to remove indoor VOC in sealed chamber. In their earliest study (Wolverton et al., 1984), the authors found that several plants could remove formaldehyde at 19,000–46,000 $\mu\text{g m}^{-3}$ to levels lower than 2500 $\mu\text{g m}^{-3}$ (detection limit) in 24 h. Similar studies were conducted with benzene and trichloroethylene at more relevant concentrations of 325–2190 $\mu\text{g m}^{-3}$ (Wolverton et al., 1989). It was then found that the 8 plants tested could remove benzene by 47–90% in 24 h compared to 5–10% in the control tests, and that the rhizosphere zone was the most effective area for removal.

Orwell et al. (2004) later investigated the potential of indoor plants for removing benzene in sealed chamber (0.216m³) and found that microorganisms of the plant

rhizosphere were mainly responsible for benzene removal ($40\text{--}80\text{ mg m}^{-3}\text{ d}^{-1}$). These results were obtained at high initial benzene concentrations ($81,000\text{--}163,000\text{ }\mu\text{g m}^{-3}$) and benzene removal rate increased linearly with the dose concentration, suggesting the system might be inefficient under typical indoor air conditions. However, the same team more recently demonstrated that plants significantly reduced toluene and xylene at indoor air concentrations of $768\text{--}887\text{ }\mu\text{g m}^{-3}$ (Orwell et al., 2006) and even the TVOC concentration in office buildings during field testing at real conditions (Wood et al., 2006). Unfortunately, the divergences in toluene removal reported in the studies of Chen et al. (2005) and Orwell et al. (2006) cannot be explained, especially as the prototype used in the earlier study was not fully described. Many parameters such as the interfacial areas, the moisture content, and the type (hydrophobicity) of the biomass used can influence pollutant removal in biological purifiers.

Therefore, there is a need for a more coordinated research in the area. Various botanical purifiers have also been patented (i.e. US5407470, US5277877) but such devices have not reached a broad market and no data on pollutant removal at relevant conditions is available. Research on the development of a commercial biological purifier has been carried out at the University of Guelph, Canada (Darlington et al., 2000; Air Quality Solution Ltd). In the first configuration, air was purified through lava rocks covered with a geotextile cloth supporting mosses (Darlington et al., 2001). This device was operated at relevant influent levels equal to or lower than $300\text{ }\mu\text{g m}^{-3}$ and displayed a purification efficiency of 30% at the lowest air flow treated. Water

was also added to the filter to compensate for water losses through evaporation (approx. 20 L d⁻¹ in 120 m² and 640 m³ room). In the second configuration, disclosed in US patent 6,676,091 from the same author, air is forced directly through a vertical (or slightly inclined) porous material serving as support for hydroponic plants which its main purpose is to support the activity of pollutants degrading microorganisms in the rhizosphere.

From the studies herein presented, it appears that the role of plants in botanical purifier is often suspected to support a microbial activity that is responsible for pollutants removal. Direct pollutants accumulation or degradation by plants is however known to occur during phytoremediation of contaminated soils (Newman and Reynolds, 2004) and the ability of plant leaves to directly take up and remove pollutants during air treatment is still debated (Wolverton et al., 1984; Schmitz et al., 2000; Schöffner et al., 2002). A recent study has suggested that bacteria growing on plant leaves could also contribute to VOC biodegradation (Sandhu et al., 2007). More generally, there is growing evidence of the complexity, and importance of interactions between plants and bacteria (Dudler and Eberl, 2006) and research in this area is highly important for IAQ. There is a lack of peer-reviewed data available in the literature and an urgent need to improve our understanding of the fundamental mechanisms of VOC uptake or release by plants and their microbial hosts (Kesselmeier and Staudt, 1999). The following discussion will therefore focus on the more established microbial degradation mechanisms.

2.3.1 Biodegradability of VOC

The biological treatment of organic compounds is based upon the capability of microorganisms to use these molecules as sources of carbon, nutrients and/or energy or to degrade them cometabolically using unspecific enzymes. The intrinsic biodegradability of an organic compound depends on many factors such as its hydrophobicity to the microbial population, the most soluble being generally the most biodegradable, or its toxicity. Toxicity effects, which sometimes limit the biological treatment of industrial air, are likely not a problem at the concentrations found in indoor air (Guieysse et al., 2008) and this will not be discussed further in this review.

Many VOC are rather small molecules that are moderately soluble and in fact, are biodegradable (Table 2-2) although certain xenobiotic compounds (Guieysse et al., 2008), such as chlorinated compounds (i.e. tetrachloroethylene), may be recalcitrant. Given the high number of VOC simultaneous found in indoor air, and the huge variations in structures and properties, a biological process suitable for indoor air treatment should rely on diverse, versatile and adaptive microbial communities to ensure all pollutants are removed. This can be achieved in fixed biofilm based reactors where high microbial diversity and cell proximity favour cellular exchanges (Molin and Tolker-Nielsen, 2003; Singh et al., 2006), acclimation (long cell residence

Table 2-2 Biodegradability of typical indoor VOC

Substance	Biodegradability ^a	Henry's law constants		Biological treatment			
		H^b (atm m ³ mol ⁻¹)	References	Inlet concentration ^c (mg m ⁻³)	Removal Efficiency (%)	Biological treatment ^d	References
Acetaldehyde (Ethanal; CH ₃ CHO)	3	5.88 10 ⁻⁵	US EPA (1982)	18.1 – 180.1 ^e	40 - 80	B	Mohd Adly et al. (2001)
		5.88 10 ⁻⁵	Zhou and Mopper (1990)				
		7.69 10 ⁻⁵	Sander (1999)				
Benzene (C ₆ H ₆)	2	6.25 10 ⁻³	Staudinger and Roberts	1.6 ^e	9 – 77	B	Ergas et al. (1992)
		5.55 10 ⁻³	(1996)	0.32 – 1.28 ^e	50 to 60	BF	Wolverton et al. (1989)
		4.76 10 ⁻³	US EPA (1982)	0.048 – 0.48 ^e	20	BF	Darlington (2004)
			Sander (1999)				
Formaldehyde (Methanal; HCHO)	3	3.33 10 ⁻⁷	Sander (1999)	0.12 – 0.49 ^e	50 to 60	BF	Wolverton et al. (1989)
		3.23 10 ⁻⁷	Zhou and Mopper (1990)	0.018 – 0.18 ^e	90	BF	Darlington (2004)
		3.13 10 ⁻⁷	Staudinger and Roberts (1996)				
Naphthalene (C ₁₀ H ₈)	1	4.76 10 ⁻⁴	Sander (1999)	0.494 ^e	75	TPPB	Macleod and Daugulis

		$4.76 \cdot 10^{-4}$	US EPA (1982)				(2003)
Tetrachlorethylene	1	$2.78 \cdot 10^{-2}$	US EPA (1982)	0.678^e	0 - 8	B	Ergas et al. (1992)
(Tetrachloroethene; C_2Cl_4)		$1.69 \cdot 10^{-2}$	Staudinger and Roberts (1996)	$0.36 - 4.80^e$		BTr	Torres et al. (1996)
		$1.56 \cdot 10^{-2}$	Sander (1999)				
Toluene	2	$6.67 \cdot 10^{-3}$	US EPA (1982)	1.88^e	14 - 78	B	Ergas et al. (1992)
(Methylbenzene; $C_6H_5CH_3$)		$6.67 \cdot 10^{-3}$	Staudinger and Roberts (1996)	753.5 $0.226 - 0.301^e$	50	MS BF	Ergas et al. (1999) Darlington et al. (2001)
				$0.057 - 0.57^e$		BF	Darlington (2004)
Trichlorethylene	1	$9.09 \cdot 10^{-3}$	Sander (1999)	107.44	30	MS	Parvatiyar et al. (1996)
(Trichloroethene; C_2HCl_3)		$1.12 \cdot 10^{-2}$	US EPA (1982)	$0.081 - 0.81^e$	0	BF	Darlington (2004)
		$1.00 \cdot 10^{-2}$	Staudinger and Roberts (1996)	$0.054 - 2.149^e$ $0.01 - 0.04^e$	50 to 60 0 - 24	BF BTr	Wolverton et al. (1989) Torre et al. (1996)

Note: ^a1=low biodegradability, 2=moderate biodegradability, 3=good biodegradability (Shareefdeen and Singh, 2005; Deviny et al., 1999).

^b At standard conditions.

^c Concentrations close to the average concentration observed in indoor air.

^d B = Biofiltration; MS = Membrane Separation; BF = Botanical Filter; TPPB = Two-Phase Partitioning Bioreactor; BTr = Biotrickling Filter.

^e In mixture with other compounds

time) and synergetic effects at various growth conditions by the establishment of substrate concentration gradients through the biofilm (Beveridge et al., 1997; Marshall, 1994). Completing or combining biodegradation with a physicochemical post-treatment is also possible to ensure the complete removal of all pollutants.

Finally, great variations in total and individual pollutant concentrations leading, for instance, to long periods of time when a given compound is not found in the indoor air could lead to permanent or momentary losses in catabolic ability. Such effects need to be further studied and possibly prevented as discussed below.

2.3.2 Influence of Low Concentration on Biomass Productivity and Transfer Rates

During the biodegradation process, the concentration of an organic pollutant in the micro-environment where the microorganisms are found has a profound impact on microbial activity and ultimately on the pollutant removal rate. At reasonably high substrate concentrations, the organic pollutant can be metabolized and used to synthesize more biomass in a process that self-regenerates the biocatalyst. When the concentration is decreased further, a critical level is reached below which new cells are no longer produced. It is crucial to compare the low concentrations at which indoor VOC are typically found with known threshold for microbial growth and biodegradation.

Guieysse et al.(2008) conducted an analysis to compare typical toluene indoor concentration with known threshold for microbial growth and biodegradation. Toluene indoor air concentrations of 0.58–17 $\mu\text{g m}^{-3}$ have been reported in Californian office buildings (Daisey et al., 1994). Assuming toluene must first transfer into an aqueous phase before being biodegraded, the maximum aqueous toluene concentration (C_{aq}^*) at which microorganisms will be exposed to can be calculated from the Henry's law constant (H) coefficient:

$$C_{aq}^* = \frac{P_i}{H_i} \quad (2-1)$$

where P_i is the partial pressure of the target contaminant in the gas phase and H_i is its constant coefficient of Henry's law. For toluene ($H=6.67 \cdot 10^{-3} \text{ atm m}^3 \text{ mol}^{-1}$; Table 2-2), this will result in a C_{aq}^* of 2–60 ng L^{-1} at normal conditions of temperature and pressure. If toluene is removed by 90%, microorganisms would actually be exposed to concentrations of 0.2– 6 ng L^{-1} (at continuous treatment at a steady state). At such concentration, toluene can be reasonably considered as the limiting substrate if it is the only carbon source available. By comparison, the threshold growth concentration of bacteria from drinking-water biofilm has been estimated to about 0.1 $\mu\text{g L}^{-1}$ (Van der Kooij et al., 1995) which is in the same range of reported toluene mineralization at aqueous concentrations of 0.9 $\mu\text{g L}^{-1}$ with active bacteria (Roch and Alexander, 1997). Hence, from the data currently available, it seems unlikely that indoor air VOC can support growth.

In the same study, from other side, the authors (Guieysse et al., 2008) represented that the specific cell production rate at typical toluene indoor concentrations should range from 5×10^{-5} – $1.7 \times 10^{-6} \text{ h}^{-1}$, which are far below the death cells coefficients for *Pseudomonas putida* F1 during the degradation of toluene (0.06 h^{-1} ; Alagappan and Cowan, 2003). Therefore, in this particular situation, neither would pollutant supply meet maintenance requirements nor would the specific growth rate meet the cellular decay rate.

Benoit et al., (2008) also mentioned that indoor air biological treatment will likely require the development of specific methods to provide and maintain a suitable catabolic activity. First, due to the complexity and variability of indoor air, an inoculum that possesses the suitable catabolic ability might be difficult to obtain. These microorganisms would also likely need to be pre-cultivated at higher VOC concentration to obtain a significant cell number in a relative short time, which might impair their ability to take up substrates at trace levels (microorganisms can lose selective traits when the corresponding selection pressure is released). Second, maintaining catabolic activity (and not only cell mass or cellular activity) could be challenging as microorganisms can lose their ability to biodegrade certain substrates when deprived from them during long periods of time. Finally, even at conditions when suitable degradation-enzymes are expressed, microbial activity must be capable to reduce the contaminant at concentration low enough to permit significant mass transfer. Roch and Alexander (1997) showed toluene mineralization at $0.9 \mu\text{g L}^{-1}$ but

the pollutant still remained at 79 ng L^{-1} after 8 days of incubation. Similar findings were reported by Pahm and Alexander (1993) when studying the biodegradation of p-nitrophenol at trace concentration although addition of a secondary carbon source was capable to trigger pollutant removal at concentrations of $1 \text{ } \mu\text{g L}^{-1}$. However, the feasibility of removing estrogens at 100 ng L^{-1} to below 2.58 ng L^{-1} (detection limit) with pure laccase from *T. versicolor* was recently demonstrated (Auriol et al., 2007), showing biological systems should be able to perform at indoor air concentrations.

Clearly, the development of biological methods for indoor air filtration faces several challenges and requires more research on the microbial mechanisms of acclimation, survival, substrate recognition, accumulation and uptake at trace concentration. Low concentrations are common in the environment and certain microorganisms have developed original survival strategies at such conditions by for instance accumulating limiting substrate before starting to growth (Singh et al., 2006). New models to correlate growth with substrate concentration are therefore needed at trace concentration, as suggested by Butterfield et al. (2002) in a study on drinking-water biofilm formation at carbon-limited conditions (2 mg L^{-1}).

The simultaneous presence of many contaminants in indoor air might sustain microbial growth or, at least, induce pollutant mineralization, as suggested by the experience of Pahm and Alexander (1993) described above. In addition, certain microorganisms are able to grow both heterotrophically and autotrophically (Larimer et al., 2003) or on myriads of different organic compounds (Chain et al., 2006). Such

metabolic versatility would give obvious advantages at conditions where numerous potential carbon and energy sources are simultaneously found at very low concentrations and would greatly enhance the treatment of indoor air. The question is therefore not if microbial growth would occur, but if it will cause VOC reduction. Wood et al. (2006) suggested that a TVOC concentration of 100 ppb was sufficient to induce a biological response that could reduce the TVOC concentration up to 75%.

Several authors have also challenged the mass transfer and microbial uptake theories used to predict the effect of substrate concentration in biological purifiers. Active transfer by enzymatic transformation has for instance been reported and mechanisms of direct uptake at the air-cell interface have been suggested. For instance, Miller and Allen (2005) reported that direct pollutant diffusion through the aqueous layer surrounding the biofilm could not explain the surprisingly high performances of biological systems treating the highly hydrophobic alpha-pinene. Likewise, it has been suggested that the aerial mycelia of fungi, which are in direct contact with the gas phase, might promote the direct uptake of VOC from the gas phase. This uptake is faster than if a flat biofilm of bacteria directly contacts the gas phase because of a high gas–mycelium interfacial area of the fungal mat and the highly hydrophobic nature of the fungal cell wall (Arriaga and Revah, 2005; Kennes and Veiga, 2004; Van Groenestijn and Kraakman, 2005; Vergara et al., 2006).

2.3.3 Impact of Design on Purification Efficiency

It is not only the single pass purification efficiency of the biofiltration device but the overall purification capacity that is important, explaining why the concept of clean air delivery rate (CADR, the amount of purified air delivered per unit or time) was introduced to evaluate and compare the various devices proposed for air removal (Shaughnessy and Sextro, 2006). Interestingly, at equivalent CADR, purification devices with high single pass efficiencies should be preferred because of their lower energy requirement (lower required flow rate).

Models are used to estimate the single pass efficiency of purification devices in sealed chamber test where pollutant are introduced at a certain amount but where there is no production (Chen et al., 2005). Thus, Wolverton et al. (1989) reported a decreased benzene concentration from 765 to 78 $\mu\text{g m}^{-3}$ in 24 h in a sealed chamber containing a plant, which resulted in a coefficient which is composed of the pollutant leakage rate from the system (Q/V) and the pollutant removal in the air purifier ($\text{CADR}/V = \text{purifier refreshment capacity}$). The same author conducted a leak experiment which calculating the leak contribution to approx. 0.01 h^{-1} . Hence, the botanical purifier used in this study generated an amount of purified air equivalent to 0.09 room volume per hour (CADR of $0.075 \text{ m}^3 \text{ h}^{-1}$) and would not significantly improve IAQ at realistic conditions. Low refreshment rates of $0.02\text{--}0.3 \text{ h}^{-1}$ were also achieved by Orwell et al. (2006) in sealed-chambers containing potted plants and initially supplied with 768–886 $\mu\text{g m}^{-3}$ of m-xylene or toluene, based on VOC

exponential removal rate constants of $0.52\text{--}7.44\text{ d}^{-1}$. Likewise, Chen et al. (2005) achieved the highest CADR of $8.3\text{ m}^3\text{ h}^{-1}$ (refreshment rate of 0.15 h^{-1}) with the botanical purifier compared to values above $200\text{ m}^3\text{ h}^{-1}$ with other portable devices. Despite this, a significant TVOC removal was recorded when using potted plants during field testing in office (Wood et al., 2006) and even if such results should be reproduced at better controlled conditions, they might indicate that our current evaluation models are inadequate.

2.3.4 Design of Biological Purifiers

Common biological processes for VOC abatement include bio-scrubbers, biotrickling filter, and bio-filters (Iranpour et al., 2005; Burgess et al., 2001; Delhoménie and Heitz, 2005; Revah and Morgan- Sagastume, 2005). In bio-scrubbers, the air is washed with an aqueous phase into which the pollutants transfer, and the aqueous phase is transferred into a bioreactor where the pollutants are biodegraded. In Bio-trickling filters, microorganisms are grown on an inert material (plastics resins, ceramics etc). An aqueous solution containing the nutrients required for microbial growth is continuously distributed and recirculated at the top of the reactor and percolates by gravity, thus covering the biofilm with an aqueous layer. Contaminated air is introduced as co- or counter current and the contaminants diffuse into the aqueous phase where they are biodegraded. The purpose of the packing

material is to facilitate the gas and liquid flows and enhance gas/liquid contact, to offer a surface for microbial growth, and to resist crushing and compaction. In biofilters, air is passed through a moist porous material which supports microbial growth. Water remains within the packing material and is added intermittently to maintain humidity and microbial viability. The packing material is generally a natural material (peat, compost, wood shavings, etc.) which is biodegradable and provides nutrients to the microorganisms although intensive research has been done to use synthetic materials (Jin et al., 2006).

An additional common limitation to all biological air treatment processes is the need to transfer contaminants into an aqueous phase prior to their biodegradation, which is especially problematic in the case of hydrophobic pollutants such as hexane. The addition of a hydrophobic organic phase into the bioreactors (two liquid phase partitioning bioreactors) could significantly enhance the transfer of the pollutants to the microorganisms and thereby, their removal (Muñoz et al., 2007). Other possibilities include the addition of activated carbon or other adsorbents in combination with the biological system. Such approaches should be investigated in the case of indoor air treatment as they could also concentrate the contaminants to levels suitable for growth.

2.3.5 Humidification Effect and Biohazards

Since biological purifiers are typically saturated with water and since indoor air treatment requires high flows, indoor biological purification might increase the moisture content in the room or building where it is used. This beneficial effect when indoor air is too dry (moisture contents of 30–60% are generally recommended for comfort) could also trigger to the excessive growth of fungi with negative impact on IAQ (Schleibinger et al., 2004), although these effects are still uncertain (Robbins et al., 2000; Pasanen, 2001). Darlington et al. (2000) for instance reported that the use of an indoor biological purifier significantly increased the concentrations of total suspended spores, although these values were similar to concentrations found in flats containing house plants, and still remained within healthy levels (100–200 CFU m⁻³). In addition, none of the 17 fungal species identified was known to be pathogenic. Likewise, Ottengraf and Konings (1991) reported that the concentration of microbial germs (mainly bacteria) in the outlet of full scale industrial biofilters was within the range of typical indoor air concentration, and only slightly higher than typical outdoor air concentrations, which was more recently confirmed by Zilli et al. (2005). There is however too little data available and the potential release of microorganisms from indoor biological purifiers (especially in the case of faulty equipment or accidents) should be better studied and prevented if necessary.

2.3.6 Summary

A review of the existing research in regards to biological and engineering constrains reveals numerous problems that must be solved before biologically-based air purifiers can be properly designed and implemented.

Firstly, our current knowledge on microbial kinetics and the thresholds for substrate uptake, consumption and gene expression raise serious doubt concerning the feasibility of microbial degradation of VOC at indoor air concentrations. There is experimental evidence that VOC can be biologically removed at indoor concentration even if the precise mechanisms are unknown. This apparent contradiction is perhaps explained by the fact that our current knowledge was derived from studies conducted at conditions (single strains with single substrate at high concentration) irrelevant to the indoor air environment (diverse communities exposed to multiple substrates at low concentrations and direct pollutant uptake). Clearly, there is a need for fundamental research at conditions relevant to indoor.

Secondly, the design of biological air purifiers requires the development of new technologies for highly efficient pollutant transfer (from air to the biological catalyst) in order to allow high volumetric treatment flows while maintaining high treatment efficiencies. Current biological purifiers have shown some potential but are all limited by their low treatment capacity.

Finally, as IAQ is linked to the presence of pollutants other than VOC and as

biological methods might always be limited in the cases of poorly soluble or recalcitrant substances, there is a need to develop combined physicochemical-biological methods.

2.4 Biofilter Modeling

Many investigators have created mathematical models of biofilters and biotrickling filters in their efforts to understand and improve reactor performance.

2.4.1 Biofilter and Biotrickling Filter Mechanics

Among modelers there is general agreement on the mechanisms of biofilters and biotrickling filters (Devinny and Ramesh, 2005). Contaminants are carried into the biofilter by the air at such rates that the flow is presumed to be laminar, although dispersion occurs because of the tortuosity of the pores in the porous packing. As the air passes through the packing, contaminants are transferred from the air to the water in the biofilm. The contaminants diffuse into the depths of the biofilm, and microorganisms in the biofilm absorb the contaminants and biodegrade them. Contaminants may also be adsorbed at the surface of the packing. The great majority of reactors utilize aerobic respiration, so that oxygen and nutrients must also dissolve in the water or biofilm and diffuse to the microorganisms.

2.4.2 Air Flow

Most biofilter or biotrickling filter models assume that air flow within the reactor can be adequately modeled as “plug flow”. Under these conditions, the effects of advection can be modeled in one dimension as:

$$\left[\frac{dC_{air}}{dt} \right]_{adv} = -V \frac{\partial C_{air}}{\partial z} \quad (2-2)$$

where t is time, C_{air} the concentration of the contaminant in the air, V the interstitial flow velocity, and z is the axial dimension of the biofilter. Interstitial flow velocity is higher than approach velocity.

$$V = \frac{V_A}{\theta} \quad (2-3)$$

where V_A is the approach velocity (face velocity), θ is the bed porosity.

Because there are typically no radial gradients in concentration, radial dispersion has no effect and is neglected. Axial gradients may be substantial, however, a few models have considered the possibility of axial dispersion. Hodge and Devinny (1995) produced such a model that modeled dispersion in the form

$$\left[\frac{dC_{air}}{dz} \right]_{disp} = D_f \frac{\partial^2 C_{air}}{\partial z^2} \quad (2-4)$$

where D_f is the dispersion coefficient. However, both calculations and experiment indicated that axial dispersion was negligible except for biofilters operating at high flow rates—with empty bed detention times of a few seconds (Hodge and Devinny,

1997). While dispersion occurs as a result of molecular diffusion in biofilters and biotrickling filters the dominant process is dispersion resulting from the tortuosity of flow.

2.4.3 Phase Transfer

Transfer of a contaminant from a gas to a stagnant liquid or a biofilm can be viewed as limited by diffusion resistance within a laminar layer of gas near the interface and by resistance within the liquid or biofilm. Water within the biofilm is presumed to be stagnant, so that molecular diffusion is the only transport mechanism. It has been generally accepted that phase transfer is limited by diffusion in the water phase: the pores are relatively small, dispersion caused by advection tends to mix the gas phase, and molecular diffusion constants in water are on the order of 10^4 times lower than those in air (concentrations, and therefore concentration gradients, are generally higher in the biofilm, but usually only by one order of magnitude). Typically, modelers presume that the concentration at the surface of the biofilm is determined by Henry's Law equilibrium with the concentration of contaminant in the bulk air phase, and that the flux of contaminant into the biofilm is controlled by diffusion resistance in the biofilm at the surface.

$$J_{bf} = D_w \left[\frac{\partial C_{bf}}{\partial x} \right]_{x=0} \quad (2-5)$$

where J_{bf} is the flux of contaminant per unit of surface area, D_w is the diffusion constant in the water film, C_{bf} the concentration of contaminant in the biofilm, and x is the coordinate perpendicular to the biofilm surface, which is zero at the air–biofilm interface. In a biotrickling filter, it is typical that transfer in the flowing water layer is slower than transport in the air and faster than in the biofilm. The same formulation is used for transfer from water to the biofilm, and a parallel form is used for transfer from the air to the water. However, some investigators have observed mass transfer resistance at the interface. This is most likely to occur where contaminant solubility is high and biodegradation is rapid. It is less likely in a biofilter treating volatile organic compounds, but Kim and Deshusses (2003) observed strong external mass transfer limitation in laboratory and full-scale biotrickling filters treating hydrogen sulfide. In such cases, models presume that transfer is limited by diffusion resistance in a laminar layer of gas at the surface, and transfer occurs at a rate determined by the degree to which the gas–liquid interface of the biofilm is below saturation:

$$J_{bf} = k_{air-bf} \left[\frac{C_{air}}{H} - C_{bf} \right] \quad (2-6)$$

where k_{air-bf} is the gas transfer coefficient and H is the Henry's Law constant for the contaminant. Li et al.(2003) further approximated the gas transfer coefficient for spherical packing particles as:

$$k_{air-bf} = \frac{D_{air}}{2R_p} \left[2 + 1.1 \text{Re}^{0.6} \text{Sc}^{0.33} \right] \quad (2-7)$$

where D_{air} is the gas-phase diffusion constant, R_p the particle, Re the Reynolds number, and Sc is the Schmidt number.

2.4.4 Diffusion within the Bio-film

Diffusion of the contaminant into the biofilm is presumed to follow Fick's Law:

$$\left[\frac{\partial C_{bf}}{\partial t} \right]_{diff} = D_{bf} \frac{\partial^2 C_{bf}}{\partial x^2} \quad (2-8)$$

where D_w is the molecular diffusion constant of the contaminant in water. While there is general agreement on this form of the equation, there is less certainty about the appropriate values for the diffusion constant. Molecular diffusion constants have been measured in pure water for most compounds, but diffusion within biofilms may be different. The abundance of cells and exuded polysaccharides reduces the cross-section of water actually available for diffusion and restricts the contaminant to diffusion along tortuous pathways. Some investigators have used the empirical equation developed by Fan et al.(1990) that relates the diffusion coefficient in the biofilm to the diffusion coefficient measured in water and the total biomass density in the film (in g/L):

$$D_{bf} = D_w \left[1 - \frac{0.43 X^{0.92}}{11.19 + 0.27 X^{0.99}} \right] \quad (2-9)$$

Miller and Allen noted that additional complications are possible. In biofiltration

of α -pinene, they showed that biological materials in the biofilm would adsorb the contaminant, causing an initial delay in transport but not affecting the steady-state rates of transport. They also found that in biological films, but not in abiotic films, enzymatic reactions rapidly convert α -pinene to a secondary product that is far more soluble, greatly increasing the effective solubility and degradation rates over those predicted for the parent compound.

2.4.5 Adsorption on the Solid Phase

Contaminants that diffuse to the bottom of the biofilm, particularly during the early stages of treatment when the biofilm is thin, may be adsorbed on the surface of the packing. Adsorption capacities vary widely with packing material. For biofilters using activated carbon packing, for example, modeling adsorption is necessary for accurate description of treatment of waste streams in which the concentration varies with time. Some modelers have also assumed that the particles are porous and contain significant amounts of water that can absorb contaminant (Deshusses et al., 1995; Zarook et al., 1997; Jorio et al., 2003). For biofilters using lava rock, at the other extreme, adsorption of contaminant is negligible. For all of the packing materials, biofilm exopolysaccharides and other biofilm compounds may compete for adsorption sites, reducing adsorption of the contaminant. Finally, adsorption has no effect on steady-state conditions: the adsorbed material is simply an inactive reservoir that has

no influence on treatment efficiency.

Adsorption and desorption have been included in nonsteady-state models, where it is generally presumed that the mass of material adsorbed per unit surface area at equilibrium is linearly proportional the concentration of the contaminant in the biomass at the bottom of the biofilm, C_{bfbot} .

$$C_{adseq} = K_{ads} C_{bfbot} \quad (2-10)$$

where K_{ads} is an empirically determined constant. Ranasinghe et al. (2002) took this approach but further modeled the adsorption constant as having Arrhenius-type dependence on temperature:

$$K_{ads} = K_0 \exp\left[\frac{-\Delta H}{RT}\right] \quad (2-11)$$

where ΔH is the heat of adsorption, R the gas constant, T the temperature, and K_0 is a constant. Zarook et al. (1997) and Ranasinghe et al. (2002) also considered non-equilibrium adsorption, assuming the flux from the biofilm to the surface occurred at a rate proportional to the degree to which it was below equilibrium. Their formulations were equivalent to:

$$J_{ads} = k_{adseq} (C_{adseq} - C_{ads}) \quad (2-12)$$

where J_{ads} is the flux per unit surface area, k_{ads} the rate constant, and C_{ads} is the concentration adsorbed.

2.4.6 Biomass Growth and Biodegradation

Biodegradation rates are a fundamental controlling factor for the effectiveness of biofilters. Most commonly, Monod kinetics are assumed for growth as a function of existing concentrations of biomass and the concentrations of contaminant

$$\frac{dX_{act}}{d_t} = \mu X_{act} \quad , \quad \mu = \frac{\mu_{max} C_{bf}}{K_S + C_{bf}} \quad \frac{dX_{act}}{d_t} = Y \frac{dC_{bf}}{d_t} \quad (2-13)$$

where X_{act} is the biomass density, μ is the growth constant, μ_{max} is the maximum value of the growth constant, K_S is the Monod or half-saturation constant, and Y is the biomass yield. For high values of C , the growth rate is constant, and some modelers have presumed that growth follows zero-order kinetics. For low values of C , growth is with contaminant concentration, and some modelers have presumed first-order kinetics. However, when the model includes sufficient detail to show biodegradation rates as a function of depth within the biofilm, concentrations will range from the Henry's equilibrium value at the surface of the biofilm to zero at the maximum depth of penetration, so it is likely that both regimes will be encountered and the full form of the Monod equation will be needed. Often the appropriate values for K_S and μ_{max} are uncertain. Both values are strongly dependent on the conditions under which they are determined and most data in the literature are from experiments performed on microorganisms in stirred, well-aerated suspensions, rather than in biofilms (and are highly variable even so). Thus, these parameters are often fitted to the biofilter data developed in the experiment being modeled.

2.4.7 Summary

Current models for mass transport in the air and within simple biofilms seem adequate. The major remaining uncertainty is in the determination of appropriate diffusion constants for various contaminants that reflect conditions in biofilms rather than water.

Biodegradation rates and biofilm growth models remain somewhat uncertain because of the lack of knowledge of Monod constants and maximum growth rate constants for actual conditions in biofilters.

2.5 Major Findings

The major findings of the literature review are:

➤ The potential of botanical filter to remove indoor VOC has been demonstrated by researchers, while there are very limited data available to understand the real VOC removal mechanisms;

➤ Most of the studies related to botanical air filtration were in terms of the static effect of the plant to VOC removal, which means there was no air flow passing through the root bed;

➤ Most of the studies related to botanical air filtration were conducted at relatively high VOC concentration level (ppm), and therefore, experimental investigation at low VOC concentration level is needed;

➤ It has been pointed out that the microbial community plays an important role in the botanical air filtration system, while the bio-degradation rate of the microbial community has not been further studied;

➤ Mathematical model on biofilter or biotrickling filter has been well developed, while there is no simulation model for botanical air filtration.

Further needed studies are:

- ✓ The VOC removal performance of botanical air filtration with air passing through the root bed is needed to be investigated;
- ✓ Studies at both relatively high concentration pollutant level (ppm) and low concentration pollutant level (ppb) are needed;
- ✓ Studies are needed to improve the understanding of the VOC removal mechanisms;
- ✓ The bio-degradation rate of botanical air filtration system needs to be determined;
- ✓ A numerical model is needed to simulate the botanical air filtration system and to help optimizing the design.

Chapter 3. Performance Testing, Evaluation, and Analysis

3.1 Introduction

As discussed in the last chapter, previous studies have indicated that the plant's root bed has the potential of improving indoor air quality. The microbial communities may play an important role in degrading VOC. Most previous studies have been focus on the VOC removal by potted plant without any air passing through the root bed, which severely limits the chance of contact between VOC and microbial communities. A dynamic botanical air filtration system (DBAF) prototype based on the principle of physical adsorption by activated carbon, absorption by water ("wet scrubber"), and VOC degradation by microorganisms in the plant's root system was developed in this study in collaboration with Phytofilter Technologies Inc. In this system, the polluted indoor air is forced to pass through the plant root bed to improve the removal performance.

The objectives of this chapter were to: 1) determine the single pass efficiency of the filter in removing both water soluble and non-soluble VOC and the equivalent clean air delivery rate (CADR) at a relative high pollutant level (1–3 ppm) in a full-scale test chamber, as well as at a typical room level (2–17 ppb) in a newly constructed office room; 2) evaluate the long-term performance in the real-world environment by monitoring its single pass efficiency for 10 months; 3) investigate the effect of moisture content in the root bed on the toluene and formaldehyde removal

performance, and determine the best moisture content range for removing both water soluble and insoluble compounds; and 4) investigate the possible effect of the DBAF may bring to the indoor air temperature and relative humidity (RH).

3.2 Methods

The DBAF system (Figure 3-1) used mixture of activated carbon and porous shale pebbles as root bed of selected plants (Golden Pothos (*Epipremnum aureum*)) with microorganisms growing in the root system. The filter bed was 1.8 m in length, 0.6 m in width and 0.2 m in depth. The average diameter of the granular activated carbon and shale pebbles was 0.005 m, and the mixed ratio is 50/50 by volume. Eight Golden Pothos were evenly placed in the bed. The filtration system was operated with periodical irrigation and airflow passing-through. An axial flow fan was installed. The maximum air flow through the bed was 1014 m³/h. Gas pollutants such as VOC were adsorbed by the activated carbon sorbent, and the wet root bed also acted as a scrubber for formaldehyde and other water soluble compounds. The adsorbed and/or absorbed organic compounds would be degraded by the microbes, regenerating the sorbent-based root bed. The purified air could be returned to indoor environment directly or fed to the supply air of an HVAC system to improve indoor air quality. The DBAF had a controller that automatically sequences the operation of the irrigation system and fan based on the signal from a moisture content sensor. The irrigation control sensor was buried in the center of the bed. When the moisture

content was below the lower limit, the fan was stopped, and irrigation system triggered and operated until the moisture content was higher than the higher limit. Three minutes after the irrigation was stopped, the fan was triggered and operated until the moisture was below the lower level again. Three Campbell CS616-L water content reflectometers (M.C. Sensors) were buried inside the bed in sequence for accurate moisture content measurement in experiments conducted in the real-world condition (a newly constructed office building), as shown in Figure 3-1(b).

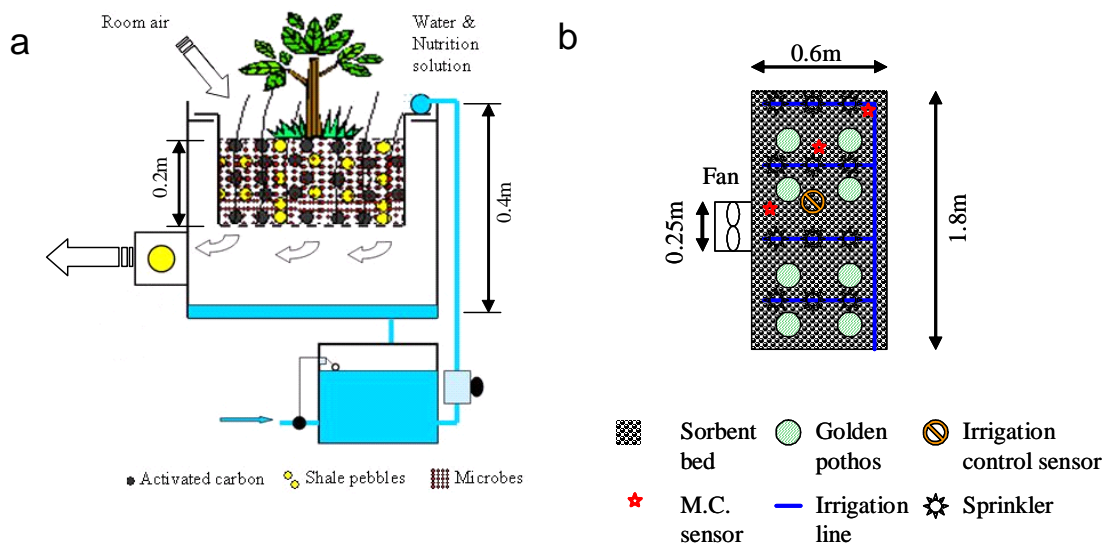


Figure 3-1 Schematic of full-sized dynamic botanical air filtration system: (a) side view, (b) top view. Moisture content sensor (M.C. sensor).

3.2.1 Experiments in a Full-scale Environmental Chamber

The chamber used had interior dimensions of 4.84 m long x 3.63 m wide x 3.05

m high (54.4 m^3 in air volume), and was maintained at $23 \pm 0.6^\circ\text{C}$ and $60 \pm 3 \%$ RH. It was operated at full-recirculation mode with a total supply airflow rate of $680 \text{ m}^3/\text{h}$ (12.5 ACH). The relatively high air change rate and use of a square air diffuser for space air distribution ensured complete air mixing inside the chamber (Chen et al., 2005).

Two sets of chamber tests were conducted to determine the initial (short-term) performance of the DBAF. In the first set of tests, the DBAF was evaluated by using the “pull-down” test procedure (Chen et al., 2005). Formaldehyde and toluene were selected as target compounds. Sulfur Hexafluoride (SF_6) was used as tracer gas. They were injected into the chamber to achieve desired initial concentration levels, and their concentrations were continuously monitored before and after the DBAF were turned on. An INNOVA 1312 photoacoustic multi-gas monitor was used for measuring the concentrations of toluene (C_{toluene}), formaldehyde (C_{formal}), and the tracer gas (SF_6) continuously until the concentrations of toluene and formaldehyde reached the background levels. Figure 3-2 shows the schematic of the chamber test set-up. The VOC removal performance of the DBAF was evaluated at three airflow rates through the DBAF ($250 \text{ m}^3/\text{h}$, $600 \text{ m}^3/\text{h}$ and $930 \text{ m}^3/\text{h}$) and two filter bed moisture content levels ($30 \pm 2\%$ for “high VWC” test and $15 \pm 1\%$ for “low VWC” test).

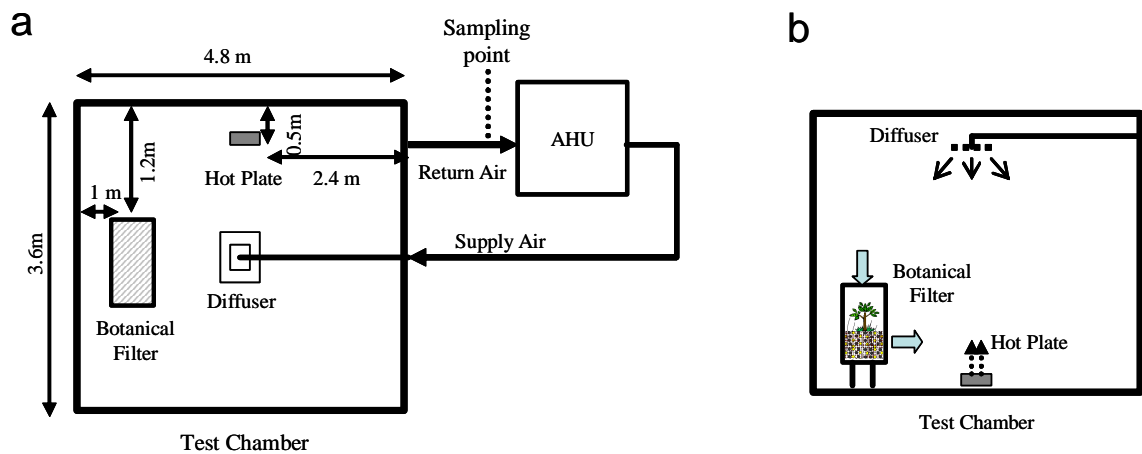


Figure 3-2 Schematic of the environmental chamber test setup: (a) top-view, (b) side-view. Air handling unit (AHU).

In the second set of chamber tests, a new working station made of particle board was placed inside the test chamber to simulate a typical emission source in an office environment. No clean air was supplied to the chamber and the VOC concentrations were allowed to increase or decrease depending on the operation of the DBAF. The test lasted for four days, and the DBAF ran eight hours per day. The air flow rate passing through the filter bed was $\sim 510 \text{ m}^3/\text{h}$ when the DBAF was turned on. The same INNOVA gas monitor was used to monitor formaldehyde and TVOC (quantified as toluene equivalent) concentrations.

Clean air delivery rate (CADR) represents the “effective” clean airflow rate delivered by the air cleaner (ANSI/AHAM standard: AC-1 2006). The performance parameter measured directly by the “pull-down” test method was CADR. The analysis was based on the well-mixed single zone model. Assuming that: 1) the air was well mixed in chamber (as confirmed by tracer gas testing), and 2) the contaminant

removal mechanisms other than air cleaning (e.g. surface adsorption effect and chamber leakage effect) were could be characterized by a first-order rate constant k_n , the mass conservation of contaminant in the “pull-down” test can be written as (Chen and Zhang, 2006):

$$V \frac{dC}{dt} = -(k_n V + CADR) \cdot C = -k_e V \cdot C, (C=C_0 \text{ at } t=0) \quad (3-1)$$

then

$$CA DR = (k_e - k_n) V \quad (3-2)$$

where, V is the testing chamber system volume, m^3 ; k_n is the exponential decay constant of the contaminant concentration without air cleaner operating (empty chamber effect), h^{-1} ; k_e is exponential decay constant with air cleaner operating (that includes both the empty chamber and air cleaner effects), h^{-1} ; C_0 is the initial contaminant concentration inside the chamber at $t=0$, mg/m^3 ; C is the contaminant concentration inside the chamber at time t , mg/m^3 .

The decay rate constant of SF_6 was 0.031 air change per hour (ACH) (corresponding to 1.68 m^3/h or 1.0 CFM), indicating that chamber leakage rate was acceptable. When there was no air cleaner in the chamber, the overall decay rate constant for each individual VOC ranged from 0.031–0.048 ACH (i.e., very close to that of SF_6 , indicating minimal surface adsorption effect of the chamber at the experimental conditions). Therefore the chamber surface adsorption effect was neglected and only the chamber leakage rate (characterized by SF_6 decay rate for each test) was used to determine k_n .

The equivalent single pass efficiency (SPE) can be calculated by following equation (Chen and Zhang, 2006):

$$\eta = \frac{CADR}{G \cdot E_d} \quad (3-3)$$

where η is single pass efficiency of the air cleaner, %; G is the air flow rate through the air cleaner, m³/h; E_d is short-circuiting factor of the air cleaner, ($E_d = 1$ at well-mixed condition).

3.2.2 Experiments as Part of an Office HVAC System

Following the full-scale chamber tests, the botanical air filtration system was integrated into the HVAC system of a newly constructed office room in Syracuse, NY, as shown in Figure 3-3. The total volume of the test room was 265 m³ (approximately 16.4 m long, 5.4 m wide and 3.0 m high). There were 16 work cubicles in the room. The botanical filter was connected with the supply air duct by steel pipes with diameter of 0.25 m. An independent fan was installed on the filter system, which provided an air flow rate of ~815 m³/h. The total amount of supply air for this room was 2378 m³/h during the tests. Tests were started in the winter (December 2008 - March 2009). During this test period, the test room was maintained at 22 °C with a relative humidity of 15%. The effect to the room temperature and RH was investigated. The effect of filter bed moisture content to the single pass efficiency was also investigated. The improvement of the indoor air quality by using the

botanical filter was evaluated as well. The single pass efficiency of the botanical in removing formaldehyde and toluene was kept on being monitored until October 2009, a ten-month-continuous monitoring.

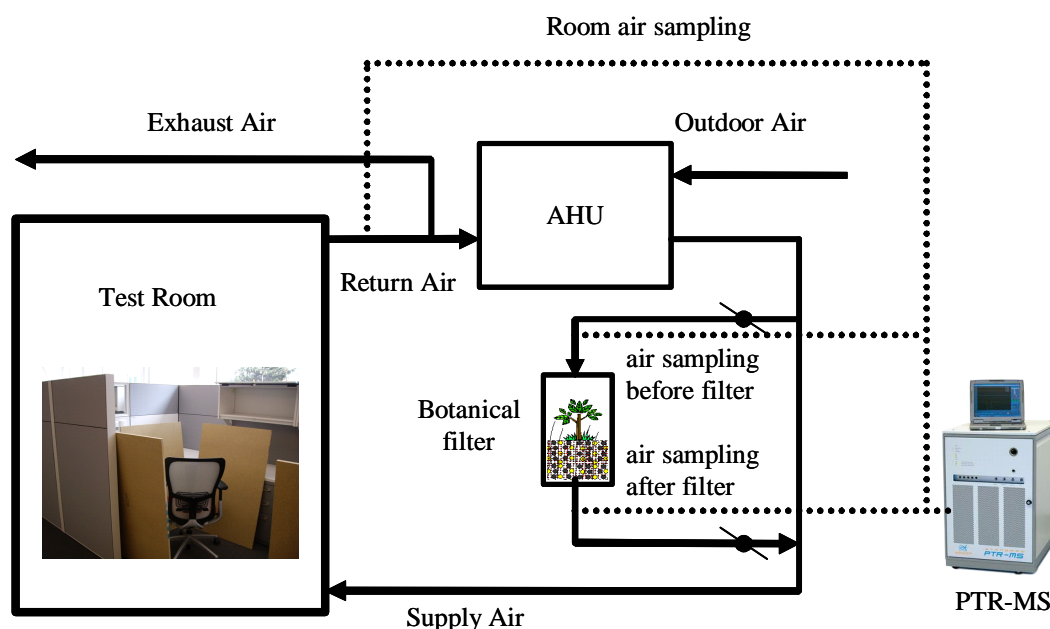


Figure 3-3 Integration of botanical filter into an HVAC system and setup for monitoring. Air handling unit (AHU). Proton Transfer Reaction Mass Spectrometer (PTR-MS).

Preliminary tests revealed that the test room had unusually low pollutant concentration due to the low emitting materials used. In order to simulate pollutant level at a more typical office conditions, 48 pieces of unused particleboard were placed in the test room. The size of each piece was 1.2 m by 0.8 m. After the particleboards were placed into the test room, an air sample was taken at the return air duct by using a tenax sorbent tube, and analyzed by gas chromatography-mass spectrometry (GC/MS). Pentanal, toluene, hexanal, xylene, α -pinene were found to

have the highest concentrations. Toluene was selected as the target VOC in current study since it is commonly used as calibration reference for the total volatile organic compounds (TVOC) (Hodgson et al., 2000). Meanwhile, another air sample was taken at the same location by using 2,4-dinitrophenylhydrazine (DNPH) cartridge, and analyzed by high-performance liquid chromatography (HPLC). Formaldehyde and acetaldehyde were also detected. Formaldehyde was chosen as the other target compounds as it is typically identified as a major compound of concern in emission testing of composite wood materials and office furniture (ANSI/BIFMA standard: M7.1 2007). A proton transfer reaction mass spectrometer (PTR-MS) was used to monitor these target compounds in real-time. The detection limits of PTR-MS are 0.06 ppb for toluene and 0.2 ppb for formaldehyde. The sampling inlet of PTR-MS was connected to the return air duct, as shown in Figure 3-3.

To study the effect of the filter bed on the air temperature and RH, air temperature and RH sensors were installed in four different locations: air duct right before entering DBAF, air duct immediately after DBAF, return air duct and supply air duct of the test room. In the one-day test period, the DBAF was turned on for eight hours, from 12th hour to 20th hour, and was turned off during the rest of hours of the day.

To investigate the maximum clean air flow rate that the DBAF could provide, tests were conducted at four different HVAC system operation modes: 50% outdoor air (OA) (1138 m³/h), 25% outdoor air, 10% outdoor air, and 5% outdoor air plus the DBAF (i.e., filter on). The room VOC sampling location was in the return air duct.

The 24-hour tests (three-hour-background measurement at 5% OA and the switch to the test ventilation mode) were conducted. The concentrations at the third hour (start point of ventilation mode change) were taken as the reference for normalization, 17 ppb for formaldehyde and 2 ppb for toluene, respectively.

To investigate the effect of filter bed moisture content on the toluene and formaldehyde removal performance, three Campbell CS 616-L water content reflectometers were used to measure the moisture content in the bed. Average of the readings from these three sensors was taken as the bed water content. The filter bed was saturated with water at the beginning of the test, and then the fan was kept on running until the bed water content decreased to less than 5% in VWC. The filter inlet and outlet contaminant concentrations were measured periodically, and then the single pass efficiency was calculated by using the following equation:

$$\eta = \frac{G(C_{in} - C_{out})}{GC_{in}} = \frac{C_{in} - C_{out}}{C_{in}} \quad (3-4)$$

where G is the airflow rate through the air cleaner, m^3/h ; C_{in} is the contaminant concentration at the inlet of air cleaner, mg/m^3 ; C_{out} is the contaminant concentration at the outlet of air cleaner, mg/m^3 .

The filter was then kept on running for 10 months. The filter inlet and outlet contaminant concentrations were measured periodically. The calculated single pass efficiencies were used to study the long-term performance of the DBAF.

3.3 Results and Discussions

3.3.1 Full-scale Chamber Experiments

3.3.1.1 Results from the First Set of Chamber Tests

Pollutant Removal Performance. Figure 3-4 presents the normalized formaldehyde concentration with three different air flow rates passing the filter bed: 250 m³/h, 600 m³/h and 930 m³/h. Formaldehyde concentration in the chamber at the time “0 hr” in the tests was 2 mg/m³ (1.64 ppm). The background pollutant concentration in the chamber was measured for two hours before the test was started, and all the concentrations measured later were subtracted by the average background concentration. Then the concentrations were normalized by using the initial concentration at time $t = 0$ as reference) to facilitate the comparison. The negative concentration at the later period of the test means that the concentration achieved was lower than initial background level. Tracer gas (Sulfur hexafluoride (SF₆)) concentration was also presented, and the chamber leakage rate from SF₆ calculation was 0.031 ACH, which corresponded to 1.68 m³/h and was excluded in the final CADR calculation for the DBAF. The formaldehyde concentration decreased quickly to the background level after the fan was turned on. With higher airflow rate passing the sorbent bed, the formaldehyde concentration decreased faster. It means more clean air was delivered in a fixed time period.

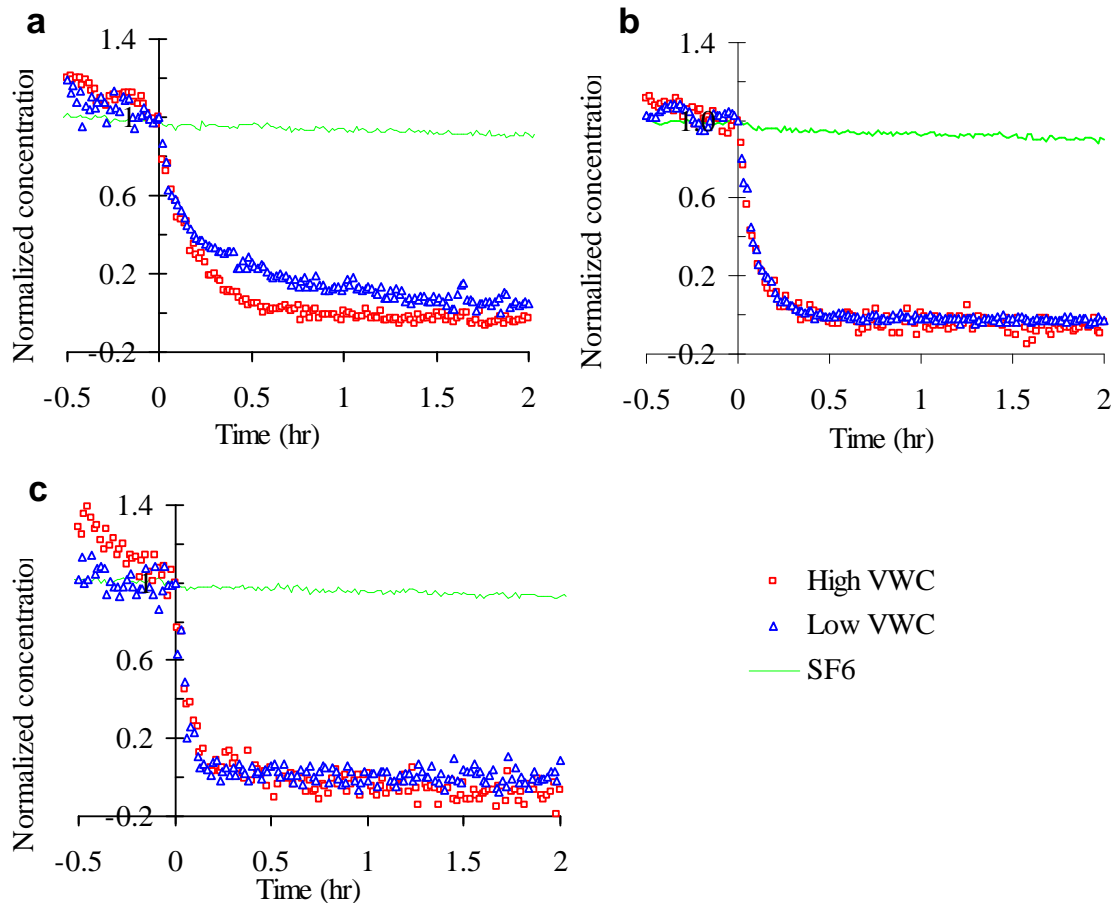


Figure 3-4 Normalized formaldehyde concentration at different air flow rate: (a) 250 m³/h airflow rate passing the bed, (b) 600 m³/h airflow rate, (c) 930 m³/h air flow rate. Volumetric water content (VWC) in the filter bed.

Toluene concentrations were also monitored at the same test conditions, as shown in Figure 3-5. Toluene concentration at the time “0 hr” in the tests was ~8 mg/m³ (2.16 ppm). Similar trend was observed for the effect of air flow rate, toluene concentration decreased faster at higher airflow rate test. Results also indicated that the single pass efficiency (SPE) at higher air flow rate was less than that at lower air flow rate in general due to smaller residence time, but more clean air can be delivered during a fixed period of time at higher airflow rate test. That is why formaldehyde or

toluene decreased faster at higher airflow rate test.

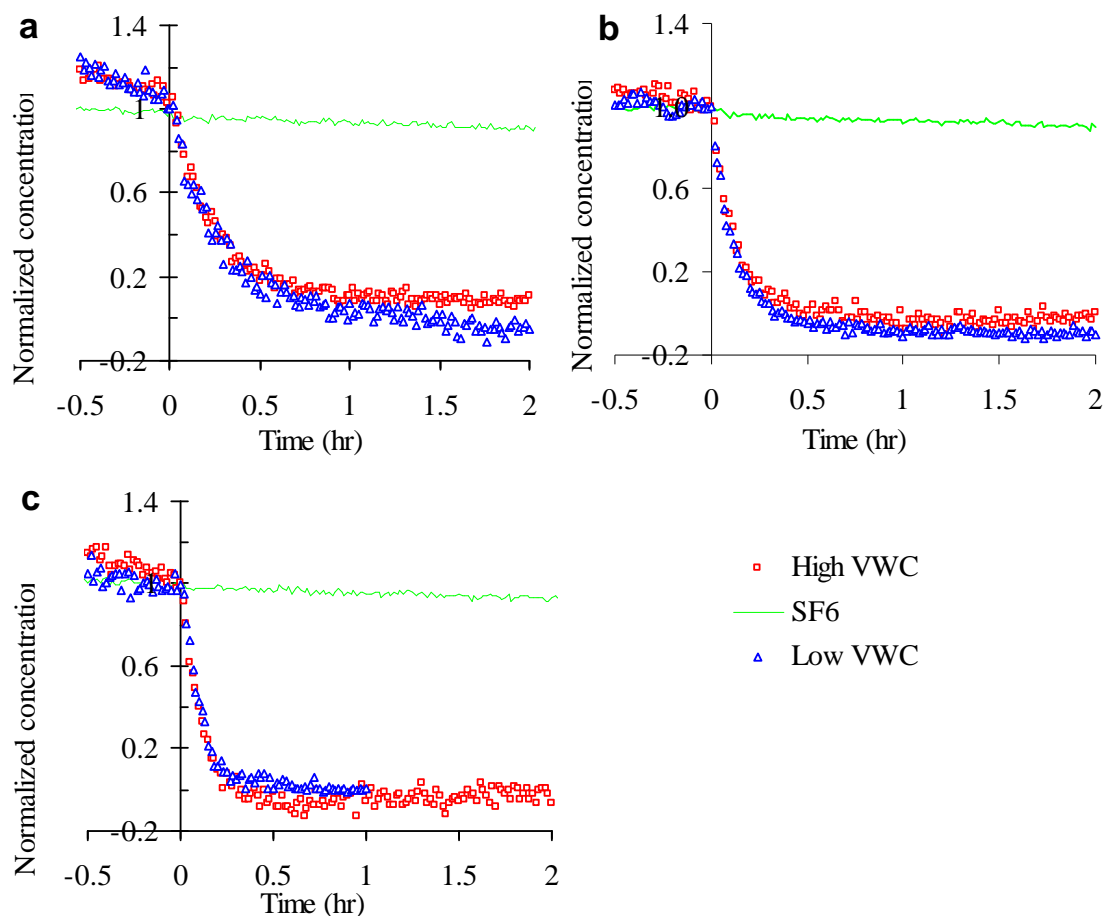


Figure 3-5 Normalized toluene concentration at different air flow rate: (a) 250 m³/h airflow rate passing the bed, (b) 600 m³/h airflow rate, (c) 930 m³/h air flow rate.

Volumetric water content (VWC) in the filter bed.

Table 3-1 lists the CADR and SPE for formaldehyde and toluene in the first set of chamber tests. Overall, the CADR or SPE was not significantly affected by the test moisture condition because both high and low VWC conditions in the tests were well within the range of 5–32% bed water content, which is the range where the botanical

filter worked well for both water soluble and insoluble compounds as to be further discussed later in this paper.

Table 3-1 CADR and SPE for formaldehyde and toluene removal

Air flow (m ³ /h)	Pollutant	Formaldehyde		Toluene	
		High VWC (30±2%)	Low VWC (15±1%)	High VWC (30±2%)	Low VWC (15±1%)
250±10	CADR (m ³ /h)	266.9	253.7	247.9	232.4
	SPE (%)	98.7	93.8	91.7	85.9
600±15	CADR (m ³ /h)	582.4	581.7	529.1	436.7
	SPE (%)	94.4	94.3	85.8	70.7
930±20	CADR (m ³ /h)	698.1	731.8	759.7	492.0
	SPE (%)	69.0	73.2	77.2	50.1

ASHRAE 62.1-2010 specifies that the requirement of outdoor air for office buildings is 5 cfm (8.48 m³/h) per person plus 0.06 cfm (1.02 m³/h) per square foot floor area. ASHRAE 62.1-2010 also specifies a maximum occupant density for office spaces of five people per 1000 ft² or per 100 m². Take this maximum value as example, the requirement of outdoor air for per 1000 ft² office building is 85 cfm (144 m³/h). The maximum CADR of the filter for formaldehyde was 731.8 m³/h. Therefore, the DBAF could serve an office building with 5000 ft² (465 m²) floor area

if formaldehyde is the target pollutant for air cleaning.

Effect of DBAF on the Chamber Air Temperature and RH. The test chamber air was maintained at $23\pm 0.6^{\circ}\text{C}$ and $60\pm 3\%$ RH at the beginning of test, which is common in a conditioned office space for a hot and humid summer. Table 3-2 lists the average temperature and relative humidity change in chamber return air with three different air flow rates passing through the filter bed: 250 ± 10 , 600 ± 15 and 930 ± 20 m^3/h . For the same air flow rate, tests were also conducted at two different volumetric water content (VWC) levels in the filter bed: High VWC ($30\pm 2\%$) and Low VWC ($15\pm 1\%$). The VWC level was measured by the filter bed moisture control sensor. The sensor was located in the center of the DBAF. Although it does not exactly represent the average moisture condition of the entire filter bed, the sensor represents relative levels of VWC in different tests. It can be found that the chamber air was cooled slightly at high VWC levels. With air flow rate of 250 ± 10 m^3/h , temperature decreased by $0.2\text{--}0.5^{\circ}\text{C}$ while RH increased by $5.7\text{--}13.3\%$. For air flow rate of 600 ± 15 and 930 ± 20 m^3/h , temperature decreased by $0.6\text{--}1.1^{\circ}\text{C}$ and $0.8\text{--}1.0^{\circ}\text{C}$ while RH increased by $11.3\text{--}14.5\%$ and $9.4\%\text{--}13.5\%$, respectively. In summary, the chamber air temperature decreased by less than 1°C and relative humidity increased by 10% to 15% RH in most tests.

Table 3-2 Average temperature and RH change “ Δ ” in chamber return air from the initial conditions of 23 ± 0.6 °C and 60 ± 3 % RH

Airflow rate (m^3/h)	Bed moisture level (VWC)	High VWC ($30\pm 2\%$)	Low VWC ($15\pm 1\%$)	Moisture generation (kg/h)
250 ± 10	Temperature Δ (°C)	-0.5	-0.2	0.81–1.14
	Relative humidity Δ (% RH)	13.3	5.7	
600 ± 15	Temperature Δ (°C)	-1.1	-0.6	1.15–1.37
	Relative humidity Δ (% RH)	14.5	11.3	
930 ± 20	Temperature Δ (°C)	-1.0	-0.8	1.23–1.89
	Relative humidity Δ (% RH)	13.5	9.4	

Even though introducing humidity through this DBAF is not preferable, the influence to humidity load of building was analyzed for reference. In this operation condition, the application of the DBAF will introduce additional humidity that needs to be removed by the HVAC during summer condition for thermal comfort, but would improve comfort during winter condition in which humidification is needed. The prototype DBAF tested produces approximately 0.81–1.89 kg/h of moisture based on the data in Table 3-2. It should be noted that the DBAF could serve a much larger building space than the chamber (465 m^2 versus 17.6 m^2 in floor area) per the outdoor airflow rate requirement recommended by ASHARE Standard 62.1-2010. The

increase of relative humidity due to the operation of DBAF would be much smaller when it is used for a larger building space that matches its CADR capacity.

3.3.1.2 VOC Removal Performance in the Second Set of Chamber Tests

Figure 3-6(a) shows the test set-up with VOC emissions from an office workstation system (the second stage of chamber test). Figure 3-6(b) shows the pollutant concentration in chamber varied with time. It decreased significantly after the DBAF began to work. Once the filter stopped running, the pollutant concentration in chamber began to increase due to sustained VOC emissions from the furniture system. Table 3-3 lists the CADR and SPE calculation for each running period. It was found that the filter also worked well at low concentration range tested (300 – 400 ppb). The single pass efficiency for formaldehyde was over 90% after the filter had been continuously running for four days which might mainly be due to the absorption of the wet media bed, and meanwhile the SPE for TVOC (quantified as toluene equivalent) was 38%.

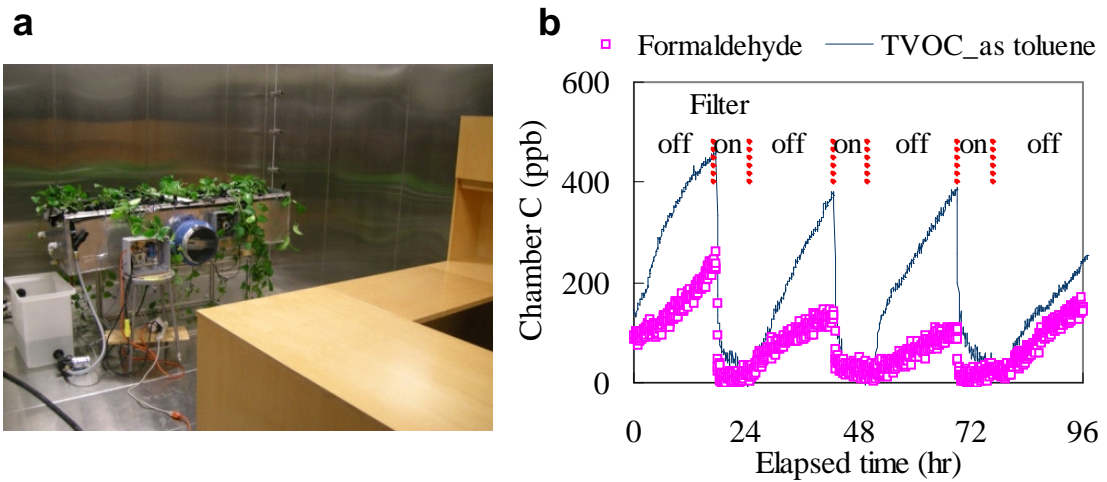


Figure 3-6 Test set-up and test chamber concentration vary with time: (a) test set-up (photo), (b) test results. The red dotted vertical lines represent the 8-hour operation period of the DBAF.

Table 3-3 CADR and SPE of DBAF for VOC emitted from an office furniture during a 4-day test

VOC	Formaldehyde				TVOC as toluene equivalent			
	1 st	2 nd	3 rd	4 th	1 st	2 nd	3 rd	4 th
Air leakage rate	0.031	0.031	0.031	0.031	0.031	0.031	0.031	0.031
calculated by SF ₆ k _n								
Decay rate calculated	16.27	14.83	8.71	8.59	4.86	5.72	3.14	3.63
after turning on AC k _e								
CADR=V(k _e -k _n)/60	510	510	470	465	260	310	169	195
(m ³ /h)								
Final single pass	100.0	100.0	92.6	91.3	51.5	60.7	33.1	38.4

3.3.2 Experiments as Part of an Office HVAC System

3.3.2.1 Effect of DBAF on the Room Air Temperature and RH

Figure 3-7 shows the impact of DBAF on the test room air temperature and RH. Table 3-4 lists the average temperature and RH at different test period. After the filter was turned on, the test room return air temperature decreased by 0.5 °C while return air RH increased by 17.7% RH. The moisture generation of DBAF was 2.54 kg/h at this test condition. Compared with the test results conducted in the test chamber, more moisture was generated due to test room low initial RH condition in the office room. The return air RH increased from 13.5–31.2%, which would improve the thermal comfort condition in dry winter climate.

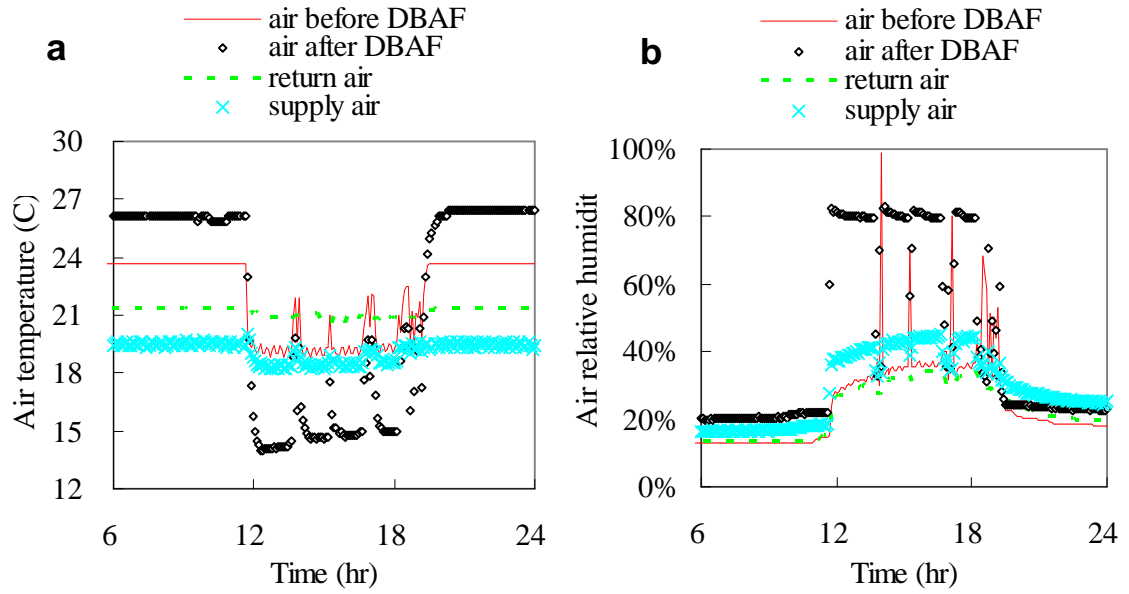


Figure 3-7 Effect of DBAF on room air temperature and RH: (a) Temperature, (b) RH.

Table 3-4 Average temperature and RH at different periods in a 24-hr-test

Air parameter	Average Temperature (°C)			Average RH (%)		
	I	II	III	I	II	III
Test Period	I	II	III	I	II	III
	6-11hr	12-19hr	20-24hr	6-11hr	12-19hr	20-24hr
Air before filter	23.7	19.7	23.7	12.9	37.6	19.2
Air after filter	26.0	15.8	26.4	20.6	71.0	23.4
Return air	21.4	20.9	21.4	13.5	31.2	20.8
Supply air	19.5	18.6	19.5	16.9	40.5	26.3

3.3.2.1 Air-cleaning Versus Ventilation: How Much Clean Air Could the DBAF Provide?

Figure 3-8 compares the normalized formaldehyde and toluene concentration in the office space among the four different operation modes. Figure 3-8(a) shows the normalized formaldehyde concentration (NFC) at different operation mode. The mode of 5% outdoor air plus filtration had the similar result as 25% outdoor air (560m³/h) without filter. The botanical filter provided an equivalent clean air delivery rate of 476m³/h for formaldehyde, which was within 10% of the value previously determined from a full-scale environmental chamber test (520m³/h). Figure 3-8(b) shows the normalized toluene concentration (NTC) at different operation mode. The operation mode with 5% outdoor air plus filtration resulted in a similar effect of 10–25% outdoor air ventilation for toluene removal.

In summary, the above results indicated that the DBAF was effective at very low pollutant concentration levels: 17 ppb for formaldehyde and 2 ppb for toluene. The botanical filter provided an equivalent clean air delivery rate of 476m³/h for formaldehyde and toluene removal, which means the requirement for the amount of outdoor air could potentially be reduced by integrating the botanical air filtration system in the HVAC system of a commercial building, while achieving adequate indoor air quality if formaldehyde and toluene were the pollutants that dictated the required outdoor ventilation rate.

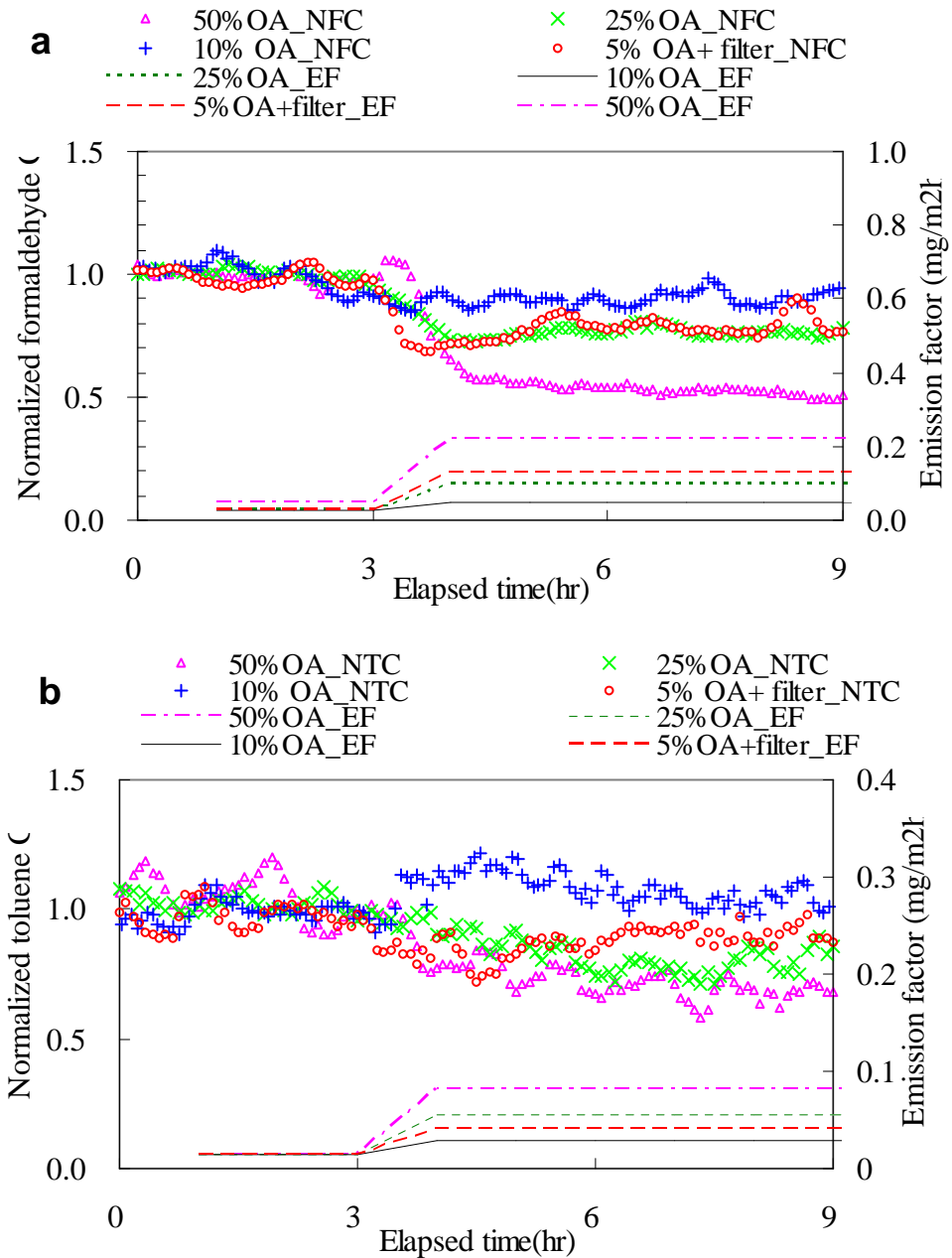


Figure 3-8 Comparison of room pollutants concentration: (a) Formaldehyde, (b) Toluene. Outdoor air (OA). Normalized formaldehyde concentration (NFC). Emission factor (EF). Normalized toluene concentration (NTC).

Figure 3-8 also shows the emission factors at different operating conditions estimated based on the following mass balance equation for the room space, assuming

that the air was well-mixed in the room:

$$V \frac{dC}{dt} = AE - QC - Q_f C \eta - \delta \quad (3-5)$$

where, V is the room volume, m^3 ; A is the total surface area of emission source, m^2 ; E is the emission factor, mg/m^2h ; Q is the outdoor air ventilation rate, m^3/h ; C is the contaminant concentration inside the chamber at time t , mg/m^3 ; Q_f is the air flow rate through the filter, m^3/h ; η is the single pass efficiency of the filter, which was determined by measuring the concentrations right before and after the DBAF ($\eta=0$ when DBAF was completely bypassed); δ is the room sink effect, mg/h .

For the same outdoor air flow rate and operation mode of the DBAF, the concentrations of both compounds had a very slow decay rate so that a quasi-steady state assumption was adopted in estimating the emission factor, E , in Equation (3-5), i.e., neglecting the transient term on the left hand side of Equation (3-5) and the sink effect term δ (which was also considered negligible comparing to the other terms in the equation), we have

$$E = \frac{1}{A} (QC + Q_f C \eta) \quad (3-6)$$

During the field test, the initial emission factors of formaldehyde and toluene were $0.046 mg/m^2h$ and $0.015 mg/m^2h$ respectively at outdoor air ventilation. Figure 3-8 shows that the emission factors increased with outdoor air ventilation or operation of botanical filter due to a higher concentration gradient between the source and the room air caused by the reduction of indoor concentration by ventilation or air cleaning.

3.3.2.3 Effect of Bed Water Content

Figure 3-9 shows the effect of bed water content on SPE of the filter. The single pass efficiency for formaldehyde was maintained at over 70% when the bed water content was higher than 10%, then it decreased very fast when the water content of the bed was less than 5%. On the contrary, the SPE for toluene was almost zero when the bed water content was higher than 40%, then it increased significantly as the bed water content decreased. The SPE for toluene was maintained at over 40% when the water content was lower than 30%. The reason for this might be the different water solubility of these two compounds. Formaldehyde is water soluble, while toluene is not. The results indicated that 5–32% bed water content is the best range where the botanical filter worked well for both water soluble and insoluble compounds. The SPEs were around 70% and 40% for formaldehyde and toluene, respectively in this range.

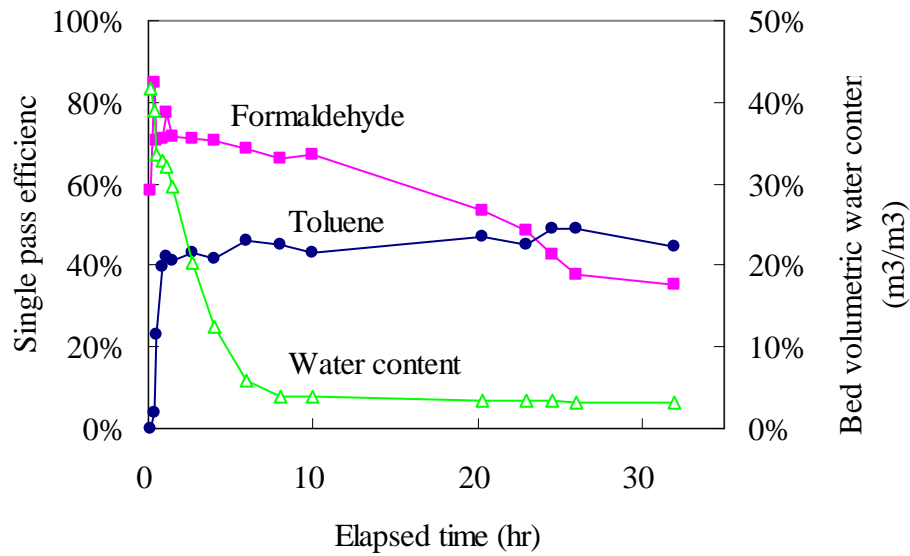


Figure 3-9 Effect of bed water content on removal of pollutants.

Formaldehyde is very weakly adsorbed on activated carbon or any other untreated adsorbent, because the formaldehyde molecules are small and light so the Van der Waals force between formaldehyde and activated carbon is very weak (Tseng et al., 1998). It appears that the “wet film” formed in DBAF worked as an effective scrubber in removing formaldehyde of the air. Formaldehyde was first absorbed by the “wet film” formed in the sorbent bed, and then degraded by the microorganisms living in the “wet film” or the microbial communities in soil from the rhizosphere of plant.

3.3.2.4 Long-term Performance

Long-term performance evaluation of the DBAF is needed to determine whether

formaldehyde and toluene retained by the bed are consumed by the microorganisms in the root system so that the removal efficiency of the bed can be maintained. During a 300-day long performance test in which DBAF operated continuously in cycles plus 5% OA ventilation, the initial formaldehyde and toluene concentration increased to 17 ppb and 2ppb, respectively, due to the emissions from the particleboards introduced into the office environment. After the filter was running for 10 days, the room formaldehyde and toluene concentration decreased to 10 ppb and 1 ppb, respectively, and then kept at a relatively constant level, meaning that the VOC continuously emitted from the particleboards were removed by the 5% OA ventilation plus DBAF. Figure 3-10 presents the SPE of the botanical filter on formaldehyde and toluene during the test period as well as the water content of the media bed. The SPE for formaldehyde almost stayed at constant, around 60%. The SPE for toluene was negatively influenced by the water content in the bed, but was still kept at 20% 300 days later. Note that without the botanical filter, concentrations in the spaces would have been 30% higher than current results, due to the continuous generation of toluene and formaldehyde by the sources.

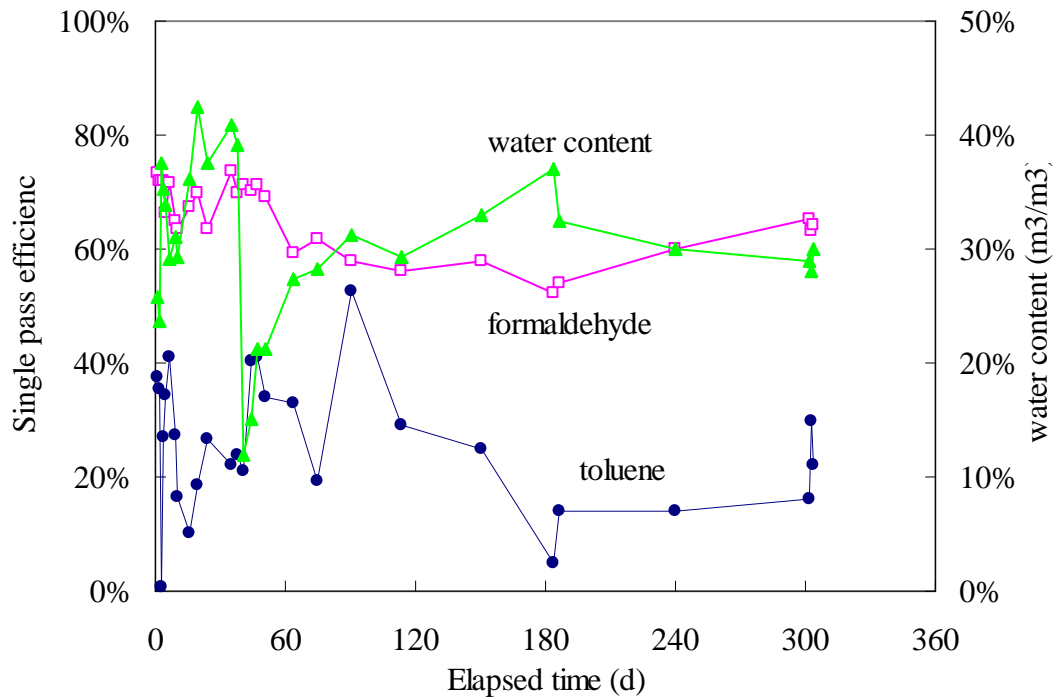


Figure 3-10 Botanical filter single pass efficiency (SPE) over 300 days.

Seven (7) bacterial species from the botanical filter system using DNA sequencing were identified, including *Arthrobacter aureescens TCI*, *Arthrobacter oxydans*, *Leifsonia xyli subsp. xyli str. CTCB07*, *Bacillus cereus*, *A. aureescens*, *Pseudomonas putida*, and *Bacillus spp* (Huang et al., 2009). Degradation of formaldehyde solution by individual species was conducted. According to Henry's law, the formaldehyde concentration in the water film around the sorbent particle was 0.001% by weight if the formaldehyde concentration in the air passing through the sorbent bed was 50 ppb. The initial liquid formaldehyde concentration in the test was 0.001% by weight. It was found that the maximum reduction rate was 86.2% after 24 hours, by *A. aureescens TCI* (Huang et al., 2009).

Therefore, as long as there are sufficient carbon sources (formaldehyde or VOC) in the air passing through the bed, the microorganisms living in the sorbent bed will degrade them. Moreover, the microorganisms that are responsible for the degradation can quickly reactivate the carbon particle so that it need not be replaced, unlike the typical carbon filters used for air cleaning which need to be replaced every three-six months.

There is a concern whether this botanical filter would cause indoor microbial pollution. A pilot test was conducted to address this issue. Five liters of filter outlet air was sampled and bubbled through Luria-Bertani (LB) medium (containing 10 g/L tryptone, 5 g/L yeast extract, and 10 g/L sodium chloride) to observe any possible microbial growth. No colony was found on the LB agar plates (LB medium supplemented with 1.5% agar) during incubation for up to 120 h at 30 °C, which means there was no microbial pollution in the sampled air. The potential release of microorganisms from indoor biological purifiers during long-term operation should be further studied and prevented.

Biofiltration system has been used for many years in the industrial setting as well as indoor air setting (Darlington et al., 2000). There are some significant differences between the DBAF and previous biofiltration system. The material used in the bioscrubber of previous biofiltration system was lava rock, while the bed of DBAF consisted of porous shale pebble and granular activated carbon. The activated carbon had a BET surface area of 900–1100 m²/g and 80% of the pore size was less than 10 nanometers, which was highly effective for adsorbing VOC. The plants used in the

previous biofiltration system were over hundreds of species of plants typically used in indoor landscaping, while the plants used in the DBAF were more selective (e.g. Golden Pothos (*Epipremnum aureum*)) for ease of maintenance and more root-zone microbial community. The previous biofiltration system has much lower face velocity than the current DBAF (0.01 m/s vs. 0.25 m/s), and delivers much less clean air airflow rate per unit surface area (360 m³/h by a 10 m² bioscrubber compared to 970 m³/h by a 1.08 m² DBAF root bed with an acceptable pressure drop of 73 Pa). As a result, the DBAF system developed in this study would be easier to be adopted for indoor air cleaning either as part of an HVAC system or operated as a standalone unit to provide the required clean airflow rate.

3.4. Major Findings

The potential usage of plant's root bed for removing indoor VOC has been demonstrated. Although potted plants alone are not efficient in real-world condition, the dynamic botanical air filtration system (DBAF) developed in this study is very promising based on the laboratory evaluation and real-field demonstration.

The full-scale chamber experimental results indicated that the DBAF had high initial removal efficiency for formaldehyde and toluene even without plants in the bed. With the plants, the filter system had even higher initial removal efficiency (90% for formaldehyde in the first four days, and over 33% for toluene). However, it was not clear if the microbes played any role in such a short term test period. The

long-term performance test results indicated that the DBAF was effective over a test period of 300 days, and the same level of single pass removal efficiency was maintained at the end of the test. This indicated the possible consumption of the VOC by the microbes. However, further study is needed to investigate the type of microbes that are responsible for the VOC removal/degradation, and the rate of degradation. More detailed and carefully controlled laboratory experiments are needed to separate out the adsorption, absorption and microbe degradation processes involved in the DBAF root bed to improve the understanding and to develop a simulation model that can be used to optimize the DBAF design.

The operation of the DBAF resulted in 1 °C temperature decrease and 9–13% RH increase in the chamber air. In the office experiments, the operation of DBAF resulted in 0.5 °C temperature decrease and 17.7% RH increase. The moisture production rate due to the use of DBAF was in the range of 0.81–1.89 kg/h. Such moisture generation would improve the thermal comfort condition in winter, while in summer contribute to little negligible effects on thermal comfort and cooling load (added 5% more humidity load).

Field experiments in the office space indicated that the use of the DBAF could reduce the percent of outdoor air supply from 25–5% of total air supply without adversely affecting the indoor air quality if formaldehyde and toluene are the target pollutants that dictate the required ventilation rate.

The effect of bed water content on the removal of formaldehyde/toluene was also

studied in the field experiments. The single pass removal efficiencies were approximately 60% for formaldehyde and 20% for toluene when the volumetric water content was within the range of 5–32% in the root bed. A moisture content that was higher than 32% resulted in significant increase of single pass efficiency (SPE) for the water soluble compound (formaldehyde) and reduction of SPE for Toluene.

Chapter 4. VOC Removal Mechanisms and Determination of Bio-degradation Rate Constant

4.1 Introduction

In previous chapter, it has been demonstrated that the DBAF performed well in removing both formaldehyde and toluene at low concentrations (less than 50 ppb), having consistently ~60% single pass efficiency for formaldehyde and ~20% for toluene over a 10-month test period, respectively. The test results represent the whole-filter performance in removing formaldehyde and toluene, but the intrinsic VOC removal mechanism is still not clear. More experimental research is needed to understand the underlying VOC removal mechanisms of DBAF. In particular, it is necessary to clarify the different roles played by the leaves, wet sorbent bed, and microbial communities.

This chapter presents the methods and results of an experimental study that was designed to: 1) improve the understanding of the mechanisms of the DBAF system in removing the volatile organic compounds, including determination of the important factors affecting the removal performance, and the roles of different transport, storage and removal processes; 2) determine the VOC biodegradation rate by the microbial community of the DBAF.

4.2 Methods

A reduced-sized dynamic botanical air filtration system was developed for laboratory evaluation, as shown in Figure 4-1. The filter bed was 0.35 m in length, 0.2 m in width and 0.15 m in depth. The average diameter of the granular activated carbon and shale pebbles was 0.005 m, and the mixed ratio was 50/50 by volume. The total weight of the sorbent material was 4900 ± 50 g. Two Golden Pothos (*Epipremnum aureum*) were placed in the bed. The filtration system was operated with periodical irrigation. A tangential flow fan was installed for driving airflow passing through the bed. The air flow through the bed was 50 ± 3 m³/h, which leads to a face velocity of ~ 0.22 m/s. A programmable logic controller was used to automatically control the operation sequences of the irrigation system and fan in the DBAF. The irrigation was triggered every two hours and lasted for 5 seconds. The irrigation water flow rate was 0.4 LPM. The fan was stopped while the irrigation was on, and was triggered 30 seconds after the irrigation stopped working and operated for 7135 seconds (~ 2 hours). The water flow rate of the irrigation was measured by a water flow meter. The actual water flow rate of the irrigation was 0.025 kg/s. One Campbell CS616-L water content reflectometers (M.C. Sensors) was buried inside the bed for accurate moisture content measurement.

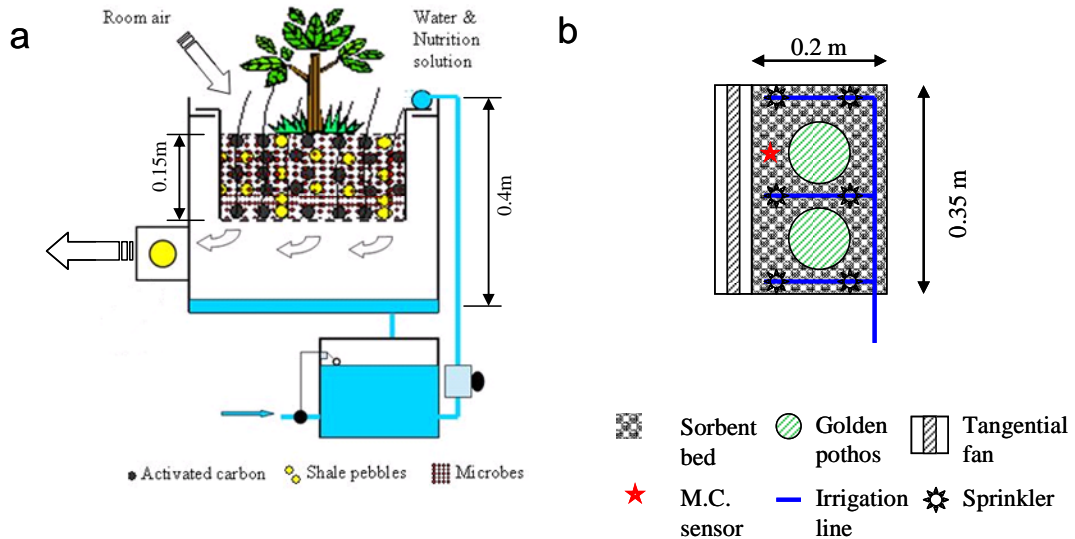


Figure 4-1 Schematic of reduced-sized dynamic botanical air filtration system: (a) side view, (b) top view. Moisture content sensor (M.C. sensor).

To achieve the objectives described above, the experiments in this chapter were designed into three parts, as shown in Table 4-1. The test methods and test purpose were also listed in Table 4-1. The detailed test conditions and procedures were discussed in the following sections.

Table 4-1 Tests conducted to investigate the VOC removal mechanisms of DBAF

Test Group	Test methods	Test purpose
A. Formaldehyde removal by potted plant without air passing through the root bed	Middle-scale chamber, No ventilation, Pull-down test	The leaf effect and soil static effect
B. Formaldehyde removal by microbial community with air flow passing through	Small-scale chamber, No ventilation, Pull-down test	The microbial community effect

C. Formaldehyde and toluene removal by DBAF	Middle-scale chamber, With ventilation, Constant source	VOC removal mechanisms of the DBAF and determination of bio-degradation rate constant
---------------------------------------------	---------------------------------------------------------------	---------------------------------------------------------------------------------------

4.2.1 Formaldehyde Removal by Potted Plant Without Air Passing the Root Bed

Tests were conducted to investigate the formaldehyde removal by the potted plants without any air flow passing the root bed. Eight-inch potted Golden Pothos (*Epipremnum aureum*) were selected (the same kind of plant used as before). The tests were conducted in a 5.1 m³ chamber with interior dimensions of 1.83 m long x 1.68 m wide x 1.68 m high. The chamber was located in a conditioned laboratory, where the temperature and relative humidity were maintained at 23±0.6°C and 50±3 %, respectively. There was no ventilation for the chamber in this test. The chamber served as a sealed space. A six-inch propeller axial fan was placed in the middle of the chamber to mix the chamber air in an acceptable manner (equivalent air change rate of 20 ACH). Para-formaldehyde powder was heated by a hot plate (250 °C heating temperature set point) to serve as an instant formaldehyde source. Sulfur Hexafluoride (SF₆) was used as a trace gas. Formaldehyde and SF₆ concentration were monitored by an INNOVA 1312 photoacoustic multi-gas monitor in real-time.

Four tests (as shown in Table 4-2) were conducted at standard test conditions: 23±0.6 °C and 50±3% RH. The initial formaldehyde concentration was 20±0.5 ppm.

The major purpose of the series of tests was to investigate the formaldehyde removal by potted plant without any air flow passing through the bed. The pot numbers effect and light effect were also studied. The detailed CADR calculation was described in section A.3.

Table 4-2 Tests conducted for formaldehyde removal by potted plant without air passing the root bed at 23 ± 0.6 °C and 50 ± 3 % RH.

Test No.	Test conditions	Formaldehyde concentration (ppm)	Test purpose
A1	Empty chamber	20 ± 0.5	Background test
A2	Leaf effect only V.S. total potted plant effect	(Initial concentration, instant source)	Study the leaf effect V.S. total effect
A3	One potted plant V.S. two potted plants		Study the potted numbers effect
A4	With light (a 60-wattz lamp) V.S. Without light		Study the light effect

The tests were conducted with following steps:

1. **Empty chamber test.** Test was conducted to check the air tightness of the chamber and the formaldehyde sink effect in empty chamber. 5 ml SF₆ was injected into the chamber. 125 mg para-formaldehyde powder was injected into the chamber by heating on the hot plate. The SF₆ and formaldehyde concentration were monitored for 48 hours. The SF₆ concentration change

will be used to determine the air tightness of the chamber. Equation (4-1) could be used to calculate the chamber air tightness and formaldehyde sink effect in empty chamber.

$$N = \frac{\ln C - \ln C_0}{t} \quad (4-1)$$

where N is the air change rate per hour due to leakage, ACH; C is the chamber concentration at time t , ppm; C_0 is the chamber concentration at time 0, ppm; t is the time of the test lasted, h.

2. **Leaf effect only V.S. total potted plant effect.** Leaf effect test was conducted when the surface of the pot soil was covered by aluminum foil. Total effect of the potted plant includes leaf, soil and microorganism effect. One eight-inch potted Golden Pothos was hanged in the middle of the chamber. The sixty-watt lamp was on during the test. 125 mg paraformaldehyde was injected into the chamber. The formaldehyde concentration was monitored for 48 hours. Formaldehyde removal by potted plant could also be calculated from Equation (4-1).
3. **One potted plant V.S. two potted plants.** Tests were conducted to study the effect of potted plant number to the formaldehyde removal. One test was conducted with only one potted plant in the chamber, and the other test was conducted with two potted plants in the chamber.
4. **With light (60-wattz lamp) V.S. without light.** Tests were conducted to check the effect of light in the chamber to the formaldehyde removal. One

test was conducted without any light in the chamber, and the other test was conducted with a sixty-watt lamp placed in the chamber. All the other test set-ups were the same.

4.2.2 Formaldehyde Removal by Microbial Community with Air Flow Passing Through

Figure 4-2 shows the schematic of the formaldehyde removal test by microbial community with air flow passing through. The entire test system was located in a conditioned chamber, where the ambient conditions were maintained at $23\pm 0.6^{\circ}\text{C}$ and $50\pm 3\%$, respectively. The test system consisted of a 50-liter stainless steel chamber (for better air mix), an air recirculation pump (with airflow rate of 2 LPM), two manually controlled three-way valves, and connection tubes. Formaldehyde concentration was monitored by an INNOVA 1312 photo-acoustic multi-gas monitor. With valve #1 and #2, the system can be switched between test loop and bypass loop. The test system was switched to the bypass loop during the period of formaldehyde injection. After the formaldehyde concentration approached to steady state, the test system was switched to the test loop.

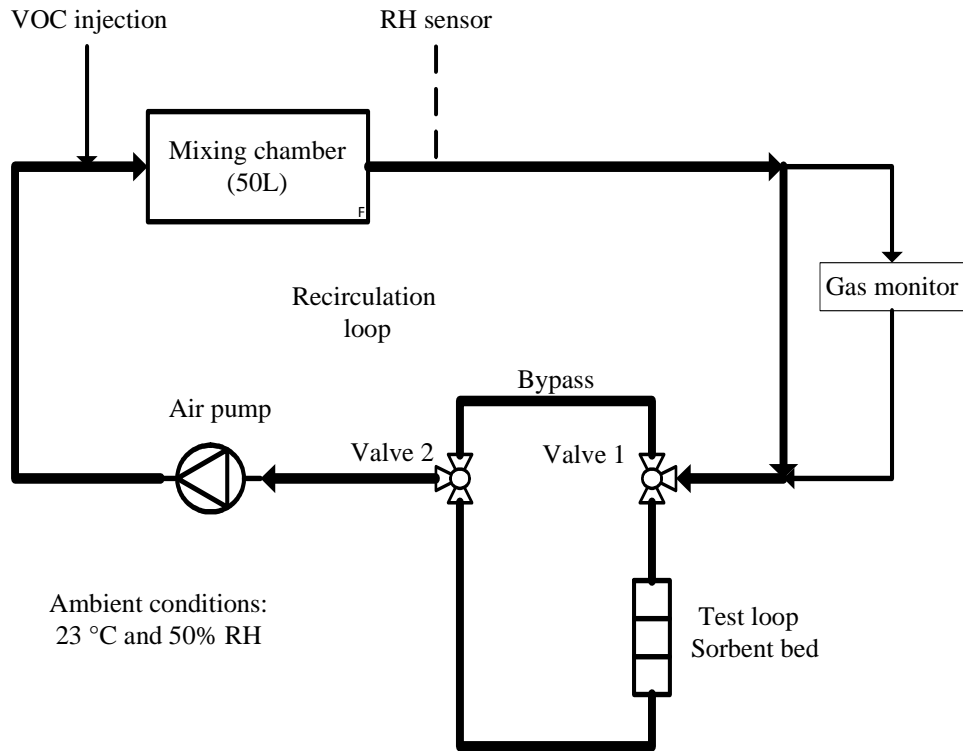


Figure 4-2 Schematics of the test set-up for formaldehyde removal by microbial community with air passing by

Table 4-3 lists the tests that were conducted for formaldehyde removal by microbial community with air flow passing by. The test temperature and RH were 23 ± 0.6 °C and 90 ± 3 %, respectively. The initial formaldehyde concentration was 7.5 ± 0.1 ppm. The main purpose of this series of tests was to study the microbial community effect to formaldehyde removal.

Table 4-3 Tests conducted for formaldehyde removal by microbial community with air flow passing through at 23 ± 0.6 °C and 90 ± 3 % RH

Test	Test conditions	Microbes	Formaldehyde	Test purpose
------	-----------------	----------	--------------	--------------

		initial number (CFU/mL)	concentration (ppm)	
B1. Single-injection w/o microbes	Wet bed only, single formaldehyde injection	0	7.5±0.1	The wet bed effect only
B2. Single-injection w microbes	Wet bed with microbes, single formaldeedhyde injection	6.78×10^{10}		The microbial community effect with single formaldehyde injection
B3. Multi-injection w microbes	Wet bed with microbes, multiple formaldeedhyde injections	2.12×10^9		The microbial community effect with multiple formaldehyde injections

The tests were conducted with following steps:

1. **Test preparation.** Two samples of sorbent material were prepared. The average diameter of the granular activated carbon and shale pebbles was 0.005 m, and the mixed ratio is 50/50 by volume. The diameter of the test cylinder was half inch. The thickness of the sorbent material was five (5) inches. The test system was pre-conditioned by 90% RH air for 24 hours. The air pump was turned on and the pre-conditioned air was re-circulated in the test system. Formaldehyde was injected to the system through the VOC injection port in Figure 4-2. The equilibrium formaldehyde concentration in the system was maintained at ~7.5 ppm.
2. **Single-injection without microbes.** The first sample of sorbent material was first saturated with Luria-Bertani (LB) medium (containing 10 g/L tryptone,

5 g/L yeast extract, and 10 g/L sodium chloride), and then placed into the test loop. After the formaldehyde concentration in the system approached to steady state, the re-circulated air was forced to pass through the test bed. The formaldehyde was monitored for 24 hours. After the baseline case test was done, the test system was flushed by lab clean air for 24 hours.

3. **Single-injection with microbes.** Firstly, the second sample of sorbent material was saturated with Luria-Bertani (LB) medium (containing 10 g/L tryptone, 5 g/L yeast extract, and 10 g/L sodium chloride) and *Arthrobacter aureescens TCI*¹ (CFU number: 6.78×10^{10} CFU/mL), and then installed into the test loop. Secondly, after the test system was pre-conditioned with 90% RH air and the same formaldehyde concentration in the system was approached again, the re-circulated air was forced to pass through the test bed. The formaldehyde in the system was monitored for 24 hours. After the proposed case test was finished, the test system was flushed by lab clean air for 24 hours.

4. **Multi-injection with microbes.** The test procedure was conducted in the same way as the single-injection test. While formaldehyde was injected into

¹ Seven (7) bacterial species from the DBAF using DNA sequencing were identified, including *Arthrobacter aureescens TCI*, *Arthrobacter oxydans*, *Leifsonia xyli subsp. xyli str. CTCB07*, *Bacillus cereus*, *A. aureescens*, *Pseudomonas putida*, and *Bacillus spp.* It is found that *Arthrobacter aureescens TCI* has the best formaldehyde removal capacity, which is 86% reduction rate in a 24-hour-test period. Therefore, *Arthrobacter aureescens TCI* was selected to conduct the formaldehyde removal.

the test system in every 6 hours. There were totally four (4) injections in the multi-injection test.

4.2.3 Formaldehyde and Toluene Removal Rate by the DBAF

Figure 4-3 shows the schematic of the set-up for low concentration test (ppb level). The tests were conducted in the same environmental chamber (5.12 m³). The RH in the chamber will be varied from 55–90% per the requirement of different tests. A six-inch propeller axial fan was placed in the middle of the chamber to have the chamber air well mixed (equivalent air change rate of 20 ACH). The chamber was ventilated by lab clean air. Sulfur Hexafluoride (SF₆) was used as a trace gas for air change rate measurement. Formaldehyde and toluene were continuously generated into the chamber by Dynacalibrator (Model 450) to serve as a constant source and monitored by proton transfer reaction mass spectrometer (PTR-MS). The DBAF was located in the middle of the chamber. A sixty-watt lamp was placed in the chamber to serve as light source for the plants.

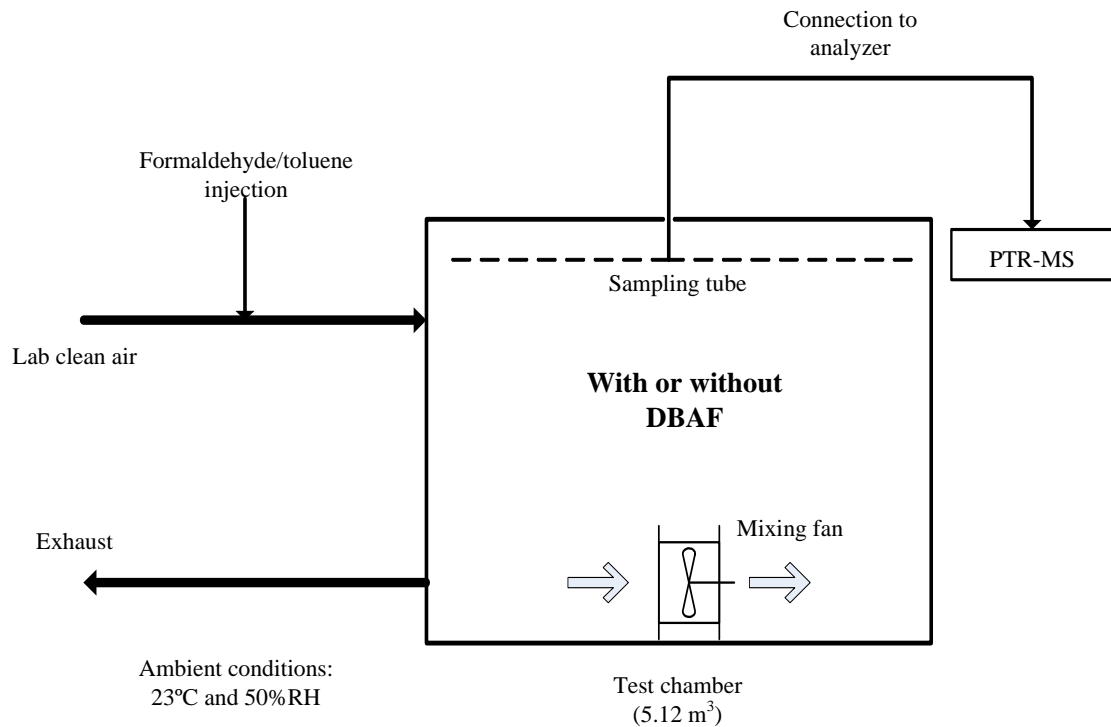


Figure 4-3 Schematic of the mid-scale chamber system for low concentration (ppb) test

Table 4-4 lists the tests that were conducted for formaldehyde removal by DBAF. The test conditions and test purpose were described in the table. There were two sets of tests. One set of tests were test C1–4. These tests were to compare the dry bed effect, wet bed effect, and the whole filter effect. The other set of tests were test C4–6. These tests were to study the whole filter effect at different RHs.

Table 4-4 Tests conducted for formaldehyde removal by DBAF

Test No.	Test media	RH (%)	Initial bed water content (m^3/m^3)	Formaldehyde concentration (ppb)	Test purpose
C1	Empty chamber	50±3	N/A	275±5	Reference test

C2	Dry bed, no plant	50±3	0.027	275±5	Effect of dry sorbent
C3	Wet bed, no plant	92±3	0.137	275±5	Effect of moisture of wet bed
C4	DBAF	92±3	0.137	275±5	Effect of RH on DBAF
C5	DBAF	75±3	0.078	275±5	Effect of RH on DBAF
C6	DBAF	55±3	0.034	275±5	Effect of RH on DBAF

Table 4-5 lists the tests that were conducted for toluene removal by DBAF. The test temperature was maintained at 23±0.6°C. The test RH decreased from 92–55%. The main purpose of this set of tests was to study the whole filter effect at different RHs.

Table 4-5 Tests conducted for toluene removal by DBAF

Test No.	Test Note	RH (%)	Initial bed water content (m3/m3)	Toluene concentration (ppb)	Test purpose
C7	Empty chamber	92±3	0.137	162±5	Background check
C8	DBAF	92±3	0.137	162±5	The whole filter effect
C9	DBAF	75±3	0.078	162±5	The whole filter effect at different RH
C10	DBAF	55±3	0.034	162±5	The whole filter effect at different RH

The tests were conducted with following steps:

1. **Empty chamber test.** Test was conducted to check the formaldehyde natural decay in empty chamber. 5 ml SF₆ was injected into the chamber. Formaldehyde and toluene were generated into test chamber as well.

2. **Test with the dry sorbent only in the chamber.** Test was conducted in the chamber with five inches dry sorbent bed only. The air flow rate passing the bed was the same as the DBAF. Formaldehyde and toluene were continuously generated into the chamber. Once the formaldehyde and toluene concentration reached the quasi steady-state, the filter with dry sorbent only was turned on.
3. **Test with the wet sorbent only in the chamber.** Test was conducted in the chamber with five inches wet sorbent bed only. The air flow rate passing the bed was the same as the DBAF. The sorbent bed has an initial water content of 0.137 (g/g). Irrigation was triggered for 5 seconds in every 2 hours. The test chamber RH for this test was $90\pm 3\%$. Formaldehyde and toluene were continuously generated into the chamber. Once the formaldehyde and toluene concentration reached the quasi steady-state, the filter with wet sorbent only was turned on.
4. **Test with DBAF (wet sorbent bed with two Golden Pothos (*Epipremnum aureum*)).** Tests were conducted in the chamber with DBAF. Two Golden Pothos (*Epipremnum aureum*) were placed in the filter bed. The plant density was 28 plant/(m² bed). Formaldehyde and toluene were continuously generated into the chamber. Once the formaldehyde and toluene concentration reached the quasi steady-state, the DBAF was turned on.

Single pass efficiency and equivalent clean air delivery rate (CADR) were obtained through the following analysis. Formaldehyde mass balance for empty chamber test can be expressed:

$$V \frac{dC_1}{dt} = R - Q_v \cdot C_1 \quad (4-2)$$

where, V is the testing chamber system volume, m^3 ; R is the formaldehyde generation rate, mg/h ; Q_v is the ventilation air flow rate, m^3/h ; C_1 is the formaldehyde concentration for empty chamber test at steady state, mg/m^3 . At the steady state,

where $\frac{dC_1}{dt} = 0$, Equation (4-2) becomes:

$$R = Q_v \cdot C_1 \quad (4-3)$$

Mass balance for test with dry bed/wet bed/DBAF in the chamber is:

$$V \frac{dC_2}{dt} = R - Q_v \cdot C_2 - Q_f \cdot \eta \cdot C_2 \quad (4-4)$$

where, C_2 is the formaldehyde concentration for test with dry bed/ wet bed/ DBAF in the chamber at steady state, mg/m^3 ; Q_f is the air flow rate of the DBAF, m^3/h ; η is

the single pass efficiency of the DBAF. At the steady state, where $\frac{dC_2}{dt} = 0$,

Equation (4-4) becomes:

$$R = Q_v \cdot C_2 + Q_f \cdot \eta \cdot C_2 \quad (4-5)$$

The formaldehyde generation rate is the same for the two tests, so:

$$Q_v \cdot C_1 = Q_v \cdot C_2 + Q_f \cdot \eta \cdot C_2 \quad (4-6)$$

Therefore, the single pass efficiency of the DBAF can be derived as follows:

$$\eta = \left(\frac{C_1}{C_2} - 1 \right) \cdot \frac{Q_v}{Q_f} \quad (4-7)$$

The equivalent clean air delivery rate (CADR) can be obtained as follows:

$$CADR = Q_f \cdot \eta \quad (4-8)$$

4.3 Results

4.3.1 Formaldehyde Removal by Potted Plant Without Air Passing the Root Bed

Effect of Leaf. Figure 4-4 shows the formaldehyde removal by potted plant without any air passing through the root bed. Normalized concentrations (i.e. concentration divided by the initial concentration at time $t = 0$) were used to determine the air tightness of the test chamber. Brown cross points are the normalized concentration of the trace gas (SF_6). The decay rate SF_6 shows that the air leakage of the chamber was 0.002 ACH (air change per hour), which indicates that air tightness of chamber was acceptable for the test. The chamber formaldehyde concentration was up to 20 ppm at the beginning of the test. Normalized concentrations (i.e. concentration divided by the initial concentration at time $t = 0$) were used to facilitate the comparison. Dark blue points show the formaldehyde concentration decay over time for the empty chamber test. Pink triangle points show the formaldehyde

concentration decay for the leaf effect only (The top surface of the pot was covered by aluminum foil to void contact between air and soil). Red square points show the total effect of the potted plant, including leaf effect and soil effect. Equation (3-1) and (3-2) can be used to calculation the clean air delivery rate. Equivalent clean air delivery rates (CADR) of leaf effect test and total effect by the plant were 0.086 and 0.161 m^3/h , respectively. It indicates that the formaldehyde removal capacity via static effect of potted plant is limited. Large amount of potted plant would be required to maintain acceptable pollutant concentration for a typical indoor space.

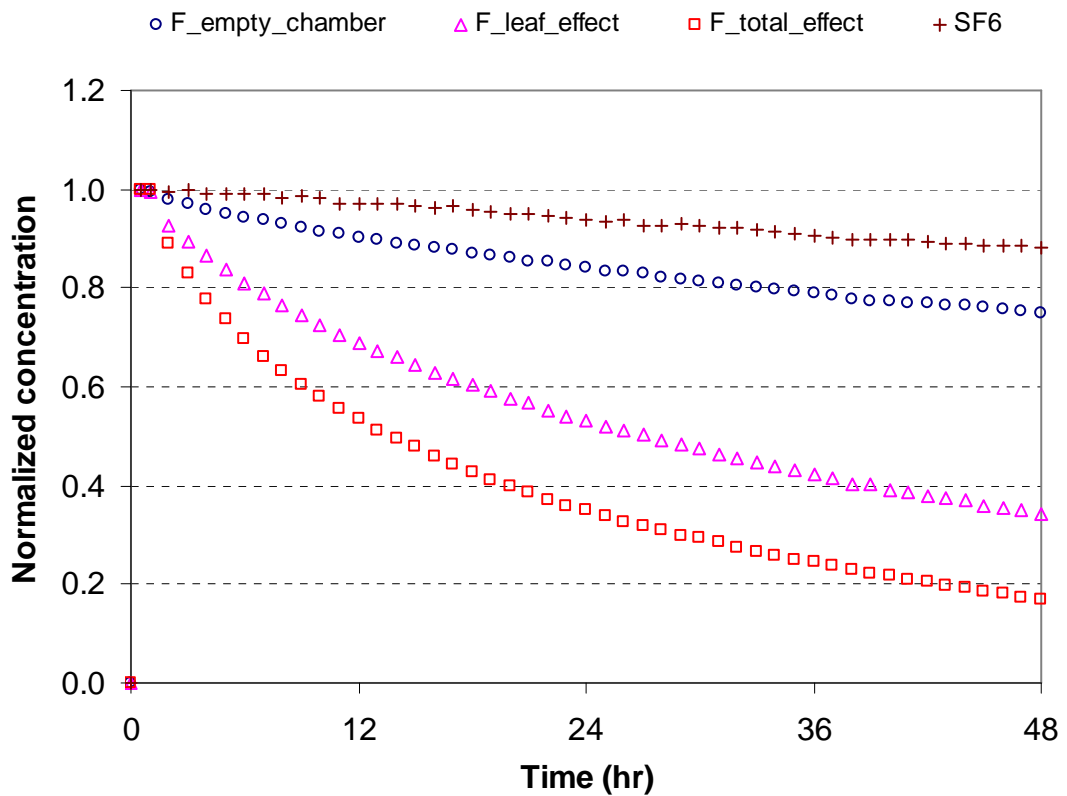


Figure 4-4 Formaldehyde removed by one 8" potted plant

Further analysis could be conducted to reflect the limited effect of formaldehyde removal by potted plant without air passing through the bed. ASHRAE 62.1-2010 specifies that the requirement of outdoor air for office buildings is 5 cfm (8.48 m³/h) per person plus 0.06 cfm (1.02 m³/h) per square foot floor area. ASHRAE 62.1-2010 also specifies a maximum occupant density for office spaces of five people per 1000 ft² or per 100 m². Take this maximum value as example, the requirement of outdoor air for per 1000 ft² office building is 85 cfm (144 m³/h). Since one eight-inch potted Golden Pothos (*Epipremnum aureum*) could only provide 0.161 m³/h equivalent clean air delivery rate, 894 potted Golden Pothos will be needed per 100 m² office building to follow ASHRAE standard, which is unpractical.

Effect of Potted Plant Numbers. Figure 4-5 shows the effect of the potted plant numbers on formaldehyde removal. The formaldehyde concentration with two potted plants placed in the chamber decayed faster than that with one potted plant. The equivalent clean air delivery rates (CADR) of total effect potted plant can also be calculated according to the concentration decay in Figure 4-5. It was found that the equivalent CADR by one potted plant and two potted plants were 0.161 and 0.256 m³/h, respectively. It reflects that the increment of the number of potted plants would provide more equivalent CADR. Still, it can not significantly improve the removal efficiency by increasing the number of plants only but without air passing through the bed.

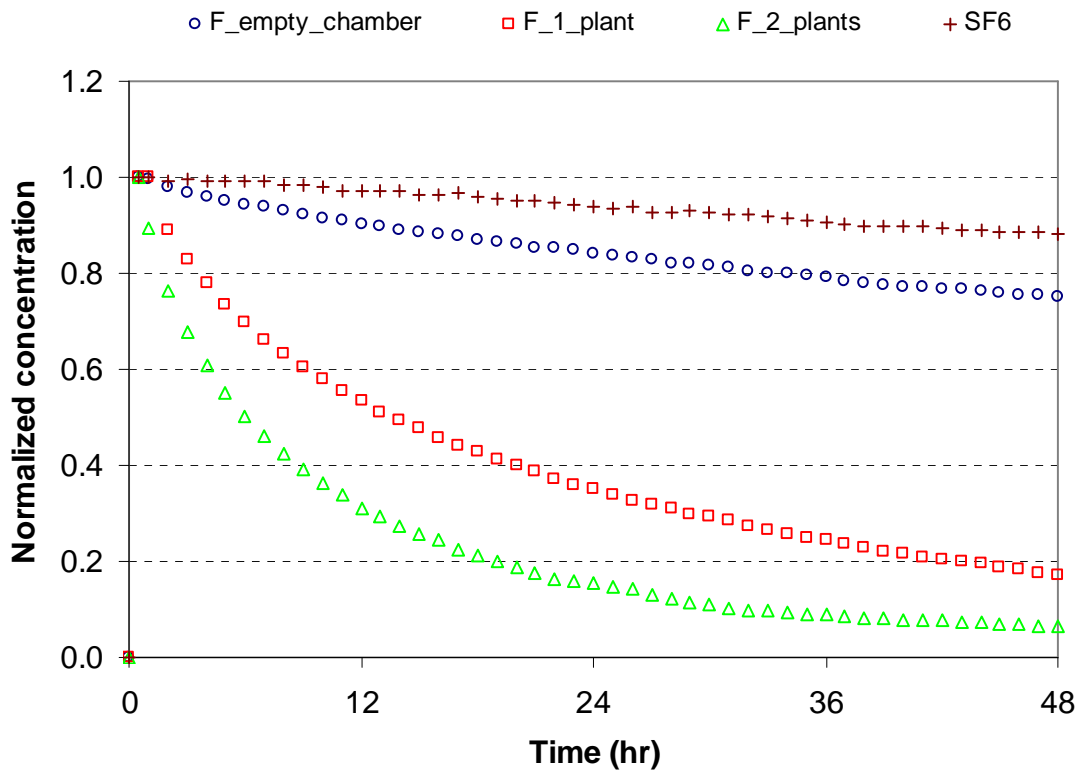


Figure 4-5 Effect of potted plant number on formaldehyde removal

Effect of Light. Figure 4-6 shows the effect of light in the chamber on formaldehyde removal. Without light in the chamber, the equivalent CADR for one potted plant decreased from 0.161–0.144 m³/h in a 24-hour test period, while there was slightly different after 24 hours. It indicates that the light had little effect after the leaves were saturated on absorbing formaldehyde. The equivalent CADR for two potted plants decreased from 0.256–0.207 m³/h, according to Equation (3-1). The presence of light can improve the performance on removing formaldehyde if the leaves have not been saturated.

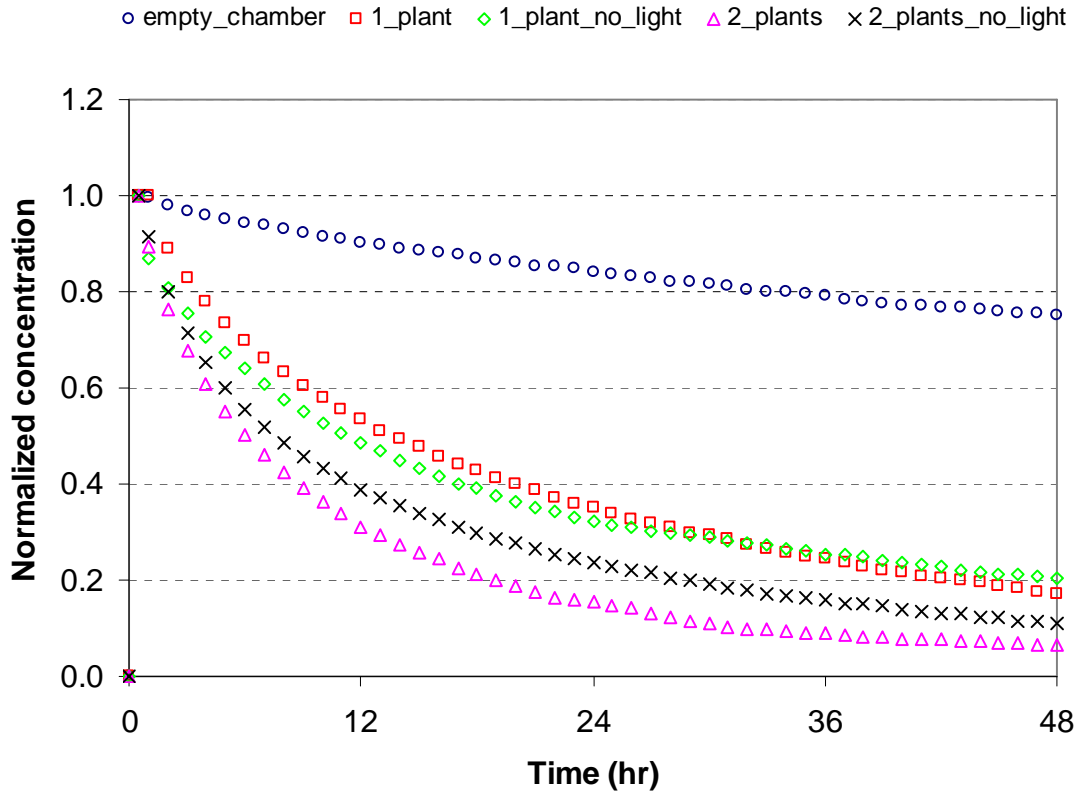


Figure 4-6 Effect of light in the chamber on formaldehyde removal

In summary, the test results show that the formaldehyde can be removed by potted plant without any air flow passing through the sorbent bed, while the removal efficiency was very limited. The equivalent clean air delivery rate for an 8” potted Golden Pothos (*Epipremnum aureum*) was $\sim 0.161 \text{ m}^3/\text{h}$. Even through the performance could be improved by increasing the number of potted plant or introducing light, the CADR of potted plant without air passing through the bed was still in an unpractical level ($\sim 0.2 \text{ m}^3/\text{h}$ CADR per potted plant). Large amount of potted plant would be needed to maintain the indoor air quality in acceptable level. If the

cross-section of the bed was taken into account, then the CADR for potted plant without air passing through the bed would become 5.1 m³/h per square meter bed.

4.3.2 Formaldehyde Removal by Microbial Community with Air Flow Passing through

It is necessary to keep the sorbent bed in a humid condition to avoid the unexpected death of microbes. Figure 4-7 shows the air RH in the recirculation loop during the test. The test system (Figure 4-2) was first pre-conditioned with 90% RH clean air for 4 hours. After the test system RH condition became steady, the test system was switched to recirculation loop. It can be seen that the test system air RH increased after the switch occurred. This is due to the test bed was initially containing certain amount of liquid solution. It can also be seen that air RH in the recirculation loop was kept at 95% in a 24-hour test period.

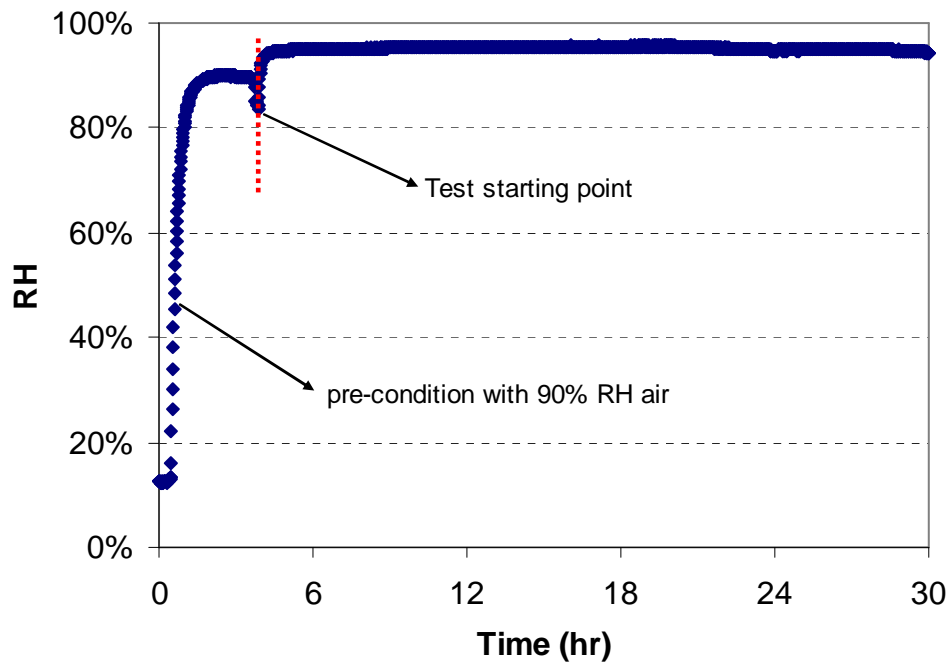


Figure 4-7 Test system relative humidity change over time

Figure 4-8 shows the normalized formaldehyde concentration in the system in a single-injection test. The steady formaldehyde concentration in the test system before switching to the test loop was ~ 7.5 ppm (9.2 mg/m^3). The formaldehyde concentration in the system decreased to 1.6 mg/m^3 with wet bed only in one hour after the switch. The system concentration was decreased to 0.6 mg/m^3 with wet bed plus microbes in one hour after the switch. The equivalent clean air delivery rates were $\sim 0.083 \text{ m}^3/\text{h}$ for wet bed only and $\sim 0.126 \text{ m}^3/\text{h}$ for wet bed with microbes. If the cross-section of the bed was taken into account, then the CADR for microbial community with air passing by would become $5.1 \text{ m}^3/\text{h}$ per square meter bed.

The formaldehyde removal rate can be calculated by multiplying the concentration difference between initial equilibrium concentration and final equilibrium concentration in the end and volume of the test system. The initial concentration was 7.5 ppm. The final concentration for wet bed and wet bed with microbes were 1.27 ppm and 0.52 ppm, respectively. By considering the test system volume of 0.05 m³, the removal rate by wet bed only was 0.38 mg/h. The removal rate by wet bed plus microbes was 0.43 mg/h. Therefore, the removal rate by microbes only would be 0.05 mg/h. The initial bed microbial density was 6.78×10¹⁰ CFU/mL. The removal rate by microbe would be 7.3×10⁻¹² mg/h per CFU/mL.

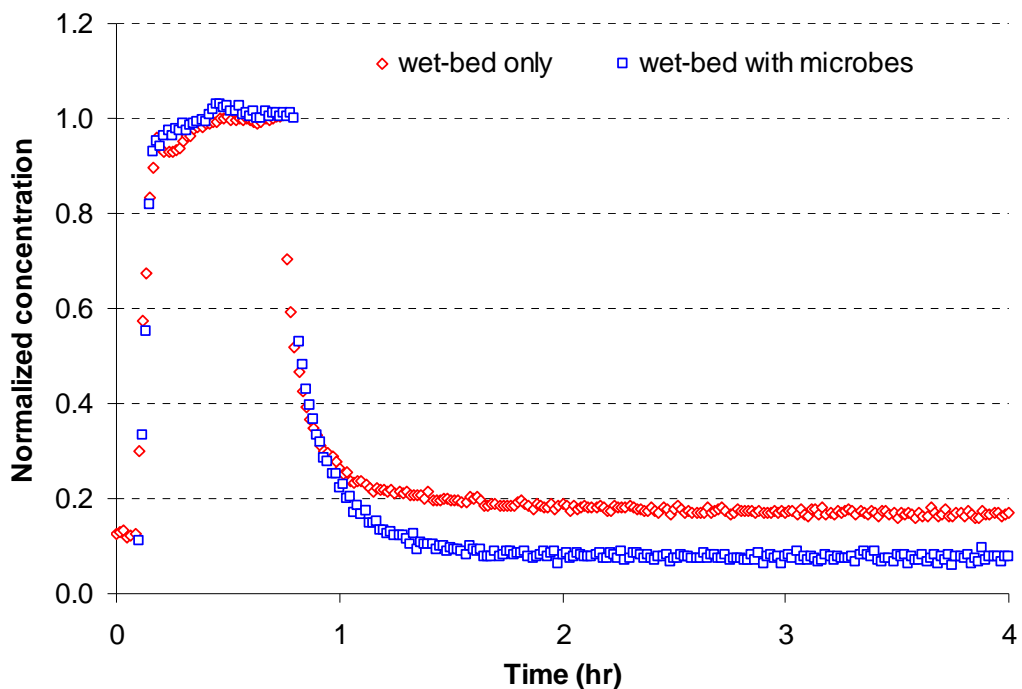


Figure 4-8 Formaldehyde removal by microbes with single-injection

After the single-injection test, the tested formaldehyde loaded sorbent bed was flushed with clean air. The downstream concentration of the sorbent bed was monitored. Figure 4-9 shows the formaldehyde concentration at the bed downstream. Desorption was observed by the presence of the concentration increase (peak) which is due to the formaldehyde adsorption capacity of the sorbent. The formaldehyde peak concentration of sorbent bed with microbes was significant lower and smaller than that without microbes. This indicates that part of the formaldehyde was degraded by the microbes. The un-degraded adsorbed formaldehyde was desorbed as indicated by the lower peak when there was clear air passing through the bed.

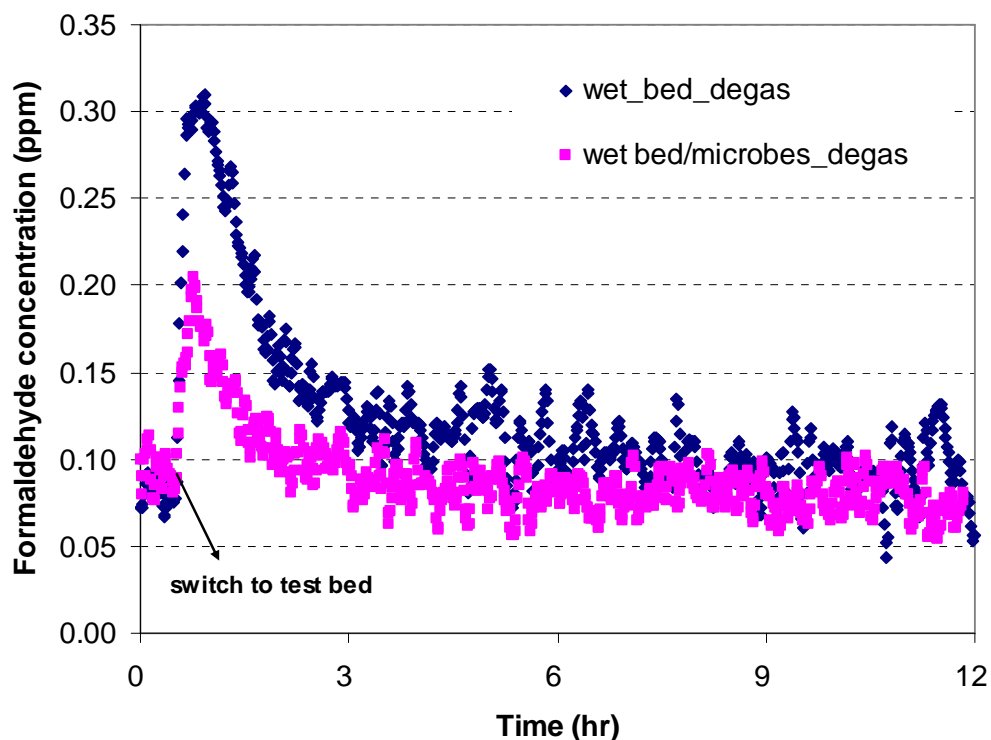


Figure 4-9 Desorption of formaldehyde from sorbent bed with and without microbes

Figure 4-10 shows the normalized formaldehyde concentration in the system vary with time in a multi-injection test. Red diamond points were for the test with wet-sorbent only. Blue square points were for the test with wet-sorbent together with microbes. The difference between these two curves after the system was switched to test loop in each cycle was due to the formaldehyde bio-degradation by microbes.

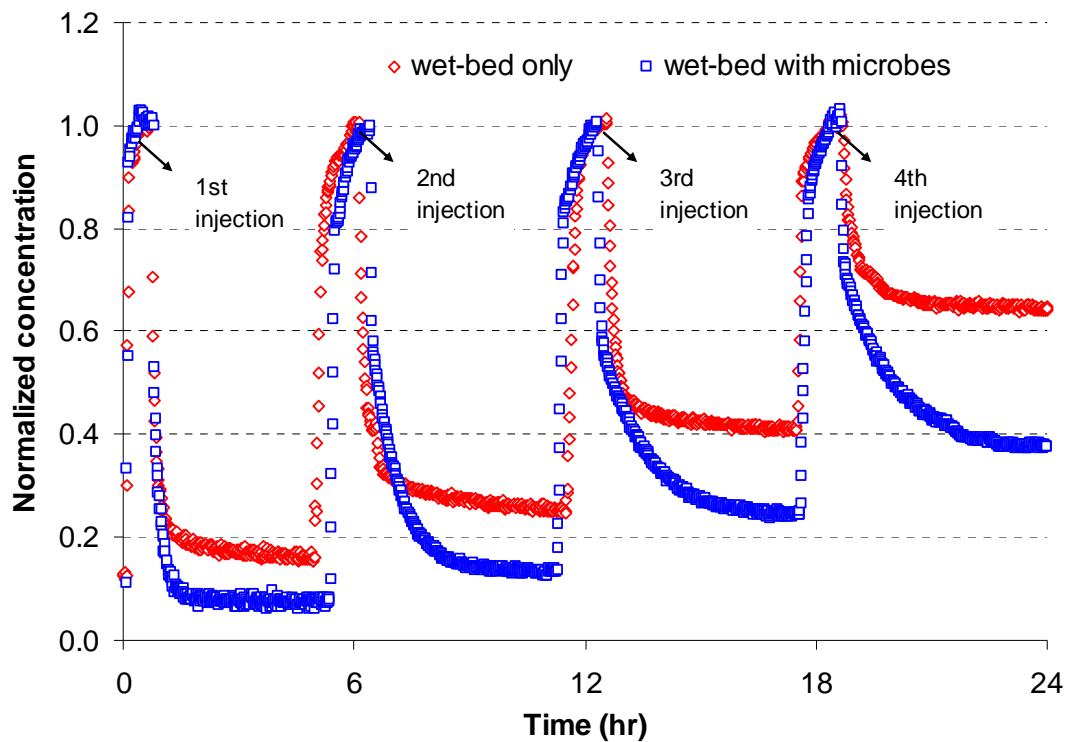


Figure 4-10 Formaldehyde removal by microbes in multi-injection test

The adsorbed formaldehyde mass at steady status of each cycle could be obtained by multiplying the system volume with concentration difference between

initial and equilibrium concentration (as shown in Figure 4-11). These were the measured absorbed mass (as shown in Table 4-6). The maximum absorbed mass could also be calculated according to Henry's Law (Smith and Harvey, 2007):

$$p = k_H \cdot c \quad (4-9)$$

where p is the partial pressure of the solute in the gas above the solution, c is the concentration of the solute and k_H is a constant with the dimensions of pressure divided by concentration. The constant, known as the Henry's law constant, depends on the solute, the solvent and the temperature. The Henry's law constant of formaldehyde is $3.27\text{E-}07 \text{ atm}\cdot\text{m}^3/\text{mol}$.

The bed water content could be obtained from the moisture retention curve (as shown in Figure 4-12). The calculated absorbed masses were also shown in Table 4-6. The measured absorbed mass generally agreed with the calculated absorbed mass. This indicates that the wet-bed had approached its formaldehyde absorption capacity; therefore the concentration reached a quasi-steady at the end of each cycle. A quasi-steady state was also reached with wet-bed with microbes at the end of each cycle. The reason may be that microbes adsorbed the formaldehyde first and it took time to degrade. If degradation process is fast enough, the concentration is expected to continuously decrease. It is also noted that there was a concentration difference between wet-bed only and wet-bed with microbes at the quasi-steady state. This was due to the degradation of absorbed formaldehyde by the microbial community

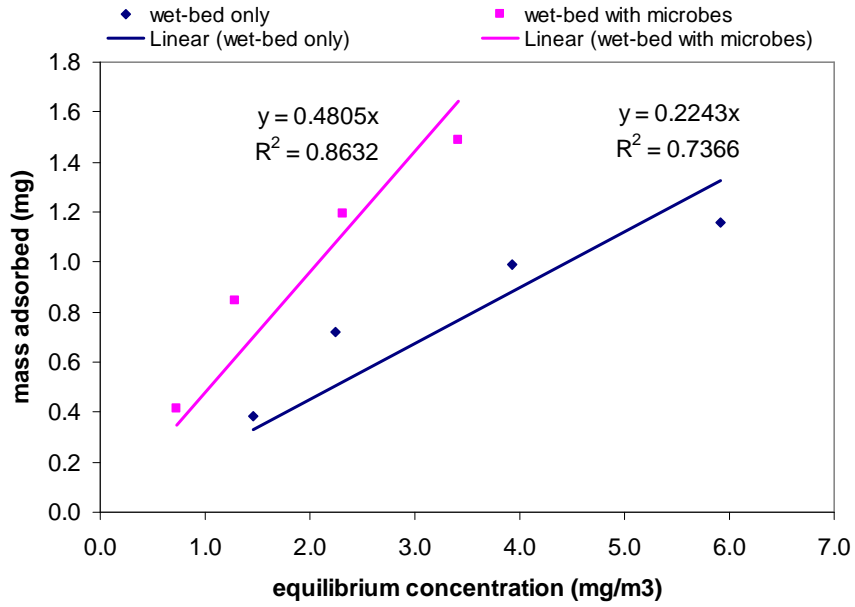


Figure 4-11 Formaldehyde removal isotherm by wet-bed with and without microbes

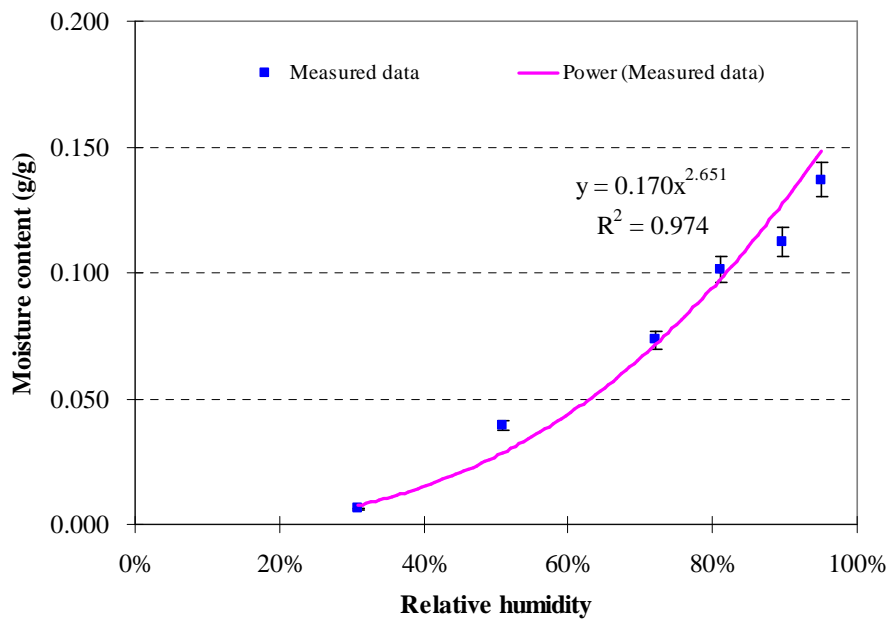


Figure 4-12 Sorbent bed moisture retention curve

Table 4-6 Comparison of calculated and measured adsorbed formaldehyde mass

Equilibrium concentration	Sorbent bed weight	Water content	Henry's law constant for	Calculated absorbed mass	Measured absorbed mass
---------------------------	--------------------	---------------	--------------------------	--------------------------	------------------------

mg/m ³	g	g	formaldehyde		
			atm·m ³ /mol	mg	mg
1.46	30.95	4.24±0.21	3.27E-07	0.455±0.023	0.383
2.25				0.700±0.035	0.720
3.93				1.223±0.061	0.991
5.91				1.842±0.092	1.157

In summary, the microbial communities were found to have significant effect on removing formaldehyde. With the best species from the plant root evenly distributed in a wet sorbent bed, the CADR became ~1050 m³/h per square meter bed.

4.3.3 Formaldehyde Removal by Dynamic Botanical Air Filtration System

Dry Bed V.S. Wet Bed V.S. DBAF. As described in section 4.2.3, empty chamber test was first conducted without the DBAF in the test chamber. Dry bed test, wet bed test and test with DBAF were then conducted. Since the equilibrium concentration for each test was stable, there was no need to monitor the concentration continuously but check for some time daily. The chamber concentration was continuously monitored by PTR-MS for two hours daily. The average of the two hour test data was used as the concentration of that test day. The chamber equilibrium concentrations for different tests were shown in Figure 4-13. It can be seen the chamber equilibrium concentration become relative stable and slightly different in a

one-week test period. Figure 4-14 shows the results of DBAF test for long term. The chamber concentration decreases slightly at the beginning of the test and then kept in a constant level after that.

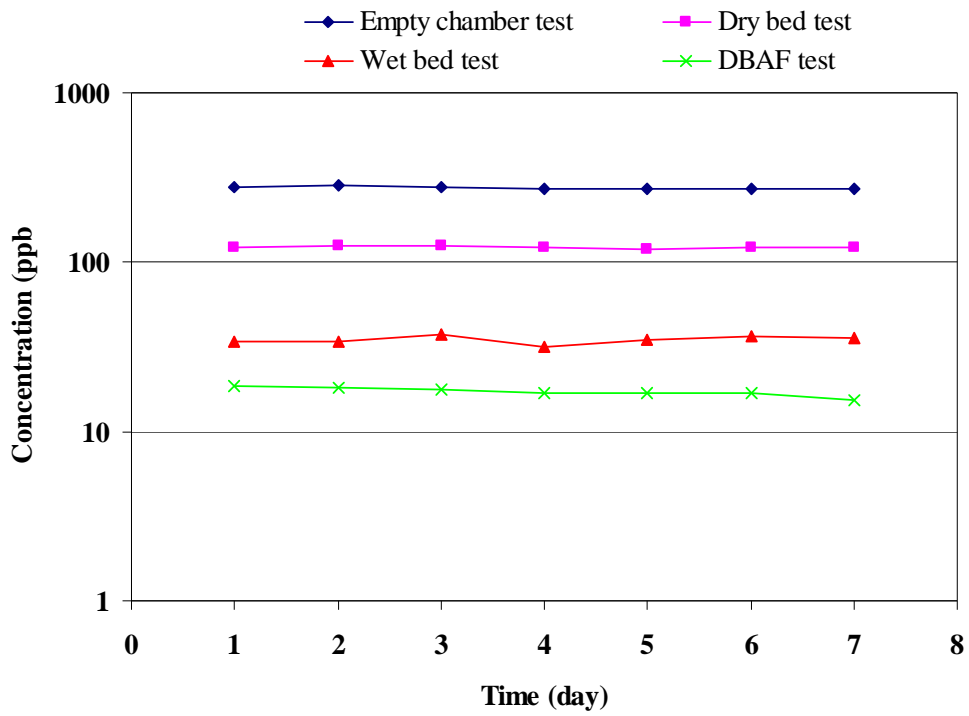


Figure 4-13 Chamber formaldehyde equilibrium concentrations at different RHs

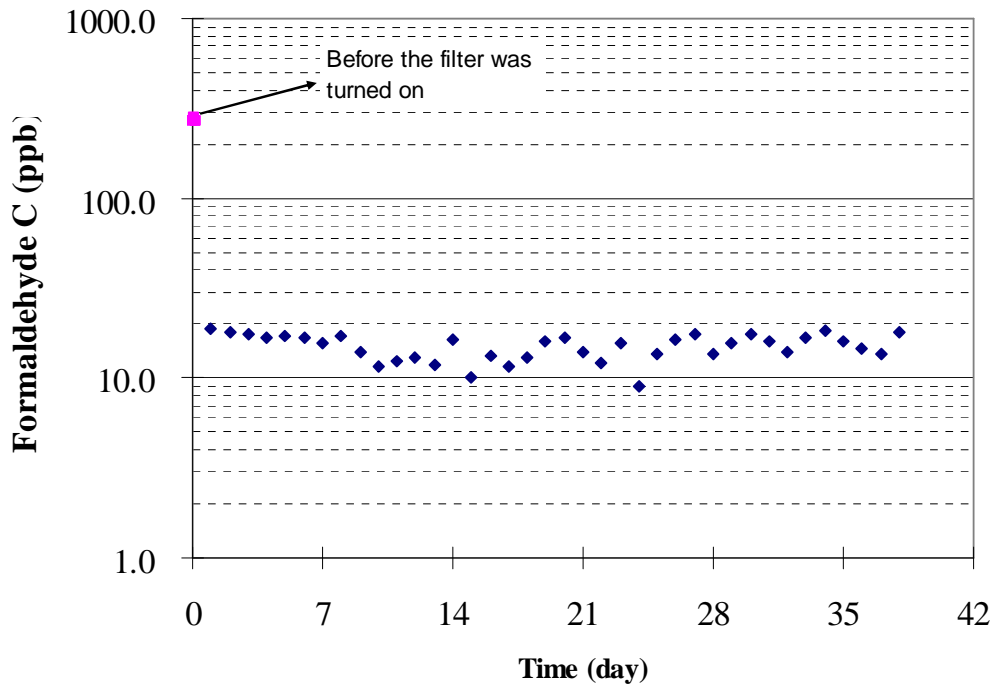


Figure 4-14 Long term formaldehyde removal efficiency by DBAF at 90% RH

Table 4-7 lists single pass efficiency and clean air delivery rate for different tests.

After one day, the SPE of dry bed and wet bed were 3% and 17%, respectively. The corresponding CADR were 1.5 and 8.5 m³/h, respectively. The SPE of DBAF was 32.7% and the CADR was 16.35 m³/h. After one week, the SPE of dry bed and wet bed were 2.6 % and 16.1%. The CADR of the dry bed and wet bed were 1.3 and 8.1 m³/h, respectively. The SPE of DBAF was 39.5% and the CADR was 19.75 m³/h.

Table 4-7 Concentration, SPE and CADR at different RHs

Test period	Empty chamber	Dry bed @ 50±3%RH	Wet bed @90±2%RH	DBAF @90±2%RH

Concentration (ppb)	1 day	278.5	123.3	34.0	18.7
	1 week	275.3	121.0	35.3	15.5
	1 month	273.7	/	/	15.0
Single pass efficiency (%)	1 day	N/A	3	17	32.7
	1 week	N/A	2.6	16.1	39.5
	1 month	N/A	/	/	40.7
CADR (m ³ /h)	1 day	N/A	1.5	8.5	16.35
	1 week	N/A	1.3	8.1	19.75
	1 month	N/A	/	/	20.35

Note: “N/A” means “not applicable”; “/” means “didn’t do”

Figure 4-15 & 4-16 show the CADR and SPE in a bar chart, the CADR due to leaf effect was only ~1% of the total CADR of DBAF. The CADR due to wet sorbent was ~52% of the total CADR. The wet sorbent bed effect includes formaldehyde absorption in water film and adsorption in dry sorbent bed, which was a combined effect. The difference between DBAF and wet sorbent bed test was due to the existence of plant. It also can be seen that the CADR of DBAF increased to 19.75 m³/h one week later, which indicates that the plant microbial community continuously performed well on removing formaldehyde.

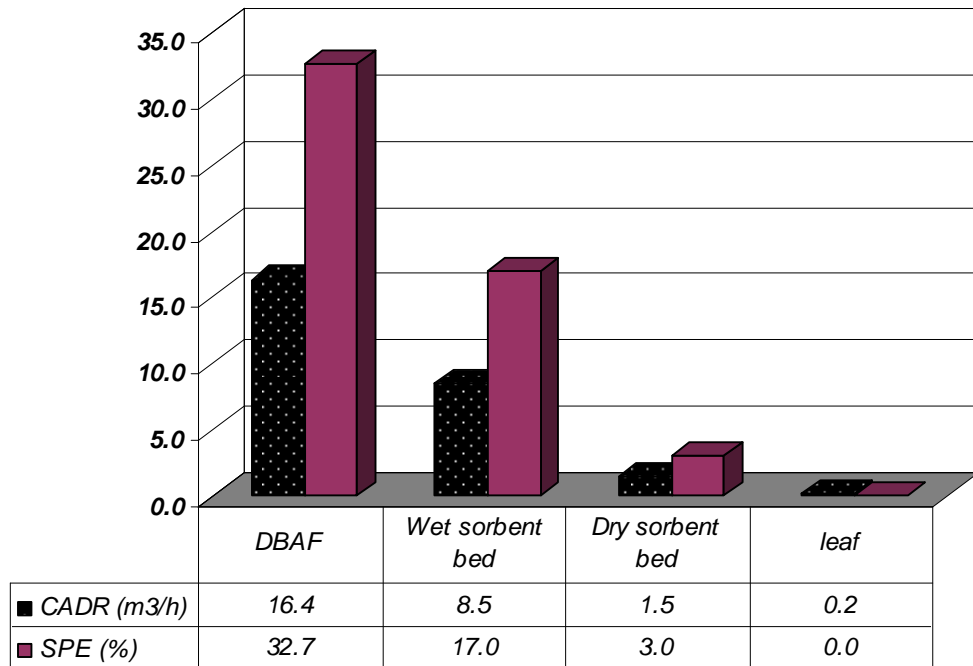


Figure 4-15 CADR and SPE after one day

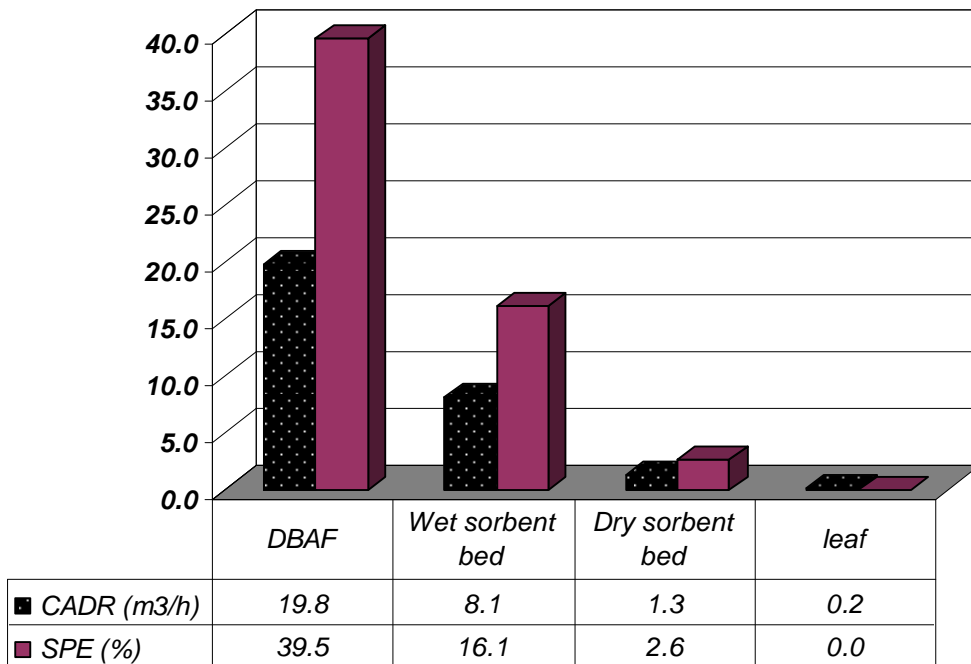


Figure 4-16 CADR and SPE after one week

DBAF at Different RHs. The tests were conducted at three different RH levels: 92%, 75%, and 55%. The different RH level was achieved by adjusting the ventilation. Figure 4-17 shows the chamber RH for different tests. There was slight fluctuation of the RH due to the irrigation, with standard deviation of < 2%. The bed moisture contents for each RH level according to the moisture retention curve were as listed in Table 4-8.

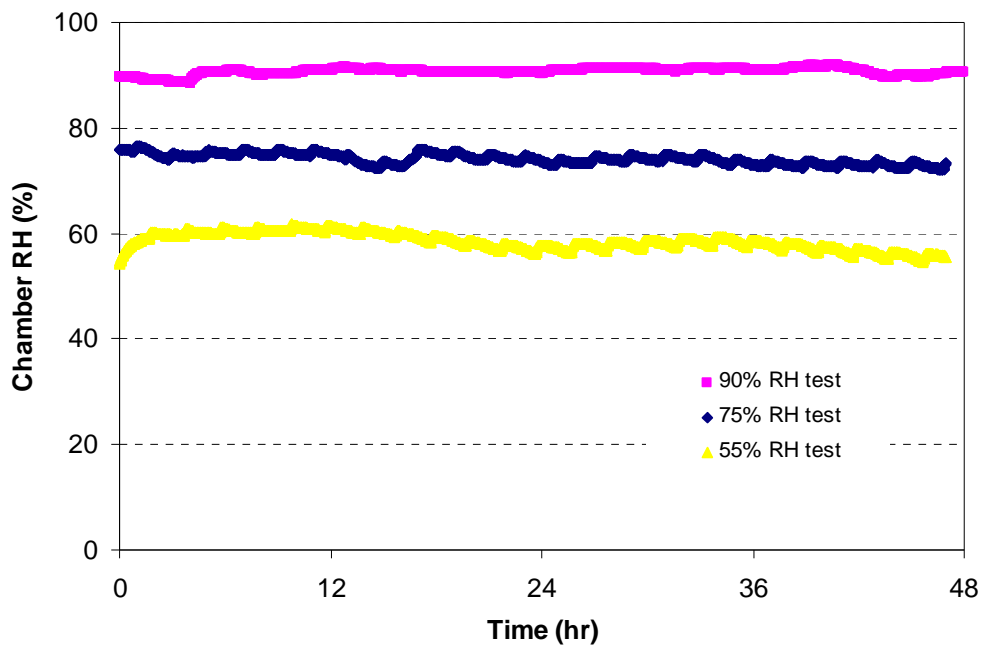


Figure 4-17 Chamber monitored RH at different RHs

Table 4-8 Chamber ventilation and DBAF bed moisture content at different RHs

Chamber RH	Ventilation air flow	Bed moisture content
%	m ³ /h	m ³ /m ³
92±1	1.18	0.137
75±2	5.48	0.078
55±3	7.02	0.034

The formaldehyde removal tests at 75% RH and 55% RH were also conducted. Table 4-9 lists the SPE and CADR of the DBAF in removing formaldehyde at different RHs. After one day, the SPE of DBAF decreased from 32.7–19.9% as RH reduced from 90–55%. The corresponding CADR decreased from 16.35–9.95 m³/h. After two days, the SPE of DBAF reduced from 33.5–20.5%. The CADR reduced from 16.75–10.25 m³/h accordingly.

The single pass efficiency and clean air delivery rate decreased as the RH decreases. Since formaldehyde is a water soluble compound, water vapor in the DBAF bed plays a positive role in removing formaldehyde. As the RH level decreases from 90–55% RH, less water film is available for absorbing formaldehyde. Therefore, the SPE and CADR will decrease. It is consistent with the test results in the real-condition test.

Table 4-9 The formaldehyde SPE and CADR of the DBAF at different RHs

	Test period	DBAF @90%RH	DBAF @75%RH	DBAF @55%RH
Single pass efficiency (%)	1 day	32.7	24.5	19.9
	2 days	33.5	24.7	20.5
CADR (m ³ /h)	1 day	16.35	12.25	9.95
	2 days	16.75	12.36	10.25

Equivalent clean air deliver rate is a useful parameter to evaluate the performance of gas filter. Table 4-10 lists the comparison of equivalent clean air delivery rate for different series of tests. It shows that the CADR was only ~5.1 m³/h per square meter bed without air flow passing through the bed. The test of microbial community with air flow passing by provides equivalent CADR of ~1050 m³/h per square meter bed. While this test was for best species from the plant root system, and the initial microbial density was 9.78E+10 CFU/ml, which was higher than the normal microbial density of 1.0E+06–1.0E+08 CFU/ml. The whole effect of DBAF has a CADR of ~233 m³/h per square meter bed.

Table 4-10 Comparison of CADR at different series of tests

Test set	Potted plant without air flow passing through the bed	Microbial community with air flow passing through	whole effect of DBAF
Test temperature (°C)	23±0.6	23±0.6	23±0.6
Test RH (%)	50±3	90±3	90±3
Test air velocity passing by (m/s)	0	0.25	0.25
Filter bed cross section area (m ²)	3.14E-02	1.26E-04	7E-02
Filter bed thickness (m)	0.15	0.15	0.15
Concentration (ppb)	20000	7500	15
CADR (m ³ /h)/(m ² bed)	5.1	1050	233

Biodegradation Rate Constant Determination. Two processes happened in series for the formaldehyde biodegradation. The first one is the gas phase formaldehyde absorption by the water film, which is followed Henry's Law. The second one is the liquid phase formaldehyde degradation by microbial community, which is followed the first-order kinetics. It should be noted that these two processes are combined with each other. The concentration in the liquid phase and biodegradation rate constant are the two unknown parameters. The biodegradation rate constant can not be directly obtained from experimental data. It has to be fitted from the comparison between the simulation result and experimental data. Nevertheless, the biodegradation rate constant still can be calculated based on the following analysis, which could be used as a reference value.

Biodegradation rate constant calculation can be calculated as follows: the VOC mass balance in the chamber can be expressed as Equation (4-10).

$$V \frac{dC}{dt} = R - Q_v \cdot C_2 - Q_{CADR-total} \cdot C_2 \quad (4-10)$$

where, V is the testing chamber system volume, m^3 ; R is the formaldehyde generation rate, mg/h ; Q_v is the clean air flow rate, m^3/h ; C_2 is the formaldehyde concentration with DBAF in the test chamber, mg/m^3 ; $Q_{CADR-total}$ is the total clean air delivery rate of the DBAF, m^3/h .

The total clean air delivery rate of the DBAF can be further separated into three parts: leaf effect, wet sorbent effect, and microbial community effect.

$$Q_{CADR-total} = Q_{CADR-leaf} + Q_{CADR-wet_sorberent} + Q_{CADR-microbes} \quad (4-11)$$

where $Q_{CADR-leaf}$ is the clean air delivery rate due to leaf effect, m³/h; $Q_{CADR-wet_sorberent}$ is the clean air delivery rate due to wet sorbent effect (including dry bed effect and water effect), m³/h; $Q_{CADR-microbes}$ is the clean air delivery rate due to microbial community effect, m³/h. The CADR of the total DBAF, leaf effect and wet sorbent effect can be calculated from experimental data, and then the CADR due to microbial community can be obtained by Equation (4-11).

The clean air delivery rate due to the microbial community effect could be used to calculate the biodegradation rate constant:

$$Q_{CADR-microbes} \cdot C_{gas} = k \cdot C_{liq} \cdot V_{bed} \cdot \theta_{liq} \quad (4-12)$$

where C_{gas} is the equilibrium gas phase formaldehyde concentration in the chamber, mg/m³; k is the biodegradation rate constant, 1/s; C_{liq} is the equilibrium liquid phase formaldehyde concentration in the filter bed, mg/m³; V_{bed} is the volume of the filter bed, m³; θ_{liq} is the volumetric water content in the filter bed, m³/m³.

The biodegradation rate constant can be obtained:

$$k = \frac{Q_{CADR-microbes} \cdot H}{V_{bed} \cdot \theta_{liq}} \quad (4-13)$$

where H is the Henry's law constant, dimensionless.

Table 4-11 Determination of formaldehyde bio-degradation rate constant

CADR due to	Henry's law	Bed	Bed	Bio-degradation
-------------	-------------	-----	-----	-----------------

microbes effect	constant(unit)	volume	water content	rate constant
m^3/h		(m^3)	(m^3/m^3)	$(1/\text{s})$
7.60	1.33E-05	0.011	0.13	2.06E-05

4.3.4 Toluene Removal by Dynamic Botanical Air Filtration System

Toluene removal by DBAF at different RHs were also conducted. Table 4-12 lists the SPE and CADR of the DBAF in removing toluene at different RHs. After one day, the SPE of DBAF increased from 10.1–37.3% as RH decreased from 90–55% RH. The corresponding CADR increased from 5.05–18.65 m^3/h . After two days, the SPE and CADR of DBAF were staying in the same level as that of one-day test.

The single pass efficiency and clean air delivery rate increased as the RH decreases. Since toluene is a water insoluble compound, water vapor in the DBAF bed plays a negative role in removing toluene. As the RH level decreased from 90–55% RH, more adsorption sites were available for adsorbing toluene. Therefore, the SPE and CADR would increase. It was consistent with the test results in the real-condition test.

The toluene biodegradation by microbial community can not be clearly determined through this series of test. It could be analyzed that the toluene biodegradation rate in the liquid phase will be very small since toluene is highly water insoluble. Still, there is a possible that the bio-degradation would occur when the microbial community expose to the adsorbed toluene directly. The tests conducted in this chapter are hard to determine the bio-degradation rate of toluene.

Table 4-12 The SPE and CADR of the DBAF in removing toluene at different RHs

	Test period	DBAF @90%RH	DBAF @75%RH	DBAF @55%RH
Single pass efficiency (%)	1 day	10.1	27.5	37.3
	2 days	10.9	29	34.8
CADR (m ³ /h)	1 day	5.05	13.75	18.65
	2 days	5.45	14.5	17.4

4.4 Major Findings

In order to improve the understanding of the mechanisms of the DBAF system in removing the volatile organic compounds, a series of further experiments were conducted to determine the important factors affecting the removal performance, and the roles of different transport, storage and removal processes were also investigated. In general, it was found that passing the air through the root bed with microbes was essential to obtain meaningful removal efficiency. Moisture in the root bed also played an important role, both for maintaining a favorable living condition for microbes and for absorbing water-soluble compounds such as formaldehyde. The role of the plant was to introduce and maintain a favorable microbe community that effectively degraded the VOCs that were adsorbed or absorbed by the root bed. While the moisture in a wet bed had the scrubber effect for water-soluble compounds such as formaldehyde, presence of the plant increased the removal efficiency by about a factor of two based on the results from the reduced-scale root bed experiments.

Moreover, for the same cross-section area of 0.35 m long and 0.2 m wide, the dry bed with airflow had an equivalent CADR of $\sim 1.5 \text{ m}^3/\text{h}$. The wet bed with airflow had an equivalent CADR of $\sim 8.5 \text{ m}^3/\text{h}$. The DBAF had an equivalent CADR of $\sim 16.4 \text{ m}^3/\text{h}$. The difference of wet bed with airflow and DBAF was due to the existence of plant. It was found that wet bed and microbial community are the two major factors to affect the formaldehyde removal. It was hard to find out which one was the dominant one in short-time test (one day), while the result shows that microbial community would become dominant gradually as time went on.

The biodegradation rate constant for formaldehyde was also determined, which was $2.06\text{E-}05 \text{ s}^{-1}$ at 92%RH and 15 ppb formaldehyde level. It should be noted that this rate constant was only for comparison. Because the transfer of formaldehyde from gas phase into liquid film and formaldehyde degradation by microbial community occurred in series but not in parallel. They can not be exactly separated from the experimental result, while it can be used as a reference for the model initial input.

Chapter 5. Model Simulation and Validation

5.1 Introduction

As noted in Chapter 2 Literature Review, “Biological purifier” is used to describe any device that includes a biological component (botanical or microbial) for VOC removal. “Bio-filter” or “Bio-trickling filter” is used to describe the devices that use a packed bed of a solid support colonized by attached microorganisms that biodegrade the VOC in the air passing through. “Botanical purifier” or DBAF is used to specifically describe the devices that use plants and their associated microorganisms. Many investigators have created mathematical models of bio-filters and bio-trickling filters in their efforts to understand and improve reactor performance (Hodge and Devinny, 1997; Devinny and Ramesh, 2005), while this study represents a first attempt to model the operation of DBAF using a numerical simulation model.

The CHAMPS-BES (Nicolai, 2009) was further developed to account for the effects of the microbes on the degradation of both water-soluble and non-soluble VOCs. The improved numerical model was then used to simulate the operation of a botanical air filtration system that used a mixture of activated carbon and porous shale pebbles as root bed of selected plants (such as Golden Pothos(*Epipremnum aureum*)). The filtration system was operated with periodical irrigation and HVAC return airflow passing-through the root bed. VOC including aldehydes were either adsorbed by the activated carbon sorbent or absorbed by water films in the wet root bed (which

acts as a wet scrubber for water soluble compounds such as formaldehyde). The adsorbed and/or absorbed organic compound could be degraded by the microorganism in the root bed, which would regenerate the sorbent in the root bed. The purified air returned to indoor environment to improve indoor air quality. These transport and removal mechanisms were discussed in Chapter 4. The laboratory and real-world environment tests discussed in Chapter 3 also demonstrated that the DBAF system had a single-pass removal efficiency of 60% for formaldehyde and 20% for toluene, and the removal efficiency for both compounds did not decrease significantly over 300-day continuous operation.

In this chapter, we present: 1) a mechanistic numerical model that can be used to optimize the design and operation of the system as well as improve the understanding of the pollutant transport and degradation processes involved; and 2) comparisons between the model simulation results and experimental data, and a method to estimate the bio-degradation rate constant required for the simulation.

5.2 Model Development

5.2.1 Model Description and Assumptions

As air passes through the filter, the processes involved in the VOC transport, adsorption/absorption and decomposition mechanism in the whole bio-filtration system include (Figure 5-1):

1. **VOC advection by airflow.** The transport of gas phase VOC by air flow through the filter bed;
2. **VOC gas phase diffusion through bed void.** The VOC diffusion through bed void occurs;
3. **VOC convective mass transfer to sorbent-air interface to be adsorbed by the sorbent.** This is the mass transfer-adsorption process of adsorbable compounds from the bulk of the gas phase to the external surface of adsorbent pellets (activated carbon). Each sorbent pellet is assumed to be homogeneous and the VOC internal diffusion in the micro-pores is not described in detail in the current model;
4. **VOC convective mass transfer to liquid-air interface to be absorbed by the liquid (water).** This is the absorption process describing transport of gaseous pollutant from the air into contacting liquid, such as water film at the surface of sorbent/pebble. The liquid serves as a solvent for the pollutant. Water film formed in the surface of pebbles or activated carbon will become the wet scrubbers, where water soluble compounds such as formaldehyde in the indoor air can be absorbed on it;
5. **VOC physical adsorption by activated carbon.** After pollutant molecules transport from gas phase to solid phase by convective mass transfer at the surface of solid, instant equilibrium between gas phase and solid phase is assumed, which is described by a constant partition coefficient;
6. **VOC absorption by liquid film.** Henry's law constant is the parameter to describe the instant equilibrium between gas phase and liquid phase;

7. **VOC consumption by microorganisms.** The microbial community in the root bed will consume the absorbed or adsorbed VOC as a food source.

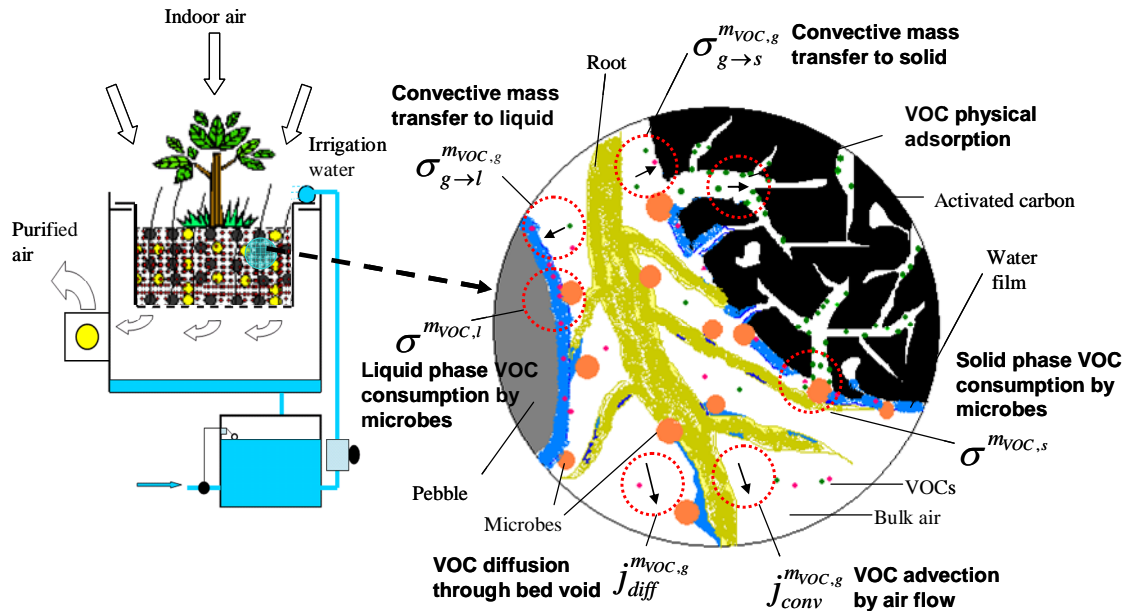


Figure 5-1 Schematic of the root bed system and associated transport and storage processes

It is not practical, nor necessarily important to model every phenomenon that occurs in the filter. As a first attempt, we adopted the following assumptions in developing the mathematical model:

- Laminar flow occurs in the bed (Reynold's number ~ 122 in this case, with superficial velocity of 0.25m/s , equivalent spherical diameter of the particle of 0.005m , and void fraction of the bed of 0.35);
- The sorbent pellet is in a spherical shape (equivalent spherical diameter of the

particle of 0.005m);

- Filter-material composition is homogeneous (e.g., porosity, density);
- Advection and diffusion of the adsorbate in the water film (liquid phase) are

negligible;

- The partition coefficient is constant for a given temperature regardless the change in concentration;

- Consumption rate of the VOC by microorganisms follows first-order kinetics.

5.2.2 Governing Equations

VOC in the filter bed are divided into three components: gas phase, adsorbed in solid and absorbed in liquid.

5.2.2.1 VOC Mass Balance in Gas

Transport of gas phase VOC can happen via convection with air, through diffusion, exchange between gas and solid, and exchange between gas and liquid. It can be expressed:

$$\frac{\partial \rho^{m_{VOC,g}}}{\partial t} = -\frac{\partial}{\partial x} \left(j_{conv}^{m_{VOC,g}} + j_{diff}^{m_{VOC,g}} \right) - \sigma_{g \rightarrow s}^{m_{VOC,g}} - \sigma_{g \rightarrow l}^{m_{VOC,g}} + \sigma^{m_{VOC,g}} \quad (5-1)$$

where $\rho^{m_{VOC,g}}$ is the VOC density in gas, kg/m³; $j_{conv}^{m_{VOC,g}}$ is VOC mass flux due to convection, kg/(m²s); $j_{diff}^{m_{VOC,g}}$ is VOC mass flux due to diffusion, kg/(m²s); the exchange between gas and solid is denoted by $\sigma_{g \rightarrow s}^{m_{VOC,g}}$, kg/(m³s); the exchange between

gas and liquid is denoted by $\sigma_{g \rightarrow l}^{m_{VOC,g}}$, kg/(m³s), whereas the arrow indicates positive transfer direction. The term $\sigma^{m_{VOC,g}}$ can be used to describe any source or sink of gas phase VOC components, such as a constant emission source. This term is zero in the current botanical filtration model.

The VOC transport by convection happens through the bulk air movement. It can be expressed as:

$$j_{conv}^{m_{VOC,g}} = c_{air}^{m_{VOC}} j^{m_g} \quad (5-2)$$

where $c_{air}^{m_{VOC}}$ is the gas phase VOC concentration (mass fraction), kg(VOC)/kg(air); j^{m_g} is air mass flux density from the airflow calculation, kg(air)/(m²s), determined by:

$$j^{m_g} = -K_a \frac{\partial p_a}{\partial x} \quad (5-3)$$

For the sorbent bed filter, the air flux can be determined by the air permeability of the bed and pressure drop across the filter as follows:

$$j^{m_g} = -K_a \frac{\Delta p}{\Delta x} \quad (5-4)$$

where K_a is air permeability through the media, s; p_a is air pressure, which equals to the sum of partial pressures of dry air and water vapor, Pa; ΔP is the pressure difference across the entire root bed, Pa; x is the coordinate in the bed flow direction, m; Δx is thickness of the bed, m.

The diffusion flux of gas phase VOC in the bed void is calculated by:

$$j_{diff}^{m_{VOC,g}} = -\frac{D_{VOC,mat}}{R_{VOC}T} \frac{\partial p_{VOC,g}}{\partial x} \quad (5-5)$$

where $D_{VOC,mat}$ is the VOC diffusion coefficient in the root-bed material system (considered as a porous medium), it is calculated by the VOC diffusion coefficient in air, $D_{VOC,air}$ (given in m^2/s), and diffusion resistance factor, μ_{voc} (dimensionless, which takes into account the tortuosity of bed-void); R_{VOC} is the gas constant for VOC, $JK^{-1}mol^{-1}$; T is the temperature, K; $p_{VOC,g}$ is the VOC partial pressure, Pa; x is the coordinate in the bed flow direction, m.

$$D_{VOC,mat} = \frac{D_{VOC,air}}{\mu_{VOC}} \quad (5-6)$$

Adsorption Flux: VOC Transfer from Gas to Solid-air Interface. When there is a concentration gradient between the gas phase concentration in the bulk air and at the surface of sorbent (gas phase at surface boundary layer, which is assumed to be in instantaneous equilibrium with the adsorbed VOC at the surface with a partition coefficient, K_{ma}), there will be an exchange flux into the direction of the lower concentration.

The mass transfer equation from gas phase to solid phase can now be given:

$$\sigma_{g \rightarrow s}^{m_{VOC,g}} = \frac{k_{m,g \rightarrow s} A_{tol} (1-w)}{V_{REV}} (\rho_{gas}^{m_{VOC,g}} - \rho_{gas}^{m_{VOC,s}}) = \frac{k_{m,g \rightarrow s} A_{tol} (1-w)}{V_{REV}} \left(\rho_{gas}^{m_{VOC,g}} - \frac{\rho^{m_{VOC,s}}}{K_{ma}} \right) \quad (5-7)$$

where $k_{m,g \rightarrow s}$ is the VOC mass transfer coefficient between gas and solid, m/s; A_{tol} is the total external surface area of the sorbent material that is available for pollutant/VOC adsorption or absorption, m^2 ; w is the wetness ratio of the surface of the activated carbon pellet (It is a function of the bed volume water content: the wetness ratio equal to zero when the bed is absolutely dry and equal to one as the bed

is total saturated with water), dimensionless. V_{REV} is the reference element volume, m^3 ; K_{ma} is the partition coefficient of the solid media.

The total surface area for spherical pellet sorbent bed can be calculated by Equation (5-8):

$$A_{tol} = \frac{(1 - \theta_{por}) V_{REV}}{\frac{4}{3} \pi R^3} 4\pi R^2 = \frac{3V_{REV} (1 - \theta_{por})}{R} \quad (5-8)$$

where θ_{por} is the porosity of the sorbent bed, dimensionless; R is the radius of the sorbent particle/pellet, m.

Absorption Flux: VOC Transfer from Gas to Liquid-air Interface. For water soluble pollutant/VOC, such as formaldehyde, when there is a concentration gradient between the gas phase concentration in the bulk air and the surface of the liquid (gas phase at the surface boundary layer of liquid, which is also assumed to be in instantaneous equilibrium with the absorbed VOC at the surface with a Henry's law constant H), there will be an exchange flux into the direction of the lower concentration.

The mass transfer equation from gas phase to liquid phase can be expressed:

$$\sigma_{g \rightarrow l}^{m_{VOC,g}} = \frac{k_{m,g \rightarrow l} A_{tol} w}{V_{REV}} (\rho_{gas}^{m_{VOC,g}} - \rho_{gas}^{m_{VOC,l}}) = \frac{k_{m,g \rightarrow l} A_{tol} w}{V_{REV}} (\rho_{gas}^{m_{VOC,g}} - H \rho^{m_{VOC,l}}) \quad (5-9)$$

where $k_{m,g \rightarrow l}$ is the VOC mass transfer coefficient between gas and liquid, m/s; w is the wetness ratio, dimensionless; $A_{tol} w$ is the total external surface area of the liquid film covering the sorbent material or pebble in filter bed, m^2 ; H is Henry's law

constant, m^3/m^3 .

5.2.2.2 VOC Mass Balance in Solid

VOC mass balance in the solid can be expressed:

$$\frac{\partial \rho^{m_{VOC,s}}}{\partial t} = \sigma_{g \rightarrow s}^{m_{VOC,g}} + \sigma^{m_{VOC,s}} \quad (5-10)$$

where $\rho^{m_{VOC,s}}$ is the VOC density in solid, kg/m^3 ; $\sigma_{g \rightarrow s}^{m_{VOC,g}}$ is the VOC transport from gas phase by convective mass transfer, $kg/(m^3s)$; $\sigma^{m_{VOC,s}}$ is considered as the common source/sink term. The consumption of adsorbed VOC by microbes is such a sink in the botanical filtration system. Another example is the chemi-sorption process (negative source term), and it is not available in the botanical air filtration system.

5.2.2.3 VOC Mass Balance in Liquid

VOC mass balance in liquid film can be expressed:

$$\frac{\partial \rho^{m_{VOC,l}}}{\partial t} = \sigma_{g \rightarrow l}^{m_{VOC,g}} + \sigma^{m_{VOC,l}} \quad (5-11)$$

where $\rho^{m_{VOC,l}}$ is the VOC density in liquid, kg/m^3 ; $\sigma_{g \rightarrow l}^{m_{VOC,g}}$ is the VOC transport from gas phase by convective mass transfer, $kg/(m^3s)$; $\sigma^{m_{VOC,l}}$ is considered as the common source/sink term. An example for such a source/sink term in the botanical filtration system is the process of pollutant/VOC degradation by microbes in the root system (negative source term).

5.2.2.4 Source/Sink Flux for Solid/Liquid Phase VOC: Microbial

Biodegradation.

The absorbed or adsorbed VOC will be served as carbon source for microorganisms. As long as there is carbon source in the liquid film or sorbent surface, the microbes will take them as nutrition, thus the VOC will be degraded. Basically, there are two main factors that affect the VOC degradation by microbes. One is the available carbon source, and the other is the number of microbes that will take charge of the degradation (Devinny and Ramesh, 2005). So the biodegradation flux can be expressed as:

$$\sigma^{m_{VOC,l}} = K\rho^{m_{VOC,l}} \quad (5-12)$$

where K is the total biodegradation rate constant for the microbial species found in the root bed, s^{-1} ; $\rho^{m_{VOC,l}}$ is the VOC density in liquid or at the solid surface, kg/m^3 .

Note that for simplification, it is assumed that the microbes live in liquid films and have access to VOCs within the film and solid surfaces though the detailed nature of the microbial activities are not known (e.g., It is conceivable that the area and spatial distribution of the liquid film in the root bed may vary or fluctuate over time giving opportunity for adsorption of water-soluble compounds at one time when uncovered by the liquid file and expose to microbes at another when covered by the liquid film).

Note: The biodegradation rate constant is dependent on the number of microbes, which depends on the density of microbial community and the area of the root bed.

The biodegradation rate constant in this study was obtained from the experimental

results. It was the total effect of DBAF. Further research is needed regarding the effect of number of microbes.

5.2.3 Determination of Model Parameters

Table 5-1 lists the key input parameters of the numerical model. The partition coefficients were obtained from experimental data. The Henry's Law constants were obtained from literature (as discussed in Chapter two). The gas to solid and gas to liquid mass transfer coefficients were calculated based on the following equation for Sherwood number (Sh) (Devinny and Ramesh, 2005).

$$k_m = \frac{D_{air}}{2R_p} \cdot Sh = \frac{D_{air}}{2R_p} \cdot [2 + 1.1Re^{0.6} Sc^{0.33}] \quad (5-13)$$

where k_m is the gas to solid or liquid mass transfer coefficient, D_{air} is the gas-phase diffusion constant, R_p is the radius of particle, Sh the Sherwood number, Re the Reynolds number, and Sc is the Schmidt number.

Table 5-1 Model key parameters determination

Parameter	Formaldehyde	Toluene
Partition coefficient	2.91E+04	4.04E+06
Henry's Law constant (C_{gas}/C_{liquid})	1.33E-05	0.28
Gas to solid mass transfer coefficient (m^3/s)	0.27	0.27

Gas to liquid mass transfer coefficient (m ³ /s)	0.55	0.55
-------------------------------------------------------------	------	------

5.3 Model Implementation

The model was implemented in CHAMPS-BES as follows: (1) VOC mass was considered existing in gas, solid and liquid phase; (2) VOC adsorption flux, absorption flux and bio-consumption flux were implemented as sink terms, which were applied as “Field Conditions”; (3) water source was enabled to simulate the irrigation of the DBAF.

5.4 Simulation Results

Model verification was first conducted to test whether the developed model could work. Model validation was then conducted by comparing to the experimental data, which also resulted in an estimate for the fitted bio-degradation rate.

5.4.1 Model Verification

In the present study, simulations were first conducted to predict the bed air flow and moisture distribution. The dimension of the filter bed was 1.8 m by 0.6 m by 0.2 m. The activated carbon particle diameter was 4×10^{-3} m. Filter inlet air was maintained at 20 °C with relative humidity of 30% RH. Air density is 1.2 kg/m³ at 20 °C. Bed initial average moisture content was $0.1 \text{ m}^3_{(\text{water})}/\text{m}^3_{(\text{bed})}$. The irrigation system

ran for 3 minutes every hour to keep the bed volumetric water content level no less than $0.08 \text{ m}^3(\text{water})/\text{m}^3(\text{bed})$.

5.4.1.1 Modeling of Air Flow through the Bed

In current model, the pressure drop between the inlet and outlet of the filter was an input parameter. It was measured to be 73 Pa with $0.229 \text{ m}^3/\text{s}$ air passing through the entire bed (cross-section area of 1.08 m^2 and thickness of 0.2 m). According to Equation (5-4), the air permeability can be calculated by airflow rate and pressure drop across the filter. The calculated air permeability was 0.00069 s, and was assigned to the material in the bed. Based on above parameter input to the model, the output air flux passing through the root-bed was $0.254 \text{ kg}/(\text{m}^2\text{s})$, which was the same as the measured air flow rate considering air density of $1.2 \text{ kg}/\text{m}^3$ at 20°C and bed cross-section area of 1.08 m^2 .

5.4.1.2 Modeling of Moisture Distribution in the Bed

The initial moisture content in the bed was set as $0.1 \text{ m}^3(\text{water})/\text{m}^3(\text{bed})$. A water source term was assigned in the field condition to simulate the periodical irrigation. The water source was activated for three minutes every hour. Water was added into the bed at the rate of $0.09 \text{ kg}/(\text{m}^3\text{s})$, which means 0.09 kg water was added in per cubic meter bed per second. Figure 5-2 shows the average bed moisture content and outlet air RH change over time from simulation. It is shown that due to the

scheduled irrigation, the average bed moisture content was maintained at 0.08~0.1 $\text{m}^3(\text{water})/\text{m}^3(\text{bed})$. Meanwhile, the bed outlet air RH was in the range of 60% to 95%. Previous field tests showed that the measured bed outlet air RH was between 74% and 82%. It is shown in Figure 5-3 that bed moisture content changes over time by simulation.

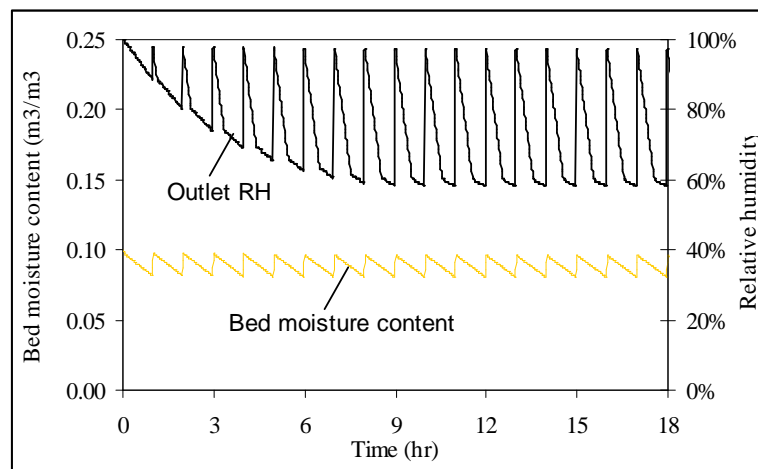


Figure 5-2 Bed average moisture content and outlet air relative humidity

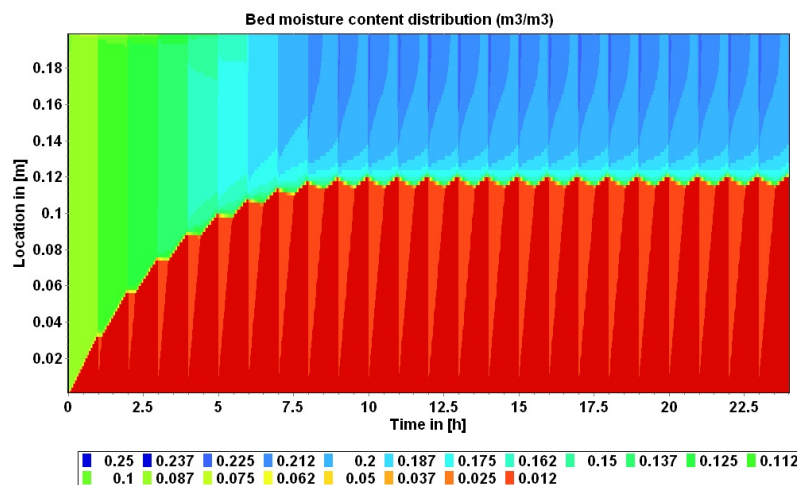


Figure 5-3 Vertical distribution of bed moisture content over time

5.4.1.3 Modeling of Breakthrough Profiles

Breakthrough curve simulation was conducted to investigate the effect of the parameters involved in the filter model to the filter performance. There are two main factors in the physical adsorption process: one is the partition coefficient, and the other is the gas-to-solid mass transfer coefficient. Partition coefficient reflects the capacity of a material on adsorbing VOC. Higher partition coefficient means bigger capability. Higher gas-to-solid mass transfer coefficient means faster mass transfer between gas and solid phase.

Effect of Partition Coefficient. In order to investigate the effect of partition coefficient, the gas-to-solid mass transfer coefficient was fixed at $0.27 \text{ m}^3/\text{s}$ (the convective mass transfer was 0.05 m/s), which was for current five inches sorbent bed based on the calculation. The partition coefficient of the sorbent material was set up at 1, 10, 100 and 1000, respectively. Figure 5-4 shows the change of outlet VOC concentration at above four different partition coefficients. The inlet pollutant concentration was maintained at 0.1 mg/m^3 . The outlet concentration reached equilibrium in less than one minute when the partition coefficient was only one. As the partition coefficient increased from 1 to 1000, it took longer time to have the outlet concentration increased to the same value as the inlet. It can be seen that the model could present the effect of partition coefficient well.

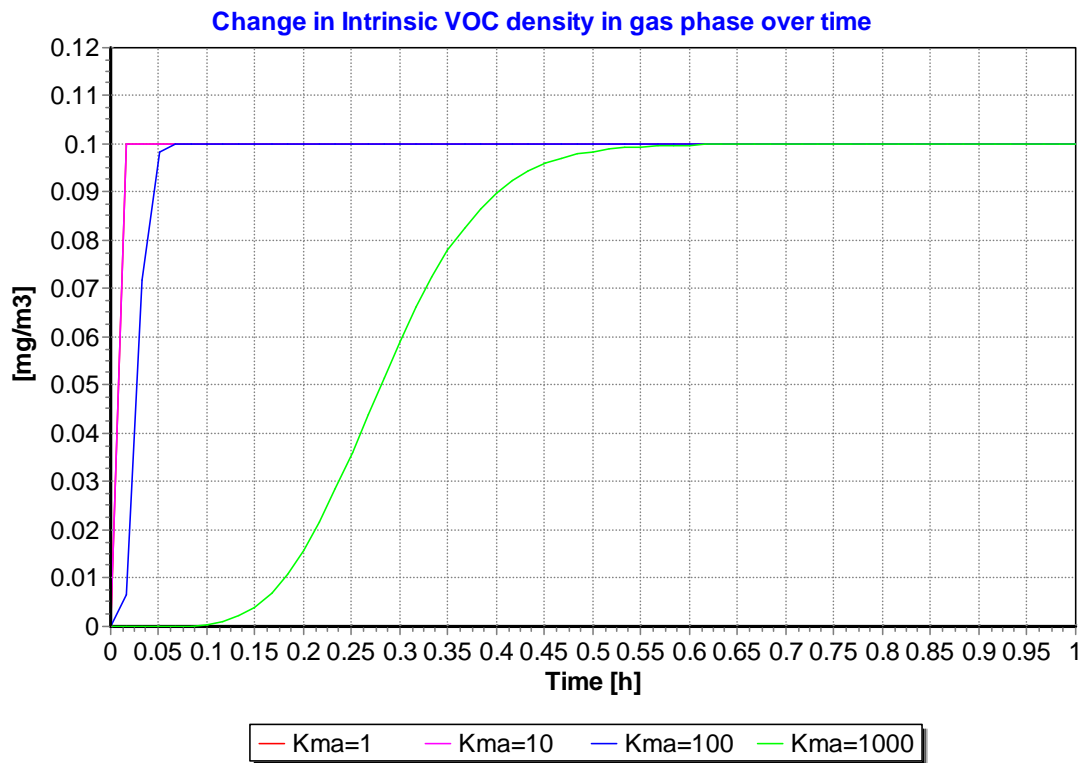


Figure 5-4 Effect of partition coefficient

Effect of Gas-to-solid Mass Transfer Constant. When it came to simulate the effect of gas-to-solid mass transfer constant, the partition coefficient was fixed at 1000, while the gas-to-solid mass transfer constant was set up at 0, 0.1, 1 and 10, respectively. The simulation result was as shown in Figure 5-5. For the gas-to-solid mass transfer constant of 0, it means that there was not any mass transfer occurred between gas phase and solid phase. The red curve in Figure 5-5 was for the mass transfer constant at 0, which was as expected that the outlet concentration increased to the same value as the inlet concentration once the simulation started. Meanwhile, as the mass transfer constant increased, it took less time to have the outlet concentration

become to the equilibrium concentration (same as inlet concentration), which indicated that the mass transfer process would become quicker as the transfer coefficient increased. The results show that the model presents the effect of gas-to-solid mass transfer constant well.

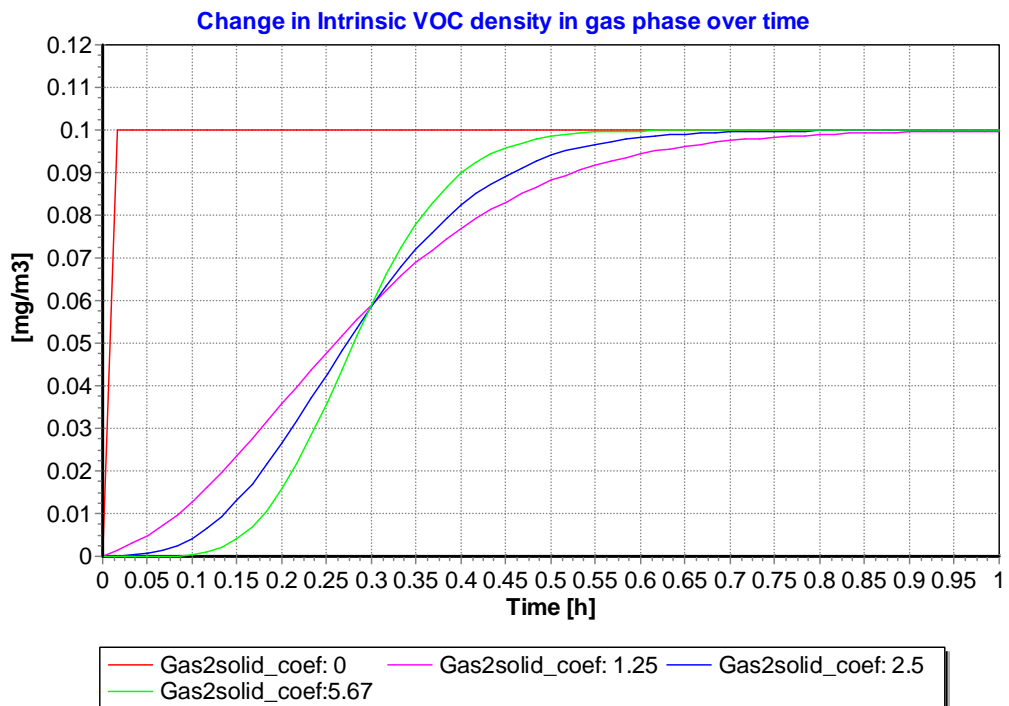


Figure 5-5 Effect of gas to solid mass transfer coefficient

Effect of Gas-to-liquid Mass Transfer Constant. The next step was to simulate the pollutant absorption by the wet surface of the sorbent particle. For the water soluble compounds, such as formaldehyde, the main principle of absorption is due to the presence of moisture (or water vapor). There are also two major impact factors in the absorption process: one is the Henry's Law constant, and the other is the

gas-to-liquid mass transfer constant. At normal operation condition (20 °C and 1 atm), the Henry's law constant is constant. For example, the Henry's law constant for formaldehyde is $1.33 \times 10^{-5} \text{ m}^3/\text{m}^3$ (Benoit et al., 2008). The gas-to-liquid transfer coefficient represents the mass flux per unit surface area and per unit concentration difference. A Higher coefficient value means higher rate of mass transfer. Figure 5-6 shows the effect of gas-to-solid mass transfer coefficient to the breakthrough curve. It can be seen that it took less time to have the outlet concentration to reach the equilibrium concentration (same as inlet concentration) as the mass transfer coefficient increased. Figure 5-7 shows the breakthrough curve at different gas-to-liquid constants with the irrigation on for 3 minutes per hour. The fluctuation of the outlet concentration was due to the irrigation (water source assigned in the field condition).

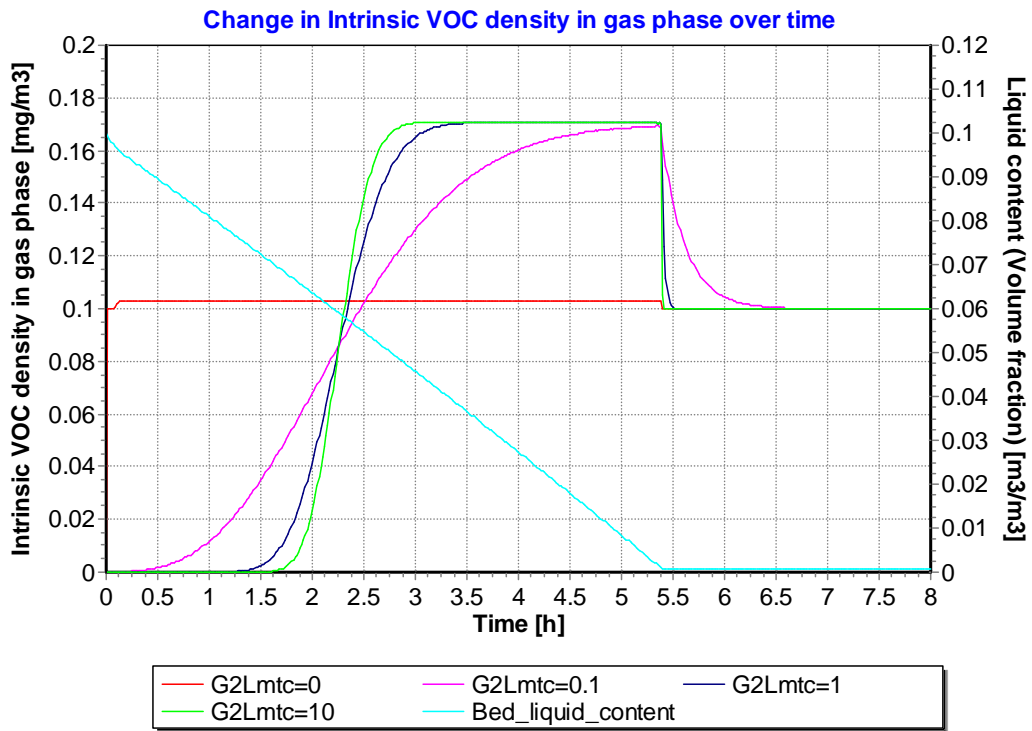


Figure 5-6 Effect of gas to liquid coefficient constant without irrigation

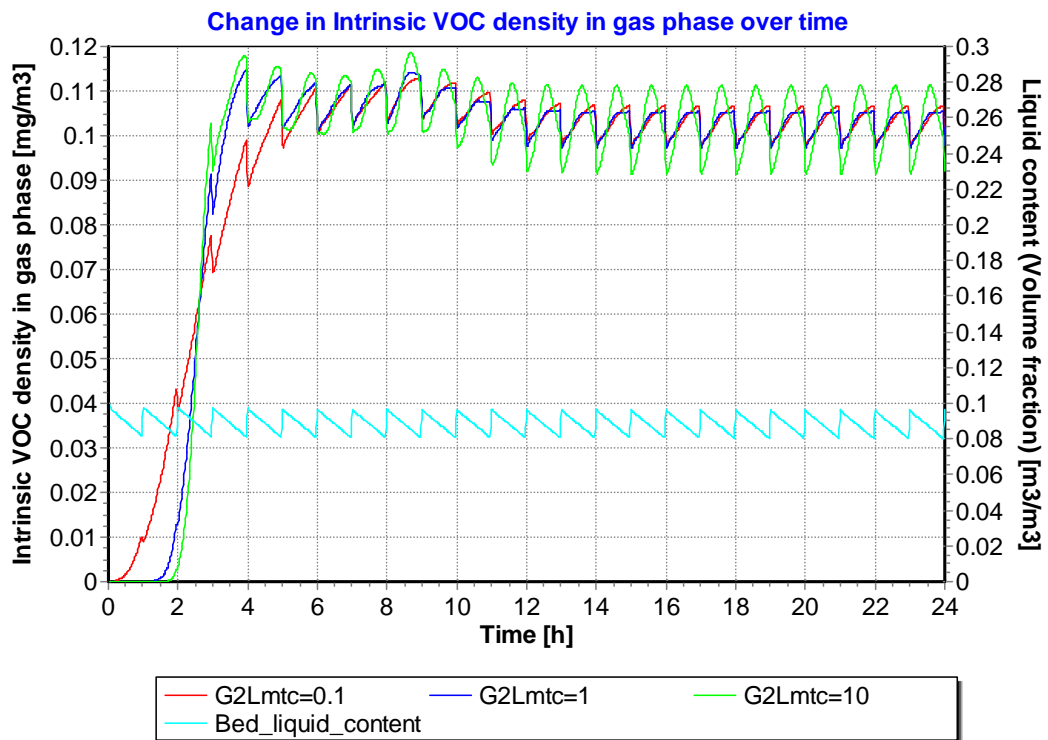


Figure 5-7 Effect of gas to liquid coefficient constant with irrigation

Effect of Bio-degradation Rate Constant by Microbes. As it mentioned in the model assumption, the pollutant bio-degradation follows the first-order kinetics. The bio-degradation rate constant reflects the pollutant removal due to the micro-organisms activities. Figure 5-8 shows the outlet concentration reduction when the bio-degradation rate constant was increased from $1 \times 10^{-7} \text{ s}^{-1}$ to $5 \times 10^{-4} \text{ s}^{-1}$. The outlet concentration was found higher than the inlet concentration. It was due to the presence of initial moisture content in the bed. Formaldehyde was first absorbed by the initial moisture content. As test went on, the initial moisture was gradually evaporated into the air passing through in addition to the amount already existed in the inlet air. Since the inlet concentration was still maintained at the same level, the downstream concentration became slight higher than upstream/inlet concentration. It can be seen that final outlet concentration was close to the inlet concentration when the rate constant was increased from $1 \times 10^{-7} \text{ s}^{-1}$ to $1 \times 10^{-6} \text{ s}^{-1}$. The final outlet concentration began to become significantly lower than the inlet concentration when the rate concentration was increased from $1 \times 10^{-6} \text{ s}^{-1}$ to $1 \times 10^{-5} \text{ s}^{-1}$. The final outlet concentration went down to half of inlet concentration when the rate increased to $1 \times 10^{-4} \text{ s}^{-1}$. Therefore, the critical bio-degradation rate constant is $1 \times 10^{-5} \text{ s}^{-1}$, which means the bio-degradation rate of the DBAF has to be maintained above $1 \times 10^{-5} \text{ s}^{-1}$ to be effective in removing formaldehyde.

Figure 5-9 shows the breakthrough curve that has all the processes together. The simulation cases were conducted in this way: (1) adsorption only; (2) absorption with

irrigation; (3) adsorption plus absorption with irrigation; (4) adsorption, absorption and bio-degradation with irrigation. It can be seen that the VOC removal capacity increased as more processes were added. These simulation results were only used to see how these removal processes were involved in the DBAF performance.

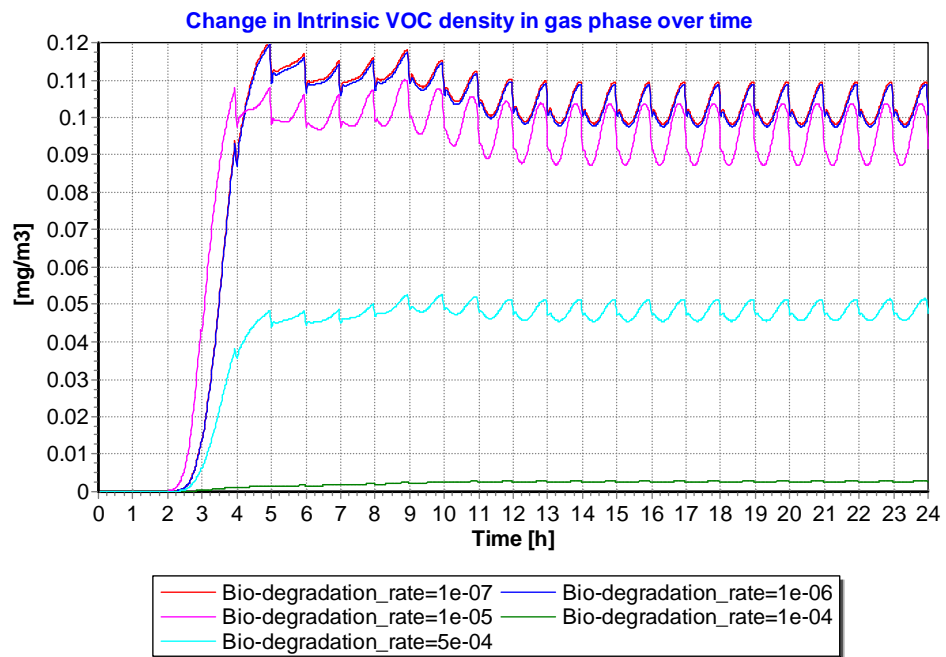


Figure 5-8 Effect of bio-degradation rate constant

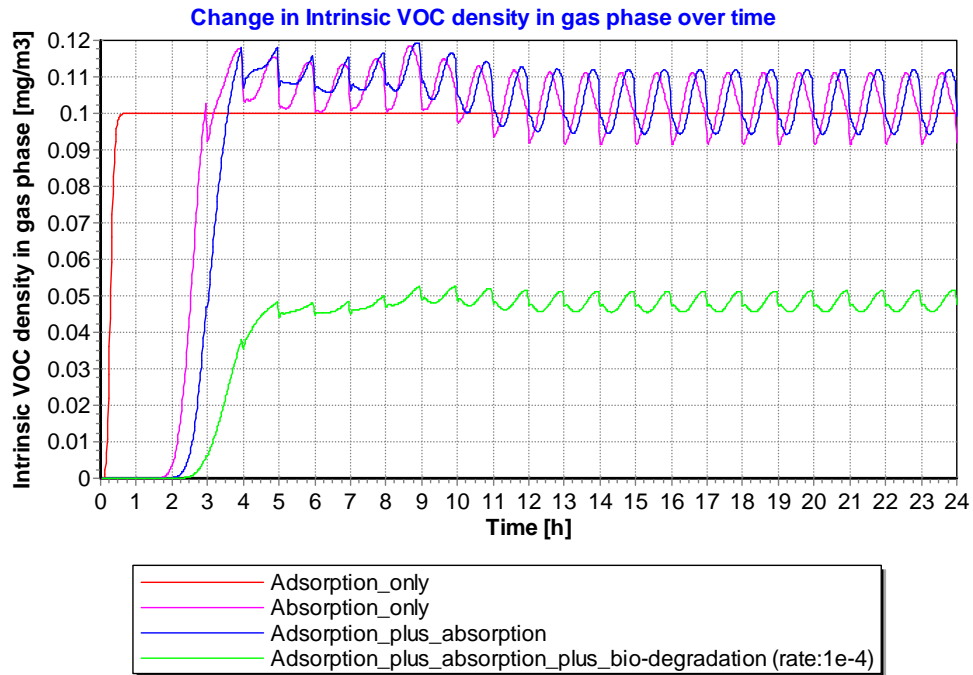


Figure 5-9 Simulation results with all the processes involved

5.4.2 Comparison with Experimental Data and Discussion

Experimental data for the reduced-scale filter are available in Chapter 4.

Formaldehyde removal tests at different RHs were conducted. The chamber steady state concentration was used as the inlet VOC concentration. The filter efficiency was calculated from measured data. The simulated efficiency varied with the input bio-degradation rate constant. When the simulated filter efficiency was equal to the measured filter efficiency, the fitted bio-degradation rate constant was obtained. Table 5-2 lists the fitted bio-degradation rate constants for different RHs. The fitted bio-degradation rate constants were $0.8 \times 10^{-4} \text{ s}^{-1}$ for 92% RH test, $1 \times 10^{-4} \text{ s}^{-1}$ for 75% RH test, and $1.5 \times 10^{-4} \text{ s}^{-1}$ for 55% RH test. It can be concluded that the

bio-degradation rate constant was in the range of $0.8\text{--}1.5\times 10^{-4}\text{ s}^{-1}$ for the reduced-scale DBAF tested in Chapter 4.

Table 5-2 The fitted bio-degradation rate constant

Model	Compound	Formaldehyde		
	Inlet RH	92%	75%	55%
	Inlet VOC concentration (mg/m ³)	0.018	0.085	0.11
	Irrigation rate (kg/m ³ s)	0.01	0.2	0.1
	Initial water content (m ³ /m ³)	0.08	0.05	0.025
	Henry's law (m ³ /m ³)	1.33E-05		
Input	partition coefficient	29084		
	Bed output RH	93%	77%	56%
	Average bed water content (m ³ /m ³)	0.079	0.049	0.026
	Bed output concentration(mg/m ³)	0.012	0.064	0.088
	Simulated removal efficiency	33%	25%	20%
	(Measured removal efficiency)	32%	24%	20%
	Fitted bio-degradation rate constant			
Output	(1/s)	0.8E-04	1.00E-04	1.50E-04

5.5 Major Findings

The modified CHAMPS-BES model is capable of simulating the operation of the DBAF system, in good agreement with the measured pressure difference, moisture content, and outlet relative humidity and concentrations. The model also correctly simulated the impact of mass transfer coefficient, partition coefficient and Henry's

Law constant on the behavior of the breakthrough curve of the DBAF system.

It was also found that the critical bio-degradation rate constant is $1 \times 10^{-5} \text{ s}^{-1}$ for formaldehyde which means that the bio-degradation rate of the DBAF has to be maintained above $1 \times 10^{-5} \text{ s}^{-1}$ to be effective in removing formaldehyde. The fitted bio-degradation rate constant was in the range of $0.8\text{--}1.5 \times 10^{-4} \text{ s}^{-1}$ for the reduced-sized DBAF tested in Chapter 4.

Chapter 6. Building Energy Efficiency Simulation and Analysis

6.1 Introduction

Buildings accounted for 38.9 percent of total U.S. energy consumption in 2005 (Buildings Energy Databook, 2006). Residential buildings accounted for 53.7 percent of that total, while commercial buildings accounted for the other 46.3 percent. There is a growing concern about energy consumption in buildings and its likely adverse impact on the environment. With economic growth, buildings, especially fully air conditioned offices, will continue to be a major energy end user. Much of this energy is used to condition the air needed for ventilation to maintain good indoor air quality. Indoor Air Quality (IAQ) (sometimes also referred to as Indoor Environmental Quality or IEQ) is one critical component of constructing "green" homes and buildings. Energy efficiency is another important component of "green building". In Chapter 3, the DBAF has been demonstrated to have the potential to improve the building indoor air quality without lowering the building energy efficiency, even increasing the building energy efficiency in some cases.

In this chapter, energyPlus was first used to estimate the potential energy saving for a small commercial building due to the use of the DBAF in Syracuse, NY. Additional simulations were then conducted at other U.S. climate zones to provide suggestion of potential DBAF application at different locations in terms of energy efficiency.

6.2 Methods

Based on the performance test results conducted in the office field demonstration study in Chapter 3, the outdoor air could be reduced from 560–119 m³/h with the DBAF (filter bed of 1.2 m by 0.8 m) integrated into the HVAC system. To estimate the potential benefit in building energy saving due to the use of the botanical air filter, the energy consumption of the building integrated with the DBAF prototype was first simulated through EnergyPlus over an entire year using representative climate data in Syracuse, NY for the Syracuse center of excellence (COE) Headquarters building. Thereafter, the same office building was simulated at different U.S. climate zones.

The COE building is a 5-story office structure (main tower) with an integrated two (2) story laboratory building. The energy simulation only focused on the 5-story main tower, where office, conference room and classrooms are located. The 5-story main tower is approximately 3387 m². One DBAF (with eight (8) plants and root bed of 1.2 m long by 0.8 m wide) could serve 465 m² office floor areas. Eight DBAF would be needed for the entire COE building. ASHRAE 62.1-2010 specifies that the requirement of outdoor air for office buildings is 5 cfm (8.48 m³/h) per person plus 0.06 cfm (1.02 m³/h) per square foot floor area. ASHRAE 62.1-2010 also specifies a maximum occupant density for office spaces of five people per 1000 ft² or per 100 m². The total required outdoor air will be 3731 m³/h per ASHRAE standard. The total required outdoor air can be reduced to 747 m³/h if eight DBAF are installed in the

building.

Figure 6-1 shows the COE building images generated in DesignBuilder. The building east façade consists of 25% window and 75 % frame wall. The west façade consists of 100% frame wall. The South facade consists of 100% curtain wall. The North façade consist of 28 % window and 72% frame wall. The Figures 6-2 and 6-3 show the floor plan of the main tower.

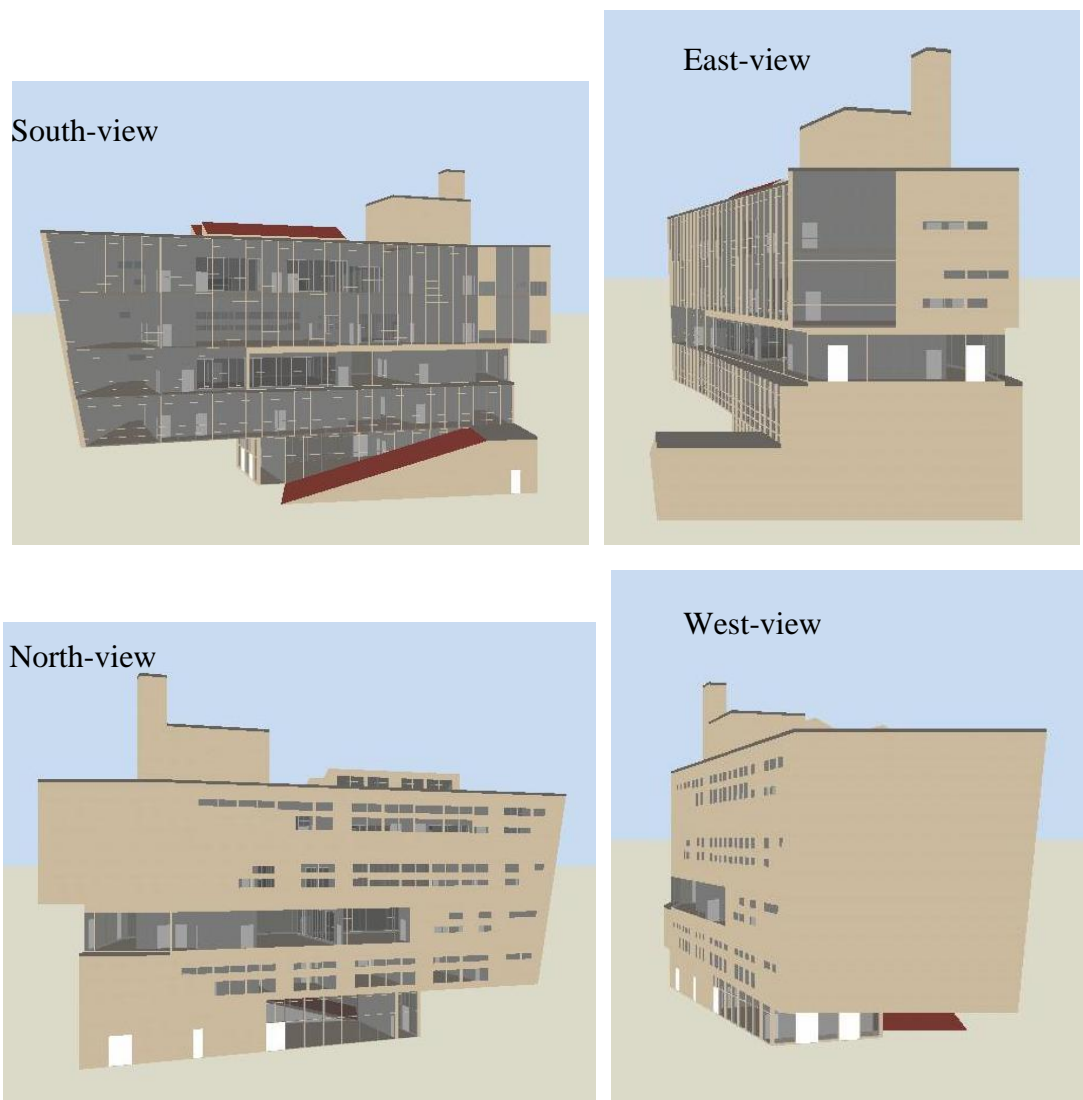


Figure 6-1 Building image for simulation (generated in DesignBuilder)

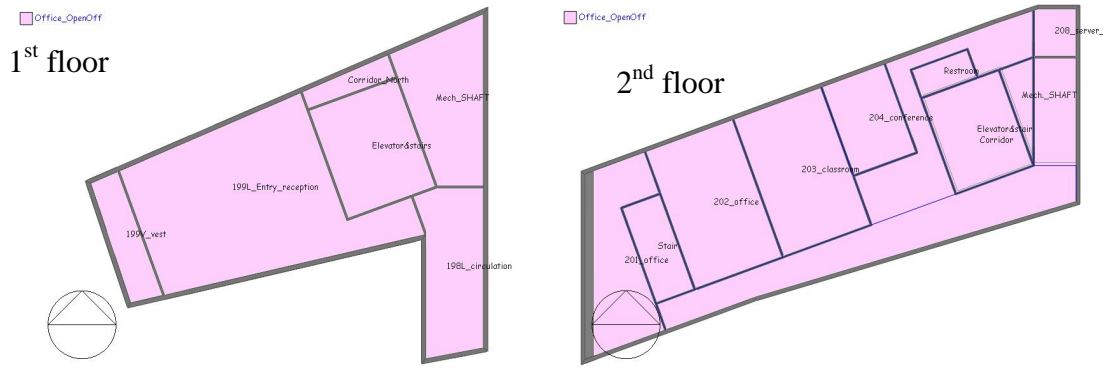


Figure 6-2 First and second floor plan of COE building main tower



Figure 6-3 Third, fourth, and fifth floor plan of COE building main tower

Table 6-1 lists the building envelope information. These are the design parameters for the building and were assigned to the building envelope as simulation

input. Table 6-2 lists the COE building internal loads for different room and these are the maximum load of the COE building. The COE building thermal control strategy was 74 °F (23.3 °C) for summer zone temperature control and 71 °F (21.6 °C) for winter zone temperature control. The zone RH is set at 30–60% all year round. No difference was set between the corridor and the office and conference spaces for the purpose of this study.

Table 6-1 COE building envelope information (from COE building design manual)

Construction	R-value(hr-ft²-°F/BTU) /U-value(BTU/hr-ft²-°F)	Solar Heat Gain Coefficient (SHGC)
Roof	R-30	N/A
Double skin (curtain wall)	U=0.25	0.12
Translucent wall panel	U=0.10	0.08
Insulated glass units	U=0.38	0.38
Framed wall	U=0.07	N/A

Table 6-2 COE building internal loads (from COE building design manual)

Floor	Room No.	Type	Floor area sf	Occupancy load		Light load W/sf	Equipment load W/sf
				Occupancy people	Density people/sf		
1	198L	circulation	530	5	0.0094	0.7	0.5
	199L	entry reception	1432	95	0.0663	0.7	0.5
2	201	office suite	770	6	0.0078	1.1	1.5
	202	office suite	1000	10	0.0100	1.1	1.5
	203	class room	1000	49	0.0490	1.1	1.0
	204	conference room	450	30	0.0667	1.1	2.0
	208	server room	145	1	0.0069	1	23000BTU/h
	other	corridor	2200	3	0.0014	0.7	0.0
3	301	conference room	916	40	0.0437	1.1	2.0
	302A	MGT room	218	2	0.0092	0.8	24000BTU/h
	302B	MGT room	100	1	0.0100	0.8	15000BTU/h
	303	BETA suite	1758	18	0.0102	1.1	1.5
	other	reception and corridor	1216	12	0.0099	0.7	0.0
4	401	monitor room	809	16	0.0198	1.1	0.5
	401B	TCR	159	3	0.0189	0.8	0.5
	402	mechanic room	2383	47	0.0197	0.8	/
	403	office suite	764	7	0.0092	1.1	1.5
	404	office suite	1185	10	0.0084	1.1	1.5
5	501	EQS suite	1122	11	0.0098	1.1	1.5
	502	TIEQ office	716	7	0.0098	1.1	1.0
	503	TIEQ office	723	7	0.0097	1.1	1.0
	504	TIEQ	453	5	0.0110	1.1	1.0
	508	office suite	1117	11	0.0098	1.1	1.5

After the building geometry and envelope parameters, internal loads, and zone thermal control were set up in the DesignBuilder, an IDF file was generated and then opened in the EnergyPlus. The HVAC system of the building was then modeled in EnergyPlus, which consists of heating/preheat/reheat coils, cooling coils, supply and

return fans, pumps, etc. The yearly energy simulation was finally conducted in EnergyPLUS.

To investigate the potential energy saving due to the use of DBAF, conventional variable air volume system was applied in the COE building HVAC system. Since the outdoor air could be reduced by 80% by using the DBAF, the baseline case was the COE building with ventilation of 3731 m³/h and the proposed case was the COE building with ventilation of 747 m³/h plus the DBAF. Comparison between above two simulated cases was conducted. In terms of the simulation set-up, the ventilation schedule was on for 12 hours (7:00 AM-6:00 PM) during weekday and off during weekend and holidays. The boiler nominal efficiency for heating was assumed 0.8. The chiller nominal coefficient of performance for cooling was assumed to be 3.2. The fan total efficiency for ventilation was assumed 0.7(power transferred to the air in Watts/fan electricity consumption in Watts). The pump motor efficiency for hot/chilled water was assumed 0.9. The total nominal power of the fans of the DBAFs was 0.75 kW.

6.3 Simulation Results

6.3.1 Base Case for Syracuse, NY Climate

With the DBAF integrated into the HVAC system, the outdoor air can be reduced from 3731–747 m³/h. It led to the change in the energy consumption related to HVAC system. Table 6-3 shows yearly energy and cost saving due to the use of

DBAF for an office building located in Syracuse, NY. The yearly heating energy saving was 80.2 MBtu (23511 kWh). The natural gas unit price was 15 dollars (\$) per MBtu. And then the yearly operation cost saving for heating was 1203 dollars (\$). The yearly energy saving for cooling and pump were 1889 and 127 kWh, respectively. The corresponding yearly operation cost saving were 283 dollars (\$) and 19 dollars (\$). It can be seen the proposed case consumed 4 kWh more electricity for fan. If all the cost savings were put together, the total yearly operation cost saving would be 1505 dollars (\$).

Table 6-3 Yearly energy and cost saving related to HVAC system

	Natural Gas Heating (MBtu)		Electricity Cooling (kWh)		Pump (kWh)		Fan (kWh)	
	Baseline Case	Proposed case	Baseline case	Proposed case	Baseline case	Proposed case	Baseline case	Proposed case
Jan.	79.5	55.2	0	0	59	49	2961	2931
Feb.	53.4	35.4	0	0	39	30	2957	2787
Mar.	26.3	17.9	0	0	19	15	3953	3512
Apr.	10.9	9.3	1571	1676	852	855	3140	3184
May	2.7	2.7	8089	8088	2808	2807	3537	3681
Jun.	0.4	0.4	13214	12745	3328	3309	3784	3922
Jul.	0.1	0.1	15600	14991	3280	3244	3709	3834
Aug.	0.3	0.3	15752	14931	3604	3571	3991	4135
Sep.	2.9	2.9	7328	7175	2470	2464	3211	3342
Oct.	13.1	11.8	1313	1372	867	868	3111	3244
Nov.	23.0	16.6	0	0	14	11	3112	3048
Dec.	51.5	31.5	0	0	37	26	3093	2942
Yearly total	264.3	184.1	62867	60978	17377	17250	40558	40561
Energy Saving	80.2		1889		127		-4	
Unit price	\$/MBtu	15	\$/kWh	0.15	\$/kWh	0.15	\$/kWh	0.15
Cost		1203		283		19		-0.6

Saving(\$)

Total cost 1505

Saving(\$)

Moreover, the energy saving listed in Table 6-3 can be analyzed further in detail.

The energy saving will be 30% if considering the heating part only, while only 3% for cooling and 0.7% for pump. The energy consumption difference for fan in the two cases was less than 0.01% and could be ignored.

The heating and cooling energy consumptions were for all the loads of the occupied floor, not just the ventilation loads. The pump energy consumption was for the water moving equipment, including hot water pump, chilled water pump, and condensed water pump. The fan energy consumption was for all the air moving equipment needed to meet the heating and cooling loads and the ventilation requirements of the occupied floor.

Note: The above simulation was based on the premise that the requirement of outdoor air can be reduced from 3731–747 m³/h after the DBAF was integrated in the building HVAC system. The energy consumption from the fan of DBAF was considered in the fan energy part. The temperature and RH effect that the DBAF may bring to the HVAC system were not reflected in the simulation. Furthermore, the climate zones also play an important role in the potential energy saving from the application of the DBAF, which will be discussed in the following section.

6.3.2 Cases for Other U.S. Climate

Figure 6-4 shows the U.S. climate zones. There are total 7 climate zones.

Simulation for the same COE building was conducted at one city in each zone. Table 6-4 lists the selected cities for different U.S. climate zones in the simulation.

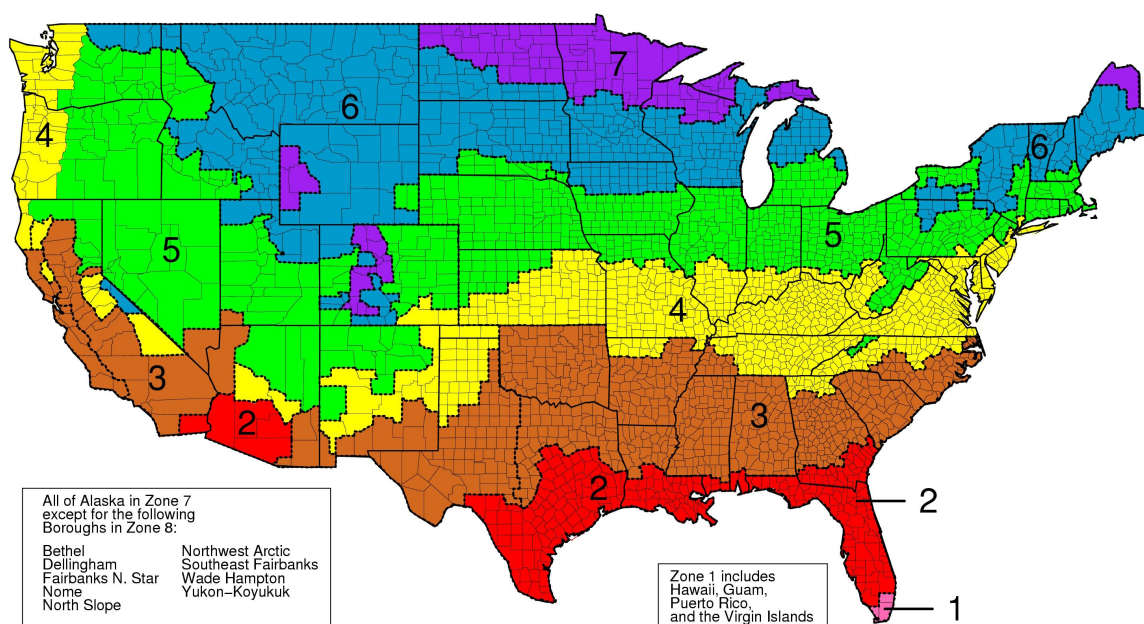


Figure 6-4 U.S. Climate zones (by county) for the 2004 Supplement to the IECC, the 2006 IECC, and ASHRAE 90.1-2004

Table 6-4 Selected cities for different U.S. climate zones in the simulation

Climate Zone No.	City, State	Weather feature
1	Miami, Florida	Hot, humid
2B	Phoenix, Arizona	Hot, dry
3B-CA	Los Angeles, California	Hot, dry

4A	Baltimore, Maryland	Mild, humid
5A	Chicago, Illinois	Cold, humid
6A	Minneapolis, Minnesota	Cold, humid
7	Duluth, Minnesota	Very cold

Table 6-5 lists the yearly operation energy and cost saving due to the use of DBAF at different U.S. climate zones. It can be seen that climate zone 1A has the highest yearly operation cost saving, which is 3450 dollars (\$). The climate zone 3B-CA has the lowest yearly operation cost saving, which is 179 dollars (\$). For climate zone one and two, most of the saving was from cooling and fan while no significant heating saving was observed. For climate zone three, there is no significant heating saving and very small cooling and fan saving were found. For climate zone four, five and six, both heating and cooling saving were observed. It seems that more heating saving and less cooling saving were found as the climate zone moves further North. For climate zone seven, the highest heating saving was observed while there was no cooling saving.

Overall, there is no need to use DBAF for climate zone 3B-CA as long as the outdoor pollutant level is in an acceptable level. It seems climate zone one could be a good place to apply the DBAF in terms of cost saving. However, the weather feature of climate zone one is hot and humid. There is always a need to dehumidify the air in summer. It has been mentioned that the DBAF would bring additional moisture to air. Therefore, further analysis regarding the dehumidification issue needs to be

conducted for the application in climate zone one. In Chapter 3, it was found that the moisture generaturion of one DBAF was ~1.89 kg/h. Eight DBAFs were needed for COE building to maintain acceptable indoor air quality. The total moisture generaturion would be 15.1 kg/h. The total moisture load for COE building applying at climate zone one was 334 kg/h (The detailed calculation was described in Appendix C). Therefore, the moisture load increament due to DBAF was ~5% of the total building humidity load. This small additional moisture load may not pose a serious limitation on the DBAF application, but its impact should be analyzed for specific application cases in Climate Zone 1. Climate zone 2B appears to be a good place to apply the DBAF due to its hot and dry weather feature.

Table 6-5 Yearly operation energy and cost saving due to use of DBAF at different U.S. climate zones

Climate Zone	City, State	Natural Gas		Electricity			Total	
		Heating	Cost	Cooling	Pump	Fan	Cost	Cost
			saving				saving	saving
		MBtu	\$	kWh	kWh	kWh	\$	\$
1A	Miami, FL	0.14	2	16153	684	6150	3448	3450
2B	Phoenix, AZ	1.3	20	4477	385	2389	1088	1108
3B-CA	Los Angeles, CA	0.2	3	755	33	383	176	179
4A	Baltimore, MD	39.7	595	5348	264	-306	795	1390
5A	Chicago, IL	76.9	1154	3835	243	180	639	1793

6A	Minneapolis, MI	121.1	1817	2116	281	-211	328	2145
7	Duluth, MI	161.7	2426	-103	256	-442	-43	2383

6.4 Conclusions

Whole building energy simulation results showed that using the DBAF to substitute 80% of the outdoor air supply without adversely affecting the IAQ could save 30% saving in heating, 3% in cooling and 0.7% in pump energy consumption for yearly operation in Syracuse, NY.

Based on the simulation results for different U.S. climate zones, it was found that a higher percentage of energy savings was achieved for climate zones where more heating is required than Syracuse climate (zone five), such as zone six and seven. Dehumidification issue needs to be considered for climate zone one even though it has the highest operation cost saving. While it was estimated that the presence of DBAF only added 5% more load into the whole building humidity load. Climate zone two might be a good place to apply the DBAF per its hot and dry weather feature. Climate zone three in California area (Zone 3B-CA) might not be a good place to apply the DBAF due to little yearly operation cost (~\$179).

Chapter 7. Summary and Conclusions

The potential usage of plant's root bed system for removing indoor VOC has been demonstrated. Although potted plants alone are not efficient in real-world condition, the studied dynamic botanical air filtration system (DBAF) with polluted air passing through the plant's root bed is very promising based on the laboratory evaluation and real-field demonstration.

1) The full-scale chamber experimental results indicated that the DBAF had high initial removal efficiency for formaldehyde and toluene even without plants in the bed. With the plants, the filter system had even higher initial removal efficiency (90% for formaldehyde in the first four days, and over 33% for toluene). However, it was not clear if the microbes played any role in such a short term test period. The long-term performance test results indicated that the DBAF was effective over a test period of 300 days, and the same level of single pass removal efficiency was maintained at the end of the test. This indicated the possible consumption of the VOCs by the microbes as suggested by one study previously (Wolverton et al., 1989).

The operation of the DBAF resulted in 1 °C temperature decrease and 9–13% RH increase in the chamber air. In the office experiments, the operation of DBAF resulted in 0.5 °C temperature decrease and 17.7% RH increase. The moisture production rate due to the use of DBAF was in the range of 0.81–1.89 kg/h. Such moisture generation would improve the thermal comfort condition in winter, while in summer contribute to little negligible effects on thermal comfort and cooling load

(add 5% more humidity load).

Field experiments in the office space indicated that the use of the DBAF could reduce the percent of outdoor air supply from 25–5% of total air supply without adversely affecting the indoor air quality if formaldehyde and toluene are the target pollutants that dictate the required ventilation rate. In other words, the DBAF was able to provide 80% of the required outdoor air supply for the field study case.

The effect of bed water content on the removal of formaldehyde/toluene was also studied in the field experiments. The single pass removal efficiencies were approximately 60% for formaldehyde and 20% for toluene when the volumetric water content was within the range of 5–32% in the root bed. A moisture content that was higher than 32% resulted in significant increase of single pass efficiency (SPE) for the water soluble compound (formaldehyde) and reduction of SPE for Toluene.

2) In order to improve the understanding of the mechanisms of the DBAF system in removing the volatile organic compounds, a series of further experiments were conducted to determine the important factors affecting the removal performance, and the roles of different transport, storage and removal processes were also investigated. In general, it was found that passing the air through the root bed with microbes was essential to obtain meaningful removal efficiency. Moisture in the root bed also played an important role, both for maintaining a favorable living condition for microbes and for absorbing water-soluble compounds such as formaldehyde. The role of the plant was to introduce and maintain a favorable microbe community that

effectively degraded the VOCs that were adsorbed or absorbed by the root bed. While the moisture in a wet bed had the scrubber effect for water-soluble compounds such as formaldehyde, presence of the plant increased the removal efficiency by about a factor of two based on the results from the reduced-scale root bed experiments.

Moreover, for the same cross-section area of 0.35 m long and 0.2 m wide, the dry bed with airflow had an equivalent CADR of 1.5 m³/h. The wet bed with airflow had an equivalent CADR of 8.5 m³/h. The DBAF had an equivalent CADR of 16.4 m³/h. The difference of wet bed with airflow and DBAF was due to the existence of plant. It was found that wet bed and microbial community are the two major factors to affect the formaldehyde removal. It was hard to find out which one was the dominant one in short-time test (one day), while the result shows that microbial community would become dominant gradually as time went on.

The biodegradation rate constant for formaldehyde was also determined, which was 2.06E-05 s⁻¹ at 92% RH and 15 ppb formaldehyde level. It should be noted that this rate constant was only for comparison. Because the transfer of formaldehyde from gas phase into liquid film and formaldehyde degradation by microbial community occurred in series but not in parallel. They can not be exactly separated from the experimental result, while it can be used as a reference for the model initial input

3) The CHAMPS-BES model was revised and used to model the operation of the DBAF. Model verification results showed that the model could describe the pressure

drop and airflow relationship well by using the air permeability as a model parameter. The water source added in the model also lead to the similar bed moisture content and outlet air RH as that in real test case. For the VOC breakthrough curve simulation, the partition coefficient effect, effect of gas to solid and gas to liquid mass transfer coefficient were also investigated. The simulation results show the developed model work well in testing the effect of different parameters. It was also found that the critical bio-degradation rate constant is $1 \times 10^{-5} \text{ s}^{-1}$, which means the bio-degradation rate of the DBAF has to be maintained above $1 \times 10^{-5} \text{ s}^{-1}$ to be effective in removing formaldehyde.

In the model validation part, the fitted bio-degradation rate constant was obtained by comparing the simulation results with experimental data. The fitted bio-degradation rate constant was in the range of $0.8\text{--}1.5 \times 10^{-4} \text{ s}^{-1}$ for the reduced-scale DBAF tested.

4) Whole building energy simulation results showed that using the DBAF to substitute 80% of the outdoor air supply without adversely affecting the IAQ could save 30% saving in heating, 3% in cooling and 0.7% in fan energy consumption for yearly operation in Syracuse, NY.

Based on the simulation results for different U.S. climate zones, it was found that a higher percentage of energy savings was achieved for climate zones where more heating is required than Syracuse climate (zone five), such as zone six and seven. Dehumidification issue needs to be considered for climate zone one even though it

has the highest operation cost saving. While it was estimated that the presence of DBAF only added 5% more load into the whole building humidity load. Climate zone two might be a good place to apply the DBAF per its hot and dry weather feature. Climate zone three in California area (Zone 3B-CA) might not be a good place to apply the DBAF due to little yearly operation cost (~\$179).

References

- Alagappan G, Cowan R. Substrate inhibition kinetics for toluene and benzene degrading pure cultures and a method for collection and analysis of respirometric data for strongly inhibited cultures. *Biotechnol. Bioeng.* 2003; 83: 798–810.
- ANSI/AHAM AC-1 2006. Method for Measuring the Performance of Portable Household Electrical Room Air Cleaner; 2006.
- ANSI/BIFMA M7.1 2007. Standard Method For Testing VOC Emissions From Office Furniture Systems, Components And Seating; 2007.
- ANSI/ASHRAE Standard 62.1-2010. Ventilation and acceptable indoor air quality. Atlanta: American Society of Heating, Refrigerating, and Air-Conditioning Engineers, Inc.; 2010.
- Arriaga S, Revah S. Improving hexane removal by enhancing fungal development in a microbial consortium biofilter. *Biotechnol. Bioeng.* 2005; 90: 107–15.
- Auriol M, Filali-Meknassi Y, Tyagi RD, Adams CD. Laccase-catalyzed conversion of natural and synthetic hormones from a municipal waster. *Water Res.* 2007; 41: 3281–8.
- Beveridge TJ, Makin SA, Kadurugamuwa JL, Li Z. Interaction between biofilms and the environment. *FEMS Microbiol. Rev.* 1997; 20: 291–303.
- Burgess JE, Parsons SA, Stuetz RM. Developments in odour control and waste gas treatment biotechnology: a review. *Biotechnol. Adv.* 2001; 19: 35–63.

- Butterfield PW, Camper AK, Ellis BD, Jones WL. Chlorination of model drinking water biofilm: implications for growth and organic carbon removal. *Water Res.* 2002; 36: 4391–405.
- Carlsson H, Nilsson U, Ostman C. Video display units: an emission source of the contact allergenic flame retardant triphenyl phosphate in the indoor environment. *Environ. Sci. Technol.* 2000; 34: 3885–9.
- Chain P, Denev V, Konstantinidis K, Vergez L, Agullo L. *Burkholderia xenovorans* LB400 harbors a multi-replicon, 9.73-Mbp genome shaped for versatility. *PNAS* 2006; 103: 15280–7.
- Chen W, Zhang J, Zhang Z. Performance of air cleaners for removing multiple volatile organic compounds in indoor air. *ASHRAE Trans.* 2005; 111: 1101–14.
- Chen W, Gao Z, Zhang J. Reduced Energy Use Through Reduced Indoor Contamination In Residential Buildings. Final report for National Center for Energy Management and Building Technologies: NCEMBT-20061101.
- Daisey J, Hodgson A, Fisk W, Mendell M, Ten Brinke J. Volatile organic compounds in twelve Californian office buildings: classes, concentrations and sources. *Atmos. Environ.* 1994; 28: 3557–62.
- Darlington A, Chan M, Malloch D, Pilger C, Dixon MA. The biofiltration of indoor air: implications for air quality. *Indoor Air* 2000; 10: 39–46.
- Darlington A, Dat J, Dixon M. The biofiltration of indoor air: air flux and temperature influences the removal of toluene, ethylbenzene, and xylene. *Environ. Sci. Technol.* 2001; 35: 240–6.

- Delhoménie MC, Heitz M. Biofiltration of air: a review. *Crit. Rev. Biotechnol.* 2005; 25: 53–72.
- Deshusses MA, Hamer B, Dunn IJ. Behavior of biofilters for waste air biotreatment. 1. Dynamic model development. *Environ. Sci. Technol.* 1995; 29: 1048–1058.
- Devinny JS, Deshusses MA, Webster TS. Biofiltration for air pollution control. Boca Raton: Lewis Publishers; 1999.
- Devinny JS, Ramesh J. A phenomenological review of biofilter models. *Chem. Eng. J.* 2005; 113: 187–196.
- Dudler R, Eberl L. Interactions between bacteria and eukaryotes via small molecules. *Curr. Opin. Biotech.* 2006; 17:268–73.
- Ekberg LA. Volatile organic compounds in office buildings. *Atmos. Environ.* 1994;28: 3571–5.
- Ergas SJ, Schroeger ED, Chang DP. Biodegradation technology for volatile organic compound removal from airstream. Final report. Contract No. A032-127. California Environmental Protection Agency, Air Resources Board, Research Division; 1992. May.
- Ergas SJ, Shumway L, Fitch MW, Neemann JJ. Membrane process for biological treatment of contaminated gas streams. *Biotechnol. Bioeng.* 1999; 63: 431–41.
- Fan LS, Leyva-Ramos R, Wisecarver KD, Zehner BJ. Diffusion of phenol through a biofilm grown activated carbon particles in a draft-tube three-phase fluidized bed bioreactors. *Biotechnol. Bioeng.* 1990; 35: 279–286.

- Fan S, Scow KM. Biodegradation of Trichloroethylene and Toluene By Indigeous Microbial Populations in Soil. *Appl. Environ. Microbiol.* 1993; 59(6): 1911-1918.
- Girman J, Philips T, and Levin H. Critical Reviews: How well do house plants perform as indoor air cleaners? *Proceedings of Healthy building 2009*: paper 667.
- Guieysse B, Hort C, Platel V, Munoz R, Ondarts M, Revah S. Biological treatment of indoor air for VOC removal: Potential and challenges. *Biotechnol. Adv.* 2008; 26: 398-410.
- Hodge DS, Deviny JS. Modeling removal of air contaminants by biofiltration, *J. Environ. Eng.* 1995; 121 (1): 21-32.
- Hodge DS, Deviny JS. Determination of biofilter model constants using mini-columns, *J. Environ. Eng.* 1997; 123 (6): 577-585.
- Hodgson AT, Rudd AF, and Chandra S. Volatile organic compound concentrations and emission rates in new manufactured and site-built houses, *Indoor Air* 2000; 10: 178-192.
- Holden PA, Firestone MK. Soil microorganisms in soil cleanup: how can improve our understanding? *J. Environ. Qual.* 1997; 26: 32-40.
- Iranpour R, Cox HJ, Deshusses MA, Schroeder ED. Literature review of air pollution control biofilters and biotrickling filters for odor and volatile compound removal. *Environ. Prog.* 2005; 24: 254-67.
- Jin Y, Veiga MC, Kennes C. Development of a novel monolith-bioreactor for the treatment of VOC-polluted air. *Environ. Technol.* 2006; 27: 1271-7.

- Jorio H, Payre B, Heitz M. Modeling of gas-phase biofilter performance. *J. Chem. Technol. Biotechnol.* 2003; 78: 834–846.
- Kennes C, Veiga MC. Fungal biocatalysts in the biofiltration of VOC-polluted air. *J. Biotechnol.* 2004; 113: 305–19.
- Kesselmeier J, Staudt M. Biogenic volatile organic compounds (VOC): an overview on emission, physiology and ecology. *J. Atmos. Chem.* 1999; 33: 23–88.
- Kim S, Deshusses MA. Development and experimental validation of a conceptual model for biotrickling filtration of H₂S. *Environ. Prog.* 2003; 22 (2): 119–128.
- Larimer FW, Chain P, Hauser L, Lamerdin J, Malfatti S, Do L. Complete genome sequence of the metabolically versatile photosynthetic bacterium *Rhodospseudomonas palustris*. *Nat. Biotechnol.* 2003; 22: 55–61.
- Li H, Mihelcic JR, Crittenden JC, Anderson KA. Field measurements and modeling of two-stage biofilter that treats odorous sulfur air emissions, *J. Environ. Eng.* 2003; 129 (8): 684–692.
- Marshall KC. Microbial adhesion in biotechnological processes. *Curr. Opin. Biotechnol.* 1994; 5: 296–301.
- Meyer, B., *Indoor Air Quality*, Addison-Wesley, Reading, MA, 1983.
- Miller M, Allen D. Modelling transport and degradation of hydrophobic pollutants in biofilms in biofilters. *Proceedings of the USC-TRG Conference on Biofiltration for Air Pollution Control*, Los Angeles, CA, October, 2004.

- Molin S, Tolker-Nielsen T. Gene transfer occurs with enhanced efficiency in biofilms and induces enhanced stabilisation of the biofilm structure. *Curr. Opin. Biotechnol.* 2003; 14: 255–61.
- Muñoz R, Villaverde S, Guieysse B, Revah S. Two phase partitioning bioreactors for the treatment of volatile organic compounds. *Biotechnol. Adv.* 2007; 25: 410–22.
- Muir DG, Howard PH. Are there other persistent organic pollutants? *Environ. Sci. Technol.* 2006; 40: 7157–66.
- Newman LA, Reynolds CM. Phytodegradation of organic compounds. *Curr. Opin. Biotechnol.* 2004; 15: 225–30.
- Nicolai A. Modeling and numerical simulation of salt transport and phase transitions in unsaturated porous building materials. Ph.D. thesis, 2009.
- NRC, Committee on Indoor Air Pollutants: Indoor Pollutants, National Research Council, National Academy Press, Washington, DC, 1981.
- Otake T, Yoshinaga J, Yanagisawa Y. Analysis of organic esters of plasticizer in indoor air by GC-MS and GC-FPD. *Environ. Sci. Technol.* 2001; 35: 3099–102.
- Orwell RL, Wood RL, Tarran WJ, Torpy F, Burchett MD. Removal of benzene by the indoor plant/substrate microcosm and implications for air quality. *Water Air Soil Pollut.* 2004; 157: 193–207.
- Ottengraf SP, Konings JG. Emission of microorganisms from biofilters. *Bioprocess Eng.* 1991; 7: 89–96.

- Orwell RL, Wood RA, Burchett MA, Tarran J, Torpy F. The potted-plant microcosm substantially reduces indoor air VOC pollution: II. Laboratory study. *Water Air Soil Pollut.* 2006; 177: 59–80.
- Owen SM, Clark S, Pompe M, Semple KT. Biogenic volatile organic compounds as potential carbon source for microbial communities in soil from the rhizosphere of *populus tremula*. *FEMS microbial. Lett.* 2007; 268: 34-39.
- Pahm MA, Alexander M. Selecting inocula for the biodegradation of organic compounds at low concentration. *Microb. Ecol.* 1993; 25: 275–86.
- Parvatiyar MG, Govind R, Bishop DF. Treatment of trichloroethylene (TCE) in a membrane biofilter. *Biotechnol. Bioeng.* 1996; 50: 57–64.
- Ranasinghe MA, Jordan PJ, Gostomski PA. Modelling the mass and energy balance in a compost biofilter. *Proceedings of the A&WMA 95th Annual Meeting and Exhibition, Baltimore, MD, June 18–24, 2002.*
- Revah S, Morgan-Sagastume JM. Methods for odor and VOC control. In: Shareefdeen Z, Singh A, editors. *Biotechnology for odour and air pollution.* Heidelberg: Springer- Verlag; 2005. p. 29–64.
- Robbins CA, Swenson LJ, Nealley ML, Gots RE, Kelman BJ. Health effects of mycotoxins in indoor air: a critical review. *Appl. Occup. Environ. Hyg.* 2000; 15: 773–84.
- Roch F, Alexander M. Inability of bacteria to degrade low concentrations of toluene in water. *Environ. Toxicol. Chem.* 1997; 16: 1377–83.

- Sander R. Compilation of Henry's law constants for inorganic and organic species of potential importance in environmental chemistry; 1999. <http://www.mpch-mainz.mpg.de/~sander/res/henry.html>.
- Sandhu A, Halverson LJ, Beattie GA. Bacterial degradation of airborne phenol in the phyllosphere. *Environ. Microbiol.* 2007; 9: 383–92.
- Schäffner A, Messner B, Langebartels C, Sandermann H. Genes and enzymes for in planta phytoremediation of air, water and soil. *Acta Biotechnol.* 2002; 22: 141–52.
- Schleibinger H, Keller R, Rüdén H. Indoor air pollution by microorganisms and their metabolites. In: Pluschke P, editor. *The handbook of environmental chemistry*, vol. 4. Berlin Heidelberg: Springer -Verlag; 2004. p. 149–77. Part F.
- Schmitz H, Hilger U, Weinder M. Assimilation and metabolism of formaldehyde by leaves appear unlikely to be of value for indoor air purification. *New Phytol.* 2000; 147: 307–15.
- Shareefdeen Z, Singh A. *Biotechnology for odor and air pollution control*. Heidelberg: Springer-Verlag; 2005.
- Shaughnessy RJ, Levetin E, Blocker J, Sublette K. Effectiveness of portable indoor air cleaners: sensory testing results. *Indoor Air* 1994; 4: 179–88.
- Shaughnessy R, Sextro R. What is an effective portable air cleaning device? A review. *J. Occup. Environ. Hyg.* 2006; 3: 169–81.
- Singh R, Debarati PD, Jain RK. Biofilms: implications in bioremediation. *Trends Microbiol.* 2006; 14: 389–97.

- Zarook SM. Development experimental validation and dynamic analysis of a general transient biofilter model, *chemical engineering science* 1997; 52(5): 759-773.
- Smith F, Harvey A. Avoid Common Pitfalls When Using Henry's Law. *Chemical Engineering Progress*. September 2007.
- Staudinger J, Roberts PV. A critical review of Henry's law constants for environmental applications. *Crit. Rev. Environ. Sci. Technol.* 1996; 26: 205–97.
- Torres EM, Basrai SS, Kogan V. Evaluation of two biotechnologies controlling POTWair emissions. *Proceedings of 1996 USG-TRG Conference on Biofiltration*. Los Angeles, CA: University of Southern California; 1996. p. 182–97.
- Tseng C, Hsieh C, Chen S. The Removal of Indoor Formaldehyde by Various Air Cleaners. Paper 457. *Proceedings of the air & waste management association's 98th annual conference*. Minneapolis, Minnesota.
- U.S. EPA. Air and steam stripping of toxic pollutants. Tech. Rep. EPA-68-03-002. Cincinnati, OH, USA: Industrial Environmental Research Laboratory; 1982.
- U.S. EPA. Why Is the Environment Indoors Important to Us? Indoor Environment Division, U.S. Environmental Protection Agency, Washington, DC, 2000.
- U.S.EPA. Indoor Air Quality. <http://www.epa.gov/iaq/is-imprv.html>, last accessed November 30, 2008.
- U.S. Green Building Council. www.usgbc.org, last accessed January 30, 2009.
- Van D, Vrouwenvelder HS, Veenendaal HR. Kinetic aspects of biofilm formation on surfaces exposed to drinking water. *Water Sci. Technol.* 1995; 32: 61–5.

- Van Groenestijn JW, Kraakman NR. Recent developments in biological waste gas purification in Europe. *Chem. Eng. J.* 2005; 113: 85–91.
- Vergara A, Haaren B, Revah S. Phase partition of gaseous hexane and surface hydrophobicity of *Fusarium solani* when grown in liquid and solid media with hexanol and hexane. *Biotechnol. Lett.* 2006; 28: 2011–7.
- Wargocki P, Sundell J, Bischof W, Brundrett G, Fanger PO, et al. Ventilation and health in non-industrial indoor environments: report from a European Multidisciplinary Scientific Consensus Meeting (EUROVEN). *Indoor Air* 2002; 12: 113–28.
- Wolverton BC, McDonald RC, Watkins EA. Foliage plants for removing indoor air pollutants from energy-efficient homes. *Econ. Bot.* 1984; 38: 224–8.
- Wolverton BC, Johnson A, Bounds K. Interior landscape plants for indoor air pollution abatement, National Aeronautics and Space Administration, 1989. p.1–22.
- Wolverton BC, Wolverton JD. Plant and soil microorganisms: Removal of formaldehyde, xylene and ammonia from the indoor environment. *J. Miss. Acad. Sci.* 1993; 11-15.
- Wood RA, Burchett MA, Alquezar R, Orwell RL, Tarran J, Torpy F. The potted-plant microcosm substantially reduces indoor air VOC pollution: 1. Office field-study. *Water Air Soil Pollut.* 2006; 175: 163–80.
- Zarook SM, Shaikh AA, Ansar Z. Development, experimental validation and dynamic analysis of a general transient biofilter model. *Chem. Eng. Sci.* 1997; 52 (5): 759–773.

Zhou X, Mopper K. Apparent partition coefficients of 15 carbonyl compounds between air and seawater and between air and freshwater: implications for air-exchange. *Environ. Sci. Technol.* 1990; 24: 1864–9.

Zilli M, Camogli G, Nicoletta C. Detachment and emission of airborne bacteria in gasphase biofilm reactors. *Biotechnol. Bioeng.* 2005; 91: 707–14.

Appendix A. Full-scale Chamber Pull-down test procedure

A.1 Test Facility and Instrument

The pilot/formal tests for characterizing the performance of the media filter in terms of VOC removal were carried out in a full-scale stainless steel environmental chamber depicted in Figure A-1(a). The chamber has a dimension of 16 ft long x 12 ft wide x 10 ft high (4.84 m long x 3.63 m wide x 3.05 m high) and an interior volume of 1920 ft³ (54.4 m³).

INNOVA 1312 Photoacoustic Multi-gas Monitor was used for online measurements of the concentration of toluene equivalent (TVOC_{toluene}), the concentration of formaldehyde (C_{formal}), and the concentration of tracer gas (SF₆), as shown in Figure A-1(b). The monitor was based on the photoacoustic infrared detection method. For TVOC_{toluene}, the sensitivity and response factor of the instrument for different compounds were different, so the readings from the gas monitor were only used as semi-quantitative measures to monitor the change of TVOC concentrations over time and how they differed for different operation conditions for the pilot tests.



(a) IEQ chamber



(b) INNOVA 1312 gas monitor

Figure A-1 Test facility and instrument

A.2 Test Procedure

- Put the filter bed system into the chamber (as shown in Figure A-2)
- Flushed the chamber overnight then set the return air at 800 CFM to make the air in the chamber in well-mixed. The chamber was running At full-recirculation mode
- Injected SF₆ to check the air tightness of the chamber system. The concentration was monitored continuously during the entire test period
- Set up 1312 photoacoustic multi-gas monitor to continuously monitor TVOC, formaldehyde and tracer gas concentration
- Preparation of tested VOC. Weighed calculated amount of liquid toluene (target 300mg which equals to approximately 5mg/m³ initial chamber concentration) to a glass bottle with septum; weighed calculated amount of paraformaldehyde (target

120mg which equals to approximately $2\text{mg}/\text{m}^3$ initial chamber concentration) to a glass bottle with septum. The uncertainty related with injection amount would be determined from the accuracy and resolution of syringe

- Injection of tested VOC. Quickly opened the chamber door and brought the two glass bottles (one for formaldehyde and one for liquid toluene) into the chamber. Poured the solid paraformaldehyde into one petri dish and the liquid toluene into the other petri dish on the hot plate, left the bottle (on hot plate to facilitate the evaporation of VOC residuals inside the bottle) and the cap inside the chamber. Then quickly stepped out of the chamber and closed the chamber door. The whole process was taken approximately 1 to 2 minutes
- Turned on the power of hot plate from chamber control panel. Recorded the time
- Turned off the power of hot plate after 1 h. The injection period for VOC was 1 h
- Turned on the fan power of the filter bed system to start the air filtration system. Recorded the time as the test started point
- The test period lasted about 4 hours (The time depended on when the contaminant concentration decreased to the background level)
- Flushed the chamber once the test was done
- Downloaded test data and analyzed test results.

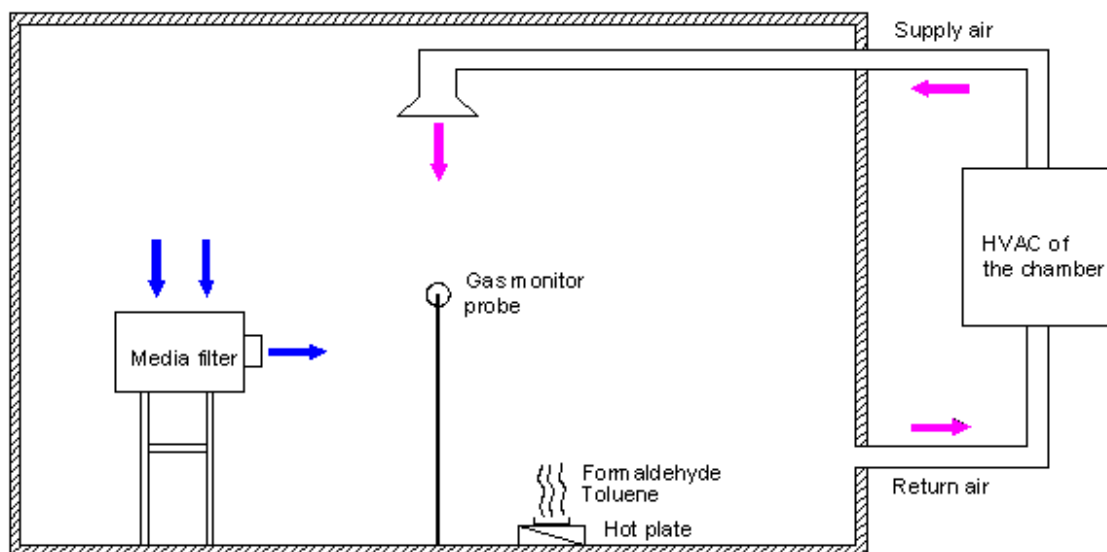


Figure A-2 Schematics of the test chamber

A.3 Calculation of CADR and Removal Efficiency

Three parameters had been commonly used to quantify the performance of air cleaning devices: single-pass efficiency (conversion), clean air delivery rate (CADR), and effectiveness of the device (Nazaroff, 2000). Single-pass efficiency and CADR were used here to evaluate the effectiveness of the filter bed.

Single-pass efficiency (η) represented the fraction of pollutants removed from the air stream as it passed through the device. It was defined as:

$$\eta = \frac{G(C_{in} - C_{out})}{GC_{in}} = \frac{C_{in} - C_{out}}{C_{in}} \quad (A-1)$$

Where,

C_{in} = contaminant concentration at the inlet of air cleaner, mg/m^3 for VOC and number of particles/ cm^3 for particulates.

C_{out} = contaminant concentration at the outlet of air cleaner, mg/m^3 for VOC and number of particles / cm^3 for particulates.

G = airflow rate through the air cleaner, CFM or m^3/h .

CADR represents the “effective” clean airflow rate delivered by the air cleaner.

It is defined as:

$$CADR = \eta \cdot G \cdot E_d \quad (\text{A-2})$$

Where, E_d = short-circuiting factor of the air cleaner, $E_d = C_{in}/C$, where C is average concentration in the test chamber ($E_d = 1$ At well-mixed condition).

CADR was calculated from the test results. The analysis was based on the well-mixed single zone model. Assuming that the air was well mixed in chamber and the contaminant removal mechanisms other than air cleaning (e.g. surface deposition effect and chamber leakage effect) were the same with and without air cleaner operating and can be characterized by a first-order rate constant k_n , the mass conservation of contaminant can be written as:

$$V \frac{dC}{dt} = -(k_n V + CADR) \cdot C, \quad (C=C_0 \text{ at } t=0) \quad (\text{A-3a})$$

Or

$$\frac{dC}{dt} = -\left(k_n + \frac{CADR}{V}\right) \cdot C = -k_e \cdot C \quad (\text{A-3b})$$

Where,

V - volume of the testing chamber system, ft³ or m³,

k_n – contaminant concentration decay rate without air cleaner operating (chamber effects), min⁻¹ or h⁻¹,

k_e – total contaminant concentration decay rate with air cleaner operating, min⁻¹ or h⁻¹,

C₀ – Initial contaminant concentration inside the chamber, mg/m³ for VOC and number of particles/cm³ for particulates.

If CADR did not change during the test period, an analytical solution could be obtained from Equation (A-3) as:

$$C = C_0 \cdot e^{-\left(k_n + \frac{CADR}{V}\right)t} = C_0 \cdot e^{-k_e t} \quad (\text{A-4})$$

CADR was then determined by linear regression of $\ln(C/C_0)$ vs. t from the measured concentration decay curve:

$$CADR = V(k_e - k_n) \quad (\text{A-5})$$

After the CADR was calculated, together with measured the airflow rate through the air cleaner, the removal efficiency could then be calculated by dividing the CADR by the airflow rate through the air cleaner. This calculated removal efficiency was the

same as the single-pass efficiency defined in Equation (A-1) since the air in the chamber was well-mixed.

The step-by-step data analysis procedure for VOC was summarized as follows:

1. Calculated k_n based on the measured tracer gas concentration decay or contaminant concentration decay before time zero (if the contaminant decay during the static period did not match the SF6 decay very well);
2. Calculated k_e by linear regression of $\ln (C/C_0)$ vs. t from measured concentration decay curve after turning on the air cleaner (dynamic period);
3. Calculated CADR according to Equation (A-5);
4. Determined the removal efficiency by dividing the calculated CADR value by the measured airflow rate through the air cleaner.

Appendix B. Application in Real-world Conditions and Test Procedure

B.1 Source Introduction

In order to simulate contaminant source in the test room, 48 pieces of unused particle board were moved into the test room. The size of each piece was 48 by 32 inches. Three (3) pieces were used in each cubical, and there were totally 16 workstations in the test room. The test room was operated At 5% outdoor ventilation flow rate with 70 CFM outdoor air and 1400 CFM total supply air.



Figure B-1 Contaminant source introduced into the test room by using particleboards

B.2 VOC Identification

After the particleboards were placed inside the test room, an air sample was taken at the return air duct by using a Tenax sorbent tube, and analyzed by GC/MS.

Table B-1 lists the detail the VOC found in the room. Pentanal, Toluene, Hexanal,

Xylene, Alpha-Pinene, (1s)-(b)-Pinene were selected as the target VOC in the room.

In addition, formaldehyde and acetaldehyde were also chosen as target compounds as they are typically identified as major compounds of concern in emission testing of composite wood materials.

Table B-1 Test room VOC identification (By GC/MS)

RT	Response area	Est.Conc. (ug/m3)	VOC Name	M.W.	Formula	CAS#	Note
2.664	169,827,440	8.37	OXIRANE, TRIMETHYL-	86	C5H10O	5076-19-7	
5.059	86,847,696	4.28	MERCAPTAMINE	77	C2H7NS	60-23-1	
6.337	118,900,960	5.86	PENTANAL(Valeralde.)	86	C5H10O	110-62-3	
7.897	147,092,128	7.25	TOLUENE	92	C7H8	108-88-3	room bkgd
8.626	186,059,488	9.17	CYCLOTRILOXANE, HEXAMETHYL-	222	C6H18O3Si3	541-05-9	tube bkgd
9.562	1,077,273,088	53.08	HEXANAL	100	C6H12O	66-25-1	
11.344	68,134,416	3.36	BENZENEETHANOL, .ALPHA.,.BETA.-DIMETHYL-	150	C10H14O	52089-32-4	
13.019	597,559,104	29.45	.ALPHA.-PINENE	136	C10H16	80-56-8	
13.714	50,035,800	2.47	CAMPHERE	136	C10H16	79-92-5	
14.348	51,328,636	2.53	CYCLOTETRASIOXANE, OCTAMETHYL-	296	C8H24O4Si4	556-67-2	
14.76	448,029,344	22.08	(1s)-(b)-pinene	136	C10H16	18172-67-3	
15.968	61,673,916	3.04	Benzaldehyde				
16.441	134,613,712	6.63	d-limonene				
16.592	88,311,400	4.35	Octanal	128	C8H16O	124-13-0	
17.88	56,756,684	2.80	Undecane				room bkgd
18.897	108,563,536	5.35	P-TRIMETHYLSILYLOXYPHENYL-BIS(TRIMETHYLS	370	C17H34O3Si3	1000079-08-1	
19.249	79,402,592	3.91	Nonanal	142	C9H18O	124-19-6	

21.382	95,913,080	4.73	PENTADECANAL-	226	C15H30O	2765-11-9
21.518	240,076,816	11.83	2-PROPENOIC ACID, 6-METHYLHEPTYL ESTER	184	C11H20O2	54774-91-3

Table B-2 lists the target compounds that were continuously monitored by PTR-MS.

It also shows the solubility of these compounds in water, which would help to understand the filter bed performance in removing water soluble vs. non-soluble compounds.

Table B-2 Target compounds monitored by PTR-MS (Ion Mass of 21)

VOC Name	M.W.	Formula	CAS#	Solubility in water
Formaldehyde	31	CH ₂ O	50-00-0	Soluble
Acetaldehyde	45	C ₂ H ₄ O	75-07-0	Soluble
Pentanal (Valeralde.)	86	C ₅ H ₁₀ O	110-62-3	Very slightly soluble
Toluene	92	C ₇ H ₈	108-88-3	Insoluble
Hexanal	100	C ₆ H ₁₂ O	66-25-1	Insoluble
Xylene	106	C ₈ H ₁₀	1330-20-7	Insoluble
Alpha-Pinene	136	C ₁₀ H ₁₆	80-56-8	Insoluble

B.3 Filter Bed Single Pass Efficiency Measurement

The filter bed single pass efficiency (SPE) would help to understand the change of the test room contaminants concentration after the filter system was turned on. The single pass efficiency was measured as follows:

- The contaminants concentration of the filter upstream was measured for a number of five minute intervals and the average of these five minutes data was taken as data 1;
- The sample system was switched to downstream. The contaminant concentration of the filter downstream was measured for five minute intervals and the average of these five minutes data was taken as data 2, and it was used as the downstream concentration;
- The monitor was switched back to measure the upstream concentration for the next five minutes and the average of these five minutes data was taken as data 3;
- The average of data 1 and data 3 was used as the upstream concentration;
- The filter single pass efficiency could be obtained as one minus downstream concentration divided by upstream concentration.

B.4 Effect of Bed Water Content to the Single Pass

Efficiency

- The media bed was irrigated with water until it became saturated, which can be realized in this way: an automatic irrigation system was setup to achieve this. A moisture control sensor was used to continuously monitor the moisture content (M.C.) in the filter bed and it was set-up at the saturation level (50%). The

irrigation was kept on running until the signal light of the moisture sensor was off, which means the media bed was saturated already

- The fan was kept running at its maximum flow rate(480cfm) until inlet air RH was close to the outlet RH: the moisture control sensor was set-up at its minimum level to avoid the fan stopping running during the test period, which means get the media bed dry gradually
- In the first half hour, PTR-MS was used to measure the contaminants concentration of upstream for five minutes, and the average was taken as data 1, and then it was switched to downstream for another 5-minute measurement and the average was taken as data 2, after that it was switched back to upstream for another five minute measurement, and the average was taken as data 3. The average of data 1 and data 3 was used as the upstream value, and data 2 was used as the downstream value. The single pass efficiency was obtained: one minus downstream value divided by upstream value
- After that, the test period was extended to 10 minutes for each side, then it took 30 minutes to get one single pass efficiency
- The procedure of measuring single pass efficiency was repeated every 30 minutes until the bed water content was lower than 5%, and then the filter bed single pass efficiency at different moisture level could be obtained.

B.5 Test Room Contaminants Concentration Monitoring

- On the first day, PTR-MS started to monitor the room concentration, and the first-two-hour test result was taken as room background, and a GC/MC sample was also taken at the same time
- After two hours, the particleboards were moved in, then four hours later, a GC/MS sample was taken to identify the VOCs existing in the room, and hexanal, pentanal, toluene, xylene, pinene, formaldehyde and acetaldehyde were selected as target compounds
- In the second day, the room ventilation was adjusted to 5% (70 CFM outdoor air) at first, then eight hours later, was increased to 50% (700 CFM outdoor air); 16 hours later, it was switched back to 5%
- Twenty four hours later, the filtration system was turned on and kept running for eight hours; then was shut off; and then the filter on/off cycle was repeated two more times
- In the second week, two more tests were done to monitor the room contaminant concentration change at ventilation of 25% and 10%.
- See Table B-3 for the schedule for the two-week test

Table B-3 The schedule for the two-week test

Test period	Time (h)	Procedure
	0	Got PTR-MS started
	2	Moved particle board in
	24	Adjusted outdoor air to 5%
	32	Adjusted outdoor air to 50%
	45	Adjusted outdoor air back to 5%
Week 1	72	Turned on the filter
	78	Turned off the filter
	100	Turned on the filter
	108	Turned off the filter
	124	Turned on the filter
	132	Truned off the filer
	0	Got PTR-MS started (with 5% outdoor air)
	8	Adjusted ventilation to 25%
Week 2	24	Adjusted ventilation back to 5%
	32	Adjusted ventilation to 10%
	48	Adjusted ventilation back to 5%

Table B-4 Air change rate for different operation modes

Room Volume	Supply air	Operation mode	Air change rate (times/h)
		50% OA	4.5
9385 ft3	1400cfm	25% OA	2.2
		10% OA	0.9
		5% OA	0.4

Appendix C. COE Building Humidity Load Calculation

Table C-1 COE building humidity load calculation

LEAKAGE & INFILTRATION LOAD		273.12 kg/Hr
<i>Formula: LOAD = (C-B) x 0.0012 x A x D x E x F</i>		
A = VOLUME OF CONDITION SPACE (m3)	11854	
B = DESIGNED HUMIDITY (g/kg)	12.000	
C = SURROUNDING HUMIDITY (g/kg)	20.000	
D = VOLUME FACTOR (Note A)	0.2	
E = PRESSURE FACTOR (Note B)	1	
F = CONSTRUCTION FACTOR (Note C)	1	
G= Delta g/kg factor (calculated)	12.00	0
HUMAN LOAD		16.58 kg/Hr
<i>Formula: LOAD = G x H x 0.15</i>		
G = NUMBER OF PEOPLE	165	
H = Work Load Coeff (0.5 Light to 1.6 Heavy)	0.67	
MADE UP AIR LOAD		44.7720 kg/Hr
<i>Formula: LOAD = (K- B) x J x 0.0012</i>		
J = Air volume in CMH	3731	
K = MADE UP AIR HUMIDITY (g/kg)	22.000	
DOOR OPENING LOAD		0.00 kg/Hr
<i>Formula: LOAD = (M- B) x 0.0012 x N x P x L x 0.3</i>		
L = TOTAL DOOR X-SECTION AREA	0	
M = NEXT DOOR AIR HUMIDITY (g/kg)	15	
N = EACH OPENING TIME (seconds)	30	
P = NUMBER OF OPENING /HOUR	2	
HYGROSCOPIC MATERIAL LOAD		0.00 kg/Hr
EXPOSED WATER SURFACE LOAD		0.00 kg/Hr
TOTAL HUMIDITY LOAD		334.47 kg/Hr

Table C-2 Determination of note A, B, and C in Talbe C-1

Note A (Volume factor)		Note B (+ve Pressure factor)		Note C (Construction factor)	
<400 CU METER	=0.4	+ 0 Pa	= 1	Wooden wall with cracks	= 2 to 3
1000 CU METER	= 0.3	+ 30 Pa	= 0.6	Basement	= 1.8 to 2.5
5000 CU METER	= 0.25	+ 60 Pa	= 0.3	4 walls exposed to rain	= 1.5 to 2
>10000 CU METER	= 0.22			Ground Floor	= 1.2 to 1.5
				Gypsum walls	= 1 to 1.3
				Normal good walls	= 1
				Oil based painted wall	= 0.8 to 0.9
				Double epoxy painted wall	= 0.7 to 0.8
				Freezer insulated seal wall	=0.6 to 0.8
				Tight sealed metal frame	= 0.3 to 0.5

VITA

Name of Author: Zhiqiang Wang

Place of Birth: Kashi, Xinjiang, China

Date of Birth: August 08, 1981

Graduate and undergraduate school attended:

Syracuse University, Syracuse, NY, USA

Tianjin University, Tianjin, China

Degrees Awarded:

M.S. Heating, Ventilating and Air-Conditioning Engineering, 2007, Tianjin University, China

B.S. Building Environment and Equipment Engineering, 2003, Tianjin University, China

Awards and Honors:

Research assistant scholarship at Syracuse University, 2007 - 2011

Professional Experience:

Research Assistant, Syracuse University, Department of Mechanical and Aerospace Engineering, 2007-2011

Technical Support, Research Center of Commercial Air-Conditioning, LG Electronics Tianjin Appliances Co., Ltd. Tianjin, China, Feb. 2004 - Aug. 2004

Publications:

Wang Z and Zhang JS. Characterization and performance evaluation of a full-scale activated carbon-based dynamic botanical air filtration system for improving indoor air quality. *Building and Environment* ; 2011, 46(3): 758-768.

- Huang W, Wang Z, Choudhary G, Guo B, Zhang JS and Ren D. Characterization of Microbial Species in a Regenerative Bio-filter System for VOC Removal. *HVAC & R journal*. Accepted for publication.
- Zhang JS, Wang Z, and Ren D. Botanical Air Filtration for Improving IAQ: Myths and Facts. *ASHRAE Journal*: 2010, 52(12): 138-140.
- Wang Z, Pei J, Zhang JS, and Ren D. 2011. Modeling and Simulation of an Activated Carbon-based Botanical Air Filtration System for Improving Indoor Air Quality. To be submitted to *Building and Environment*.
- Wang Z, Zhang JS and Ren D. 2011. Experimental Investigation on the Mechanisms of Formaldehyde Removal in a Dynamic Botanical Air Filtration System. To be submitted to *Building and Environment*.
- Huang W, Wang Z, Choudhary G, Guo B, Zhang J, Ren D. Characterization of Microbial Species in a Regenerative Bio-filter System for VOC Removal. *Proceedings of IAQVEC 2010—the 7th International Conference on Indoor Air Quality, Ventilation and Energy Conservation in Buildings*, August 15-18, Syracuse, NY, USA. Paper 104-133.
- Wang Z, Pei J, Zhang JS, Ren D. Modeling and Simulation of an Activated Carbon-based Botanical Air Filtration System for Improving Indoor Air Quality. *Proceedings of Clima 2010*, Antalya Turkey, May 9-12.
- Wang Z, Zhang JS, Mittelmark M, Wolverton BC. Performance evaluation and demonstration of an activated carbon based botanical air filtration system. *Proceedings of Healthy Building 2009*. Paper.564.

Liu J, Wang Z, Pei J. Ambient air quality measurement and assessment of a residential habitation. *Journal of Harbin Institute of Technology (New Series)*.

Vol. 14, 2007: 221-223.

Liu J, Wang Z, Sun J. Analysis of the Penetration Testing of Glass Fibrous Media by Fractional Particle Size. *China Pulp & Paper*. Vol. 26, No. 6, 2007: 23-26.

Liu J, Wang Z. Analysis and Design for the Mixing Water System of Fresh Air Pre-heater. *FLUID MACHINERY (CHINA)*. Vol. 35, No. 9, 2007: 65-69.

Liu J, Wang Z. Experimental Analysis and Research on the Filtration Efficiency of High Efficiency Air Cleaner. *FLUID MACHINERY (CHINA)*. Vol. 35, No. 7, 2007: 10-14.